Technical Analysis of Vehicle Load Reduction Potential For Advanced Clean Cars (Contract 13-313)

Draft Final Report
- Task 8 -
(Version 1.1)

by

Greg Pannone
CONTROLTEC, LLC

prepared for

California Air Resources Board
and the
California Environmental Protection Agency

March 3, 2015

DISCLAIMER

The statements and conclusions in this Report are those of CONTROLTEC, LLC and not necessarily those of the California Air Resources Board. The mention of commercial products, their source, or their use in connection with material reported herein is not to be construed as actual or implied endorsement of such products.

ACKNOWLEDGEMENTS

This research benefitted immensely from the experience and talent of Heidi Schroeder. Heidi's attention to detail and her analytical skills were key to the successful analysis of nearly 1400 vehicle models as required to support the research objectives. CONTROLTEC also appreciated the constructive input and feedback from the Air Resources Board project team.

This Report was submitted in fulfillment of Contract 13-313 by CONTROLTEC, LLC under the sponsorship of the California Air Resources Board. Work was completed as of March 3, 2015.

TABLE OF CONTENTS

ABSTRACT ix

EXECUTIVE SUMMARY x

Background x
Methodology x
Results xi
Conclusions xi

1. INTRODUCTION 1

2. METHODOLOGY 1

3. LITERATURE REVIEW 2

A. Mass 7
B. Aerodynamic Drag 8
C. Tire Rolling Resistance 10
D. Brake and Hub Drag 10
E. Model Year 2015 and Beyond 10
F. Conclusions 12

4. IDENTIFY DATA SOURCES AND COLLECT DATA 12

A. Data Sources 12
B. Selection of Vehicle Models 13
C. Data Fields and Data Set Configuration 13
D. Data Collection 16
E. Data Quality Assurance 17
F. Vehicle Data Set 18

5. CROSS REFERENCE VEHICLE CONFIGURATION DATA WITH NON-MASS LOAD REDUCTION TECHNOLOGIES 19

A. Background 19
B. Aerodynamic Drag 21
C. Method of Estimating the Coefficient of Drag 22
D. Aerodynamic Drag Results 26
E. Best-in-Class Aerodynamic Drag 28
F. Tire Rolling Resistance 36
G. Method of Estimating Tire Rolling Resistance 37
H. Tire Rolling Resistance Results 38
I. Best-in-Class Tire Rolling Resistance 43

6. DETAILED MASS REDUCTION ANALYSIS METHODOLOGY 45

A. Background 45
B. Curb Weight Reporting 48
C. Vehicle Mass Reduction and Mass Efficiency 49
D. Mass Model 49

E. Mass Model Elements 51
F. Mass Model Results 52
G. Mass Efficiency 52
H. Best-in-Class Mass Efficiency 54

7. PROJECTION METHODOLOGY 61

A. Analysis Software 61
B. Load Scenario Overview 61
C. Baseline Load Scenario 62
D. Non-Mass Load Reduction Scenario 63
E. Mass-Reduced plus Non-Mass Load Reduction Scenario 63
F. Power Source Resizing 63
G. On-board Energy Storage Resizing 64
H. Fleet Scenario 64

8. RESULTS 65

A. Load Attributes 65
B. Vehicle Energy Intensity 68
C. Energy Conversion Efficiency, Fuel Consumption, and Carbon Dioxide Emissions 72

9. SUMMARY AND CONCLUSIONS 76

10. RECOMMENDATIONS 76

REFERENCES 77

REFERENCES: MANUFACTURER WEBSITES 83

APPENDIX A: DATA QUALITY ASSURANCE CHARTS 85

APPENDIX B: TABULAR RESULTS 98

LIST OF FIGURES

Figure 1: Road Load Force vs. Vehicle Speed. 20
Figure 2: Manufacturer-Reported C_d vs. Vehicle Type. 22
Figure 3: Estimated Frontal Area vs. Manufacturer-Reported Frontal Area. 24
Figure 4: CONTROLTEC Estimated C_d vs. Vehicle Type. 27
Figure 5: CONTROLTEC Estimated C_d vs. Manufacturer-Reported C_d. 27
Figure 6: Estimated C_d from Road Load C-Coefficient vs. Manufacturer-Reported C_d. 28
Figure 7: Distribution of Estimated C_d for Coupes. 30
Figure 8: Distribution of Estimated C_d for Convertibles. 30
Figure 9: Distribution of Estimated C_d for Sedans. 31
Figure 10: Distribution of Estimated C_d for Hatchbacks and Wagons. 31
Figure 11: Distribution of Estimated C_d for SUVs. 32
Figure 12: Distribution of Estimated C_d for Vans. 32
Figure 13: Distribution of Estimated C_d for Pickups. 33
Figure 14: Estimated C_d for SUVs vs. Model Year of Renewal/Introduction. 35
Figure 15: Distribution of Estimated Tire RRC for All Vehicles. 39
Figure 16: Distribution of Tire RRC vs. Estimation Methodology. 39
Figure 17: Distribution of Tire RRC vs. Estimation Methodology. 40
Figure 18: Distribution of Tire RRC for the MY 2014 Data Set and the RMA Analysis [80]. 41
Figure 19: Estimated RRC vs. Tire Outside Diameter. 42
Figure 20: Estimated RRC vs. Tire Width. 42
Figure 21: Distribution of Tire RRC vs. Vehicle/Tire Category. 44
Figure 22: Equivalent Test Weight Class Range vs. Test Weight Class. 47
Figure 23: Example of Tailpipe CO_2 Emissions vs. Mass Reduction Scenarios. 47
Figure 24: Curb Weight vs. Vehicle Cubic Volume, MY 2014 Vehicles. 50
Figure 25: Curb Weight vs. Vehicle Type vs. Vehicle Cubic Volume, MY 2014 Vehicles. 50
Figure 26: CONTROLTEC Mass Model vs. Manufacturer Reported Curb Weight. 52
Figure 27: Distribution of Normalized Model Residuals. 53
Figure 28: Distribution of Normalized Model Residuals with Ford F-150 Overlays. 54
Figure 29: Distribution of Normalized Model Residuals for Coupes. 56
Figure 30: Distribution of Normalized Model Residuals for Convertibles. 56
Figure 31: Distribution of Normalized Model Residuals for Sedans. 57
Figure 32: Distribution of Normalized Model Residuals for Non-Luxury and Luxury Sedans. 57

Figure 33: Distribution of Normalized Model Residuals for Basic Sedans. 58
Figure 34: Distribution of Normalized Model Residuals for Hatchbacks & Wagons. 58
Figure 35: Distribution of Normalized Model Residuals for SUVs. 59
Figure 36: Distribution of Normalized Model Residuals for Vans. 59
Figure 37: Distribution of Normalized Model Residuals for Pickup Trucks. 60
Figure 38: Un-Weighted and Sales-Weighted C_d vs. Baseline and Best-in-Class (BIC) 66
Figure 39: Un-Weighted and Sales-Weighted Tire RRC vs. Baseline and Best-in-Class (BIC) 66
Figure 40: Un-Weighted and Sales-Weighted Curb Weight vs. Baseline and Best-in-Class (BIC) 67
Figure 41: Un-Weighted and Sales-Weighted ETW vs. Baseline and Best-in-Class (BIC) 67
Figure 42: Un-Weighted and Sales-Weighted Tire Rolling Force vs. Baseline and Best-in-Class (BIC) 68
Figure 43: Vehicle Energy Intensity for the Best-in-Class C_d Load Scenario 69
Figure 44: Vehicle Energy Intensity for the Best-in-Class C_d and Tire RRC Load Scenario 70
Figure 45: Vehicle Energy Intensity for the Best-in-Class C_d, Tire RRC, and Mass Efficiency Load Scenario 70
Figure 46: Average Vehicle Energy Intensity vs. Load Scenario 71
Figure 47: Reported vs. Projected Fuel Consumption (Combined Cycle) for the Baseline Condition 73
Figure 48: Reported vs. Projected Tailpipe CO_2 Emissions (Combined Cycle) for the Baseline Condition 73
Figure 49: Average Energy Conversion Efficiency vs. Load Scenario 74
Figure 50: Average Fuel/Electric Energy Intensity vs. Load Scenario 74
Figure 51: Average Fuel Economy vs. Load Scenario (Combined Cycle) 75
Figure 52: Average Tailpipe CO_2 Emission vs. Load Scenario (Combined Cycle) 75
Figure 53: Ground Clearance vs. Vehicle Type 85
Figure 54: Aerodynamic Drag Coefficient (C_d) vs. Vehicle Type 85
Figure 55: Engine Displacement per Cylinder 86
Figure 56: Engine Compression Ratio vs. Fuel System 86
Figure 57: Engine Specific Power vs. Compression Ratio, Power Source and Aspiration 87
Figure 58: Engine Specific Torque vs. Compression Ratio and Power Source Type 87
Figure 59: Rear Track vs. Front Track 88
Figure 60: Rear Brake Diameter vs. Front Brake Diameter 88
Figure 61: Rear Weight Distribution vs. Front Weight Distribution 89
Figure 62: Consumer Reports vs. Manufacturer-Reported Curb Weight 89
Figure 63: Equivalent Test Weight vs. Manufacturer-Reported Curb Weight 90
Figure 64: Equivalent Test Weight from Manufacturer-Reported Curb Weight vs. Equivalent Test Weight for Certification 90

Figure 65: Overall Width vs. Overall Length 91
Figure 66: Overall Height vs. Overall Length 91
Figure 67: Wheelbase vs. Overall Length 92
Figure 68: Vehicle Area vs. Vehicle Footprint 92
Figure 69: Manufacturer-Reported Curb Weight vs. Vehicle Cubic Volume 93
Figure 70: Fuel Tank Capacity vs. Curb Weight 93
Figure 71: Battery Capacity vs. Manufacturer-Reported Curb Weight 94
Figure 72: Manufacturer-Reported Frontal Area vs. Square Frontal Area 94
Figure 73: Tire Diameter vs. Vehicle Cubic Volume 95
Figure 74: Tire Diameter vs. Manufacturer-Reported Curb Weight 95
Figure 75: Road Force vs. Manufacturer-Reported Curb Weight 96
Figure 76: Engine Specific Power vs. Rated Power Speed 96
Figure 77: Engine Specific Torque vs. Rated Torque Speed 97
Figure 78: 0-60 mph Acceleration vs. Weight-to-Power Ratio 97

LIST OF TABLES

Table I: MY 2014 Light-duty Vehicle Load Reduction Technologies and Strategies Body, Closures, Glazing 4

Table II: MY 2014 Light-duty Vehicle Load Reduction Technologies and Strategies Brakes, Hubs, Suspension, Sub-frame, Tires, Wheels, Interior, Electrical 5

Table III: MY 2014 Light-duty Vehicle Load Reduction Technologies and Strategies Powertrain, Energy Storage, Other 6

Table IV: MY 2014 Manufacturer-Reported Mass Reduction 9

Table V: Vehicle Attribute Data Fields 14

Table VI: Manufacturer-Reported C_d Statistics vs. Vehicle Type. 22

Table VII: Example of dF_{aero}/dv and dF_{tire}/dv at 110 kph. 25

Table VIII: Estimated C_d Percentiles vs. Vehicle Type and Subcategories. 33

Table IX: Estimated C_d for ICE and Electric Powered Vehicles. 35

Table X: Proposed Best-in-Class C_d vs. Vehicle Type and Subcategories. 36

Table XI: Estimated Tire RRC Percentiles vs. Vehicle and Tire Category. 44

Table XII: Proposed Best-in-Class Tire RRC vs. Vehicle and Tire Category. 45

Table XIII: Normalized Mass Model Residuals vs. Vehicle Type and Subcategories 60

Table XIV: CT-ENERGY™ Output Variables to Support the Research Plan 62

Table XV: Vehicle Energy Intensity-to-Load Attribute Ratios. 71

Table XVI: Coefficient of Drag vs. Load Scenario 98

Table XVII: Effective Frontal Area vs. Load Scenario 98

Table XVIII: Tire RRC @ 80 kph vs. Load Scenario 98

Table XIX: Tire Rolling Force @ 80 kph vs. Load Scenario 99

Table XX: Curb Weight vs. Load Scenario 99

Table XXI: Equivalent Test Weight vs. Load Scenario 99

Table XXII: Vehicle Energy Intensity vs. Load Scenario 100

Table XXIII: Energy Conversion Efficiency vs. Load Scenario 100

Table XXIV: Fuel/Electrical Intensity vs. Load Scenario 100

Table XXV: Fuel Economy vs. Load Scenario 101

Table XXVI: Tailpipe CO_2 Emissions vs. Load Scenario 101

ABSTRACT

Reducing greenhouse gas emissions will require light-duty vehicle manufacturers to implement strategies such as aerodynamic drag improvements, reduced tire rolling resistance, and mass optimization. In support of the California Air Resources Board Advanced Clean Cars program, these vehicle load attributes were assessed for the potential to reduce carbon dioxide (CO_2) emissions from the future light-duty vehicle fleet.

Model year 2014 vehicles were studied to determine the extent to which vehicle load reduction technologies have already been applied. Using manufacturer-reported information, including certification data, the aerodynamic drag and tire rolling resistance were estimated for each vehicle model. Vehicle curb weight was obtained from the same sources and, combined with other vehicle specifications, used to evaluate mass efficiency. These analyses were then used to identify vehicles achieving best-in-class performance for each load attribute and the results cross-referenced to load reduction technologies.

The proposed best-in-class performance of each load attribute was then applied to all vehicle models in the same class and projections of fuel consumption and tailpipe CO_2 emissions were generated to determine the potential benefit to vehicle load reduction. Assuming that all current vehicles adopt similar amounts of load reduction technologies and strategies already available in today's better performing vehicles, and that the powertrains are re-optimized to the lower loads, it is estimated that a reduction in tailpipe CO_2 emissions of up to 10.4% is achievable.

EXECUTIVE SUMMARY

Background

In support of the California Advanced Clean Cars program [1][1] and the mid-term evaluation of regulations for Greenhouse Gas emissions and Corporate Average Fuel Economy [2, page 7], the California Air Resources Board requested research to determine the potential of applying currently implemented vehicle load reduction technologies to reduce carbon dioxide (CO_2) emissions from the future light-duty vehicle fleet.

Methodology

Model year 2014 light-duty vehicles were studied to determine the extent to which vehicle load reduction technologies, such as aerodynamic drag improvements, reduced tire rolling resistance, and mass optimization, have already been applied. Applying the proposed best-in-class performance of each load attribute to all vehicle models and generating projections of fuel consumption and tailpipe CO_2 emissions determined the potential benefit of vehicle load reduction.

The research began with a literature review to document all relevant load reduction strategies and technologies that are in the current fleet and can be reasonably applied to future light-duty vehicles.

To support the required analysis, a data set of specifications and attributes was assembled for each vehicle model and powertrain sub-configuration. The data set was composed of manufacturer-reported information, including certification data. Using these data, the aerodynamic drag and tire rolling resistance were estimated for each vehicle model. Vehicle curb weight was obtained from the same sources and, combined with other vehicle specifications, used to generate a mass efficiency metric.

To determine the benefits of key vehicle load reduction strategies and technologies, the results of the literature review were then combined with values for aerodynamic drag, tire rolling resistance, and mass efficiency. Additionally, the distribution of the attributes was used to determine proposed best-in-class values.

Using vehicle simulations, the fuel consumption, CO_2 emissions, and acceleration performance of each vehicle model and powertrain sub-configuration was determined to establish a baseline. The proposed best-in-class performance of each load attribute was then applied to all vehicle models and the simulations were repeated to determine the change in fuel consumption, tailpipe CO_2 emissions, and acceleration performance. The lower vehicle loads will result in improved acceleration performance and a greater driving range from the on-board energy storage. The final evaluation, therefore, included reducing the size of the power source and on-board energy storage to re-establish the baseline acceleration and driving range. All fuel consumption and CO_2 emission results were reported for the regulated drive cycles only.

---

[1] Values in brackets [ ] denote references found at the end of the document

Results

Assuming that all vehicles adopt load reduction technologies already demonstrated in today's vehicles, and that the powertrains are re-matched to the lower loads, it is estimated that a reduction in tailpipe CO_2 emissions of 8.3% to 10.4% is achievable. Of this total, 6.6% is the direct result of reducing the vehicle loads associated with aerodynamic drag, tire rolling resistance and mass. Reducing the engine displacement (or motor size in the case of electric vehicles) to maintain the baseline acceleration performance contributes an additional 1.7% (8.3% total). Further optimizing the powertrain system to the reduced vehicle loads could contribute another 2.1% (10.4% total). These improvements represent plausible levels for the potential of vehicle load reduction to reduce CO_2 emissions using technologies and strategies that exist in the MY 2014 fleet. Assuming the current fleet mix and powertrain technology deployment, the potential reduction of mobile source CO_2 emissions from deploying 2014 model year road load reduction technologies across the fleet is between 22 g/mile (8.3%) and 27 g/mile (10.4%). Combined with a new California light-duty vehicle fleet of 1.83 million units, the potential reduction in mobile source greenhouse gas load is between 40 and 50 metric tons per fleet-mile traveled. Future changes to fleet mix and powertrain technology deployment will change the absolute levels (i.e., g/mile) of potential mobile source CO_2 emissions reduction, however, the fractional benefit (~10%) is expected to remain as long as the internal combustion engine is the dominant light-duty vehicle power source.

Conclusions

Using technologies and strategies that exist on production vehicles today, the aerodynamic drag, tire rolling resistance, and mass efficiency of the light-duty fleet can be reduced to achieve a benefit in tailpipe CO_2 emissions of up to 10.4%. This improvement represents nearly one third of the 34% reduction required to support the California Air Resources Board Advanced Clean Cars program.

1. INTRODUCTION

The California Advanced Clean Cars program [1] is projecting a 34% reduction of global warming gases from model year (MY) 2012 to full implementation in MY 2025. Reducing greenhouse gas (GHG) emissions to the MY 2025 targets will require light-duty vehicle manufacturers to implement technologies to improve powertrain efficiency and reduce vehicle loads.

In support of the California Advanced Clean Cars program and the mid-term evaluation of regulations for GHG emissions and Corporate Average Fuel Economy (CAFE) [2, page 7], the California Air Resources Board (CARB) requested research [3] to determine the potential of applying vehicle load reduction technologies to reduce carbon dioxide (CO_2) emissions from the future light-duty vehicle fleet. Vehicle load reduction strategies include aerodynamic drag improvements, reduced tire rolling resistance, and mass optimization.

The objective of the research is to determine to what extent current vehicles have already adopted vehicle load reduction technologies and the plausible reduction of CO_2 emissions if all vehicles achieved the load attributes demonstrated by the best MY 2014 products. The scope of the research includes all light-duty vehicles and assumes operation over the regulated drive schedules. Although vehicle load reduction will improve CO_2 emissions over any drive cycle, off-cycle performance was not evaluated for this research. The requested research is a technical assessment and, therefore, an evaluation of technology costs is not within the study scope.

2. METHODOLOGY

As required by the research plan [3], the technical analysis was composed of six major elements: literature review, identify and collect data, cross reference vehicle configuration data source with non-mass load reduction technologies, detailed mass reduction analysis methodology, develop vehicle projection methodology, and produce vehicle projections.

The research began with an extensive literature review to document all relevant non-mass (road load) and mass reduction technologies that can be reasonably applied to light-duty vehicles. The literature review covered a variety of sources including, but not limited to, technical publications, research results from independent and government organizations, and manufacturer's new vehicle press releases. Concurrently, a data set of existing light-duty vehicles was created. The data set included vehicle and powertrain specifications, vehicle load reducing technologies being used, acceleration and capability performance, fuel consumption, and tailpipe CO_2 emissions.

Using the information from the literature review and the vehicle database, an analysis was conducted to determine the best-in-class products for aerodynamic drag, tire rolling resistance, and mass efficiency. Using vehicle modeling, the proposed best-in-class performance was then applied to all vehicles in the same class. The fuel consumption, CO_2 emissions, and acceleration performance of the modified vehicles were calculated to determine the benefits of the vehicle load actions. The power source of each vehicle was then re-sized to achieve the same level of performance as the current product. Finally, the on-board energy storage was reduced to maintain the same operating range as the original vehicle.

Sales volumes, representing the California fleet, were mapped to each vehicle to generate a fleet scenario. The sales-weighted CO_2 emissions were computed for each vehicle load scenario. The difference between the load-reduced and baseline fleet represents the plausible reduction in CO_2 emissions resulting from a fleet-wide application of currently available load reduction technologies.

Each task of the research project is described in more detail in the following sections.

3. LITERATURE REVIEW

Manufacturer sources (see Manufacturer Websites in the Reference Section) were used to develop the most comprehensive and up-to-date information regarding the non-mass and mass reduction strategies and technologies currently in production. While collecting data, the manufacturer press kits and press releases were reviewed, where available, for every MY 2014 vehicle. For vehicles that were recently launched, press kits and releases from earlier model years were accessed for additional information. From this process, over 2700 statements associated with non-mass and mass reduction strategies and technologies were collected for 764 of the 1358 vehicles in the data set. This information was combined with load reduction items from the specifications (e.g., aluminum wheels, low rolling resistance tires) to generate a list of load reduction strategies and technologies present in the MY 2014 light-duty fleet. In total, 73 non-mass and mass reduction strategies and technologies were identified. The results of this assessment are shown in tables I, II, and III.

For organization purposes, the strategies and technologies were binned under one of five vehicle systems:

1. Body (body structure, body panels, closures, glazing)
2. Chassis (sub-frame, suspension, brakes, hubs, tires, wheels)
3. Interior (seats, trim, carpet, instrument panel, seat belts, air bags)
4. Electrical (non-powertrain motors, lighting, wiring)
5. Powertrain (engine, motors, power electronics, transmission, driveline, cooling, energy storage)

Within a vehicle system, the strategy was further categorized by sub-system and load attribute (e.g., mass, aerodynamics). Strategy categories were defined as follows:

1. <u>Material substitution</u>. Substituting one material for another to reduce weight.
2. <u>Design and/or process</u>. Design and/or structural optimization (using the same materials and features) and/or manufacturing process improvements that enable mass reduction or road load reduction. Examples include unitized body versus body-on-frame construction, aerodynamic optimization of side mirrors, and roll formed cargo box versus a stamped box (pickup trucks).
3. <u>Features</u>. The addition of physical part(s) that reduce vehicle load. Examples include grille shutters, hood seals, and underbody panels for aerodynamic drag reduction.
4. <u>Dimensional Reduction</u>. Dimensional reduction of any vehicle or powertrain component or attribute. Examples include reducing fuel tank volume and battery capacity for weight reduction and reducing vehicle frontal area to reduce aerodynamic drag.

5. De-content. Removal of content that is typically included on other vehicles in its class, on the prior year's model, or included in the base vehicle. Examples include elimination of the spare tire and reduced sound insulation to minimize weight.

The technology or approach further defines the strategy, while the specific items and areas indicate which parts of the vehicle or powertrain were changed. The last column in each table represents the frequency, across manufacturers, that the strategy was referenced. This is an assessment of how many manufacturers claim use of the strategy in one or more of their products. It is not an assessment of the overall market penetration of the strategy. It is also important to note that if a manufacturer does not report a technology or strategy it cannot be concluded that the manufacturer did not incorporate the approach in their products. Rather, the manufacturer may have simply chosen not to report it, perhaps because it is considered common industry practice. For example, composite engine intake manifolds were noted by only a few manufacturers, however, many manufacturers now use this technology. Further, the level of detail varied significantly among the manufacturers. Some manufacturers provided little information beyond their specifications while others provided many references to load reduction strategies. The frequency of reference is, therefore, more likely indicative of the current areas of focus. Consequently, the information in tables I, II, and III should be viewed as a guide to the load reduction technologies on MY 2014 vehicles and not an assessment of the extent to which these technologies or strategies are used.

Mass reduction strategies and technologies can be found in all five vehicle systems. In some cases, the vehicle system was not identified. The non-mass strategies were typically associated with the body (aerodynamics), chassis (aerodynamics, tire rolling resistance, brake drag, and hub drag), and to a lesser degree powertrain (cooling drag). While all manufacturers reported a load reduction technology or strategy, there was very little information regarding the specific benefit, either as an absolute value or a percentage. The load reduction strategies, for each of the major load attributes, are discussed in the following sub-sections, in order of reference frequency.

Table I: MY 2014 Light-duty Vehicle Load Reduction Technologies and Strategies Body, Closures, Glazing

Vehicle System / Sub-System	Load Attribute	Strategy	Technology(ies) or Approach	Specific Items and/or Areas	Frequency of Reference
Body	Mass	Material Substitution	Aluminum	structure, panels, fenders, bumper/impact beam, roof, tunnel	High
Body	Mass	Material Substitution	High-Strength Steel	frame, tunnel, front rails, structure, pillars, rocker panels	High
Body	Mass	Material Substitution	Carbon Fiber Reinforced Polymer	structure, panels, hood, fenders, side blades, roof, underbody panels	Medium
Body	Mass	Material Substitution	Magnesium	structure, roof frame	Medium
Body	Mass	Material Substitution	Polymers and Polymer Composites	panels, fenders, fascias	Medium
Body	Mass	Material Substitution	Ultra High-Strength Steel	structure, pillars, rocker panels, bumper/impact beam	Medium
Body	Mass	Design and/or Process	Structural, Design, & Process Optimization	overall design, roll formed vs. stamped pickup bed, unibody vs. body-on-frame	Medium
Body	Mass	Dimensional Reduction		wheelbase	Low
Body	Aerodynamic Drag	Design and/or Process	Upper Body Design Optimization	front fascia, dealer installed air dam, air curtains, head lamps, wiper nesting, mirrors, pillars, wheel spats/strakes, tire-to-body gap, tail lamps	High
Body	Aerodynamic Drag	Dimensional Reduction	Reduce Frontal Area	overall, lower height	Low
Body	Aerodynamic Drag	Features	Underbody Panels	engine, exhaust tunnel, rear axle, rear diffuser	High
Body	Aerodynamic Drag	Features	Active Grille Shutters		Medium
Body/Closures	Mass	Material Substitution	Aluminum	impact beams, hood, door panels, door structure, convertible roof structure, tailgate	High
Body/Closures	Mass	Material Substitution	Carbon Fiber Reinforced Polymer	panels, hood, decklid, liftgate, engine cover, roof, fenders	Medium
Body/Closures	Mass	Material Substitution	Polymers and Polymer Composites	panels, doors, decklid, tailgate	Medium
Body/Closures	Mass	Material Substitution	Magnesium	structure, panels	Low
Body/Closures	Mass	Material Substitution	High-Strength Steel	door panels, door frame	Low
Body/Closures	Mass	Material Substitution	Ultra High-Strength Steel	door panels, impact beam	Low
Body/Closures	Aerodynamic Drag	Features	Hood seals, Retractable Door Handles		Low
Body/Glazing	Mass	Dimensional Reduction	Glass Thickness		Low
Body/Glazing	Aerodynamic Drag	Design and/or Process	Design Optimization	flush mount side glass	Low

Table II: MY 2014 Light-duty Vehicle Load Reduction Technologies and Strategies Brakes, Hubs, Suspension, Sub-frame, Tires, Wheels, Interior, Electrical

Vehicle System / Sub-System	Load Attribute	Strategy	Technology(ies) or Approach	Specific Items and/or Areas	Frequency of Reference
Chassis/Brakes	Mass	Material Substitution	Aluminum	calipers, rotor hub (two piece rotor)	Medium
Chassis/Brakes	Mass	Material Substitution	Carbon Ceramic	rotor	Medium
Chassis/Brakes	Mass	Material Substitution	Titanium		Low
Chassis/Brakes	Mass	Design and/or Process	Waved Rotor, Two-Piece Rotor (multiple materials)		Low
Chassis/Brakes	Brake Drag	Design and/or Process	Low Drag		Low
Chassis/Hubs	Hub Drag	Design and/or Process	Low Friction Seals and/or Bearings		Low
Chassis/ Suspension	Mass	Material Substitution	Aluminum	suspension, upper & lower control arms, steering knuckles, torque struts	High
Chassis/ Suspension	Mass	Material Substitution	High-Strength Steel	linkages, A-arms	Low
Chassis/ Suspension	Mass	Material Substitution	Ultra High-Strength Steel		Low
Chassis/ Suspension	Mass	Design and/or Process	Design Optimization	shock, hollow stabilizer bar	Low
Chassis/ Suspension	Aerodynamic Drag	Features	Active Ride Height		Low
Chassis/ Sub-frame	Mass	Material Substitution	Aluminum	sub-frame, cradle	Low
Chassis/Tires	Mass	Design and/or Process	Design Optimization		Low
Chassis/Tires	Mass	Decontent	Eliminate Spare Tire		Low
Chassis/Tires	Tire Rolling Resistance	Design and/or Process	Low Rolling Resistance		High
Chassis/Wheels	Mass	Material Substitution	Aluminum		High
Chassis/Wheels	Mass	Material Substitution	Lightweight Materials (not specified)		Low
Chassis/Wheels	Mass	Design and/or Process	Structural Optimization & Manufacturing Process		Low
Chassis/Wheels	Aerodynamic Drag	Design and/or Process	Design Optimization		Medium
Interior	Mass	Material Substitution	Lightweight Materials (not specified)		Low
Interior	Mass	Material Substitution	Aluminum	steering support bracket	Low
Interior	Mass	Material Substitution	Lightweight Fibers	instrument panel, door panels	Low
Interior	Mass	Material Substitution	Magnesium	instrument panel cross member, seat frame	Low
Interior	Mass	Material Substitution	Polymers and Polymer Composites	trunk floor	Low
Interior	Mass	Material Substitution	High-Strength Steel	seat structure, seat cross members	Low
Interior	Mass	Decontent		manual seats, reduced sound insulation	Low
Interior	Mass	Design and/or Process	Design Optimization	HVAC	Low
Electrical	Mass	Design and/or Process	Design Optimization	wiper motor	Low

Table III: MY 2014 Light-duty Vehicle Load Reduction Technologies and Strategies Powertrain, Energy Storage, Other

Vehicle System / Sub-System	Load Attribute	Strategy	Technology(ies) or Approach	Specific Items and/or Areas	Frequency of Reference
Powertrain/ Engine	Mass	Material Substitution	Aluminum	cylinder block, cylinder heads	High
Powertrain/ Engine	Mass	Material Substitution	Steel	exhaust manifold (vs. cast iron)	Low
Powertrain/ Engine	Mass	Material Substitution	Carbon Fiber Reinforced Polymer	cam covers, engine cover	Low
Powertrain/ Engine	Mass	Material Substitution	Compacted Graphite Iron	cylinder block	Low
Powertrain/ Engine	Mass	Material Substitution	Magnesium	intake manifold, valve covers, engine covers	Low
Powertrain/ Engine	Mass	Material Substitution	Polymers and Polymer Composites	intake manifold	Medium
Powertrain/ Engine	Mass	Material Substitution	Titanium	piston rods, fasteners	Low
Powertrain/ Engine	Mass	Design and/or Process	Design Optimization	cylinder head-exhaust single casting, bearing size, counterweight reduction, thin wall crankcase	Medium
Powertrain/ Transmission	Mass	Material Substitution	Aluminum	case	Low
Powertrain/ Transmission	Mass	Design and/or Process	Design Optimization	case, gears, lightweight design,	Low
Powertrain/ Driveline	Mass	Material Substitution	Carbon Fiber Reinforced Polymer	propshaft	Low
Powertrain/ Driveline	Mass	Material Substitution	Aluminum	torque tube, drive shaft	Low
Powertrain/ Driveline	Mass	Design and/or Process	Design Optimization	transfer case, 4WD system	Low
Powertrain/ Exhaust	Mass	Material Substitution	Titanium		Low
Powertrain/ Fuel Tank	Mass	Material Substitution	Polymers and Polymer Composites		Low
Powertrain/ Fuel Tank	Mass	Dimensional Reduction	Capacity Reduction		Low
Powertrain/ Battery	Mass	Material Substitution	Li-ion		Low
Powertrain	Aerodynamic Drag	Design and/or Process	Design Optimization	cooling drag	Low
Not Identified	Mass	Material Substitution	High-Strength Steel		Medium
Not Identified	Mass	Material Substitution	Ultra High-Strength Steel		Medium
Not Identified	Mass	Material Substitution	Lightweight Materials (not specified)		Low
Not Identified	Mass	Material Substitution	Aluminum		Low
Not Identified	Mass	Material Substitution	Polymers and Polymer Composites		Low
Not Identified	Mass	Design and/or Process	Structural & Design Optimization		Low

A. Mass

Mass reduction was the most frequently referenced load reduction strategy for MY 2014 vehicles. Mass reduction was achieved by material substitution, design and/or process, dimensional reduction, and de-contenting.

Within the mass reduction category, material substitution was the most commonly referenced strategy, in particular:

- Steel to aluminum (Al)
- Mild steel to high-strength (HSS) or ultra high-strength steel (UHSS)
- Steel to polymer composites
- Steel or aluminum to magnesium
- Steel or aluminum to carbon fiber reinforced polymer (CFRP)
- Steel or aluminum to titanium
- Cast iron (Fe) to steel
- Cast iron to compacted graphite iron

Material substitution to aluminum as a light-weighting strategy was the most frequent comment, followed by substitution to high-strength steels, ultra high-strength steels, polymer composites, and magnesium. Material substitution with carbon fiber reinforced polymer and titanium are applied to a few current products, all high performance or low volume vehicles.

The body and chassis appear to be the primary focus areas for material substitution, followed by the powertrain elements. Very few manufacturers referenced material substitution associated with interior components. No material substitution references were found for electrical components.

Within the body, a range of material strategies was employed depending upon the subsystem. Structural components were most often aluminum, high-strength steel, and ultra high-strength steel. Magnesium is used to a lesser extent in areas such as the roof structure and doors. For body panels and closures, the most common material substitution was to aluminum and polymer composites and, to a lesser extent, high-strength steel. Carbon fiber reinforced polymers are emerging, primarily in body panels.

In the chassis, aluminum substitution in cradles, suspension components, wheels, and brake calipers was the most common mass reduction strategy. High and ultra high-strength steels were referenced, but to a much lesser degree than aluminum. Carbon ceramic brake rotors provide a relatively large benefit and are being applied to high performance vehicles.

Material substitution on powertrain components is relatively mature. For example, aluminum is the most common material for cylinder blocks and heads. Composite engine intake manifolds (versus aluminum) and steel exhaust manifold (versus cast iron) are referenced to a lesser degree, likely because these are now commonly used materials for these sub-systems. Compacted graphite iron is emerging as a substitute material to cast iron in engine blocks. Carbon fiber and titanium are referenced as substitute powertrain materials for high performance vehicles. Carbon fiber

powertrain applications include engine covers and propshafts, while titanium is being used on engine internal components, fasteners, and exhaust systems.

Material substitution within the interior included the use of aluminum in steering supports, high-strength steel in the seat structure, magnesium for the instrument panel (IP) cross member, lightweight fibers in the IP and door panels, and plastic composites for non-structural elements such as the trunk floor.

A few manufacturers referenced design and structural optimization as a light-weighting strategy. Areas targeted for design optimization included body systems, engines, tires, suspension components, and electric motors. De-contenting (e.g., spare tire removal, reduced sound insulation) and dimensional reduction (e.g., fuel tank capacity, glass thickness) was mentioned by a few manufacturers and most often associated with performance vehicles.

Of the over 1600 comments recorded regarding weight reduction in the body and chassis, only a small fraction included actual weight savings. Of those, only a few provided specifics and none provided a baseline weight. Manufacturer-reported weight reduction claims are provided in table IV. There was no attempt to independently verify these values, however, some claims (e.g., Land Rover Range Rover Sport) are not supported by the manufacturer's own certification documents. Light-weighting is often approached holistically, consequently, the largest weight reduction claims were typically an aggregate of multiple strategies, technologies, and sub-systems and, therefore, do not provide insight to the potential of a single approach. The body, chassis, and powertrain were the only sub-systems with reported mass reduction values.

B. Aerodynamic Drag

The most common design element to reduce non-mass load reduction was improving aerodynamic drag. Most statements referred to achieving lower aerodynamic drag reduction through passive methods such as design optimization, underbody panels, hood seals, and flush side glass, rather than adding features such as active grille shutters and active ride height.

Within the passive category, the most common strategy was improving underbody airflow, followed by upper body design optimization. In particular, these passive design elements were mentioned:

- Front fascia detail
- Headlamp design
- Air curtains
- Wiper nesting
- Mirror optimization
- Wheel spats/strakes
- Tire-to-body gap
- Aerodynamic wheels
- Underbody panels
- Rear diffusor
- Tail lamp design

Table IV: MY 2014 Manufacturer-Reported Mass Reduction

System & Strategy	Mass Reduction		Product	Reference
	[kg]	[lb]		
Vehicle, Holistic	363	800	Land Rover Range Rover Sport	[4]
Vehicle, Holistic	181	400	Porsche Cayenne	[5]
Vehicle, Holistic	91	200	Mitsubishi Outlander	[6]
Vehicle, Holistic	91	200	Nissan Versa Note	[7]
Vehicle, Holistic	20-45	44-100	BMW 3/4-Series	[8] [9] [10]
Body, Steel to Al Substitution	24	52	Acura TL	[11]
Body, Steel to Al Substitution	45	100	Porsche 911	[12]
Body, Steel to HSS Substitution	18	40	Audi A3	[13]
Body/Hood, Steel to Al Substitution	7.7	17	GMC Sierra	[14]
Body/Hood, Steel to Al Substitution	8.9	19.6	Acura RLX Hybrid	[15]
Body/Hood, Steel to Al Substitution	6.8	15	Audi A3	[13]
Body/Door Panels, Steel to Al Substitution	11	24.3	Acura RLX Hybrid	[15]
Body/Fenders, Steel to Al Substitution	2.2	4.9	Audi A3	[13]
Body/Liftgate, Steel to Polymer Substitution	30%		Nissan Rogue	[16]
Chassis/Sub-frame, Steel to Al Substitution	6.4	14	Dodge Dart	[17]
Chassis/Sub-frame, Steel to Al Substitution	4	8.8	Accord Hybrid	[18]
Chassis/Sub-frame, Steel to Al Substitution	6	13.2	Audi A3	[13]
Chassis/Wheel, Design Optimization	21.9	48.3	Chevrolet Camaro	[19]
Chassis/Brakes, Fe to Ceramic Discs	9.5	21	Chevrolet Camaro	[19]
Powertrain/Engine, Al to Composite Intake Manifold	2.5	5.5	Cadillac XTS	[20]
Powertrain/Engine, Fe to Compacted Graphite Iron Cylinder Block	25	55	Volkswagen Touareg Diesel	[21]
Powertrain/Engine, Al Substitution	21	46	Audi A3	[13]
Powertrain/Engine, Al to Titanium Piston Rods & Fasteners	7.5	16.5	Bugatti Veyron	[22]
Powertrain/Engine, Design Optimization	5.9	13	Bugatti Veyron	[22]
Powertrain/Exhaust, Steel to Titanium Substitution	17	37.5	Bugatti Veyron	[22]

A few manufacturers mentioned features such as hood seals and retractable door handles. Active grille shutters and active ride height were noted by several manufactures. One manufacturer reduced the frontal area of its vehicle to reduce drag.

Many manufacturers provided the drag coefficient (C_d) of the final product. However, very few manufacturers provided actual improvement values for aerodynamic drag strategies. As with mass reduction, most aerodynamic development is holistic and, therefore, the benefit of individual approaches cannot be extracted from the available information. In only one instance was the baseline and improved state of a technology provided. Those that did provide information quoted improvements from 3% to 7%. Underbody panels were attributed to improving aerodynamic drag by 3.4% on the Honda Civic [23] and 7% on the Dodge Dart [17]. Chrysler quoted active grille shutters as having a 3% to 5% benefit [17]. Audi claims a 0.02 C_d (5%) reduction from active ride height for their Q7 [24].

C. Tire Rolling Resistance

Low rolling resistance tires were noted by more than half of the manufacturers. Of the manufacturers that reported improved rolling resistance, only two provided a benefit; 21% for the Honda Civic HFE [25] and 7% for the Porsche Boxster [26].

D. Brake and Hub Drag

Only three manufacturers referenced low friction hub bearings and low drag brakes as a load reduction strategy; none stated benefits.

E. Model Year 2015 and Beyond

In keeping with the objective of the research, this phase of the literature review focused on finding information regarding emerging technologies that could be reasonably applied to the future fleet. Consequently, the focus was on finding technologies and strategies that either provided a specific implementation date or had undergone significant validation. Information was not gathered on research that had no evaluation of production feasibility or timing.

A review of manufacturer, trade, and technical publications for emerging and new load reduction technologies for MY 2015 and beyond yielded similar strategies currently in use. Three key trends emerged after reviewing hundreds of press releases, articles, and technical papers:

1. Current technologies and strategies will see expanded use.
2. Current technologies and processes will be refined.
3. The cost of some current technologies may become much more affordable

Manufacturers are expanding their key mass reduction strategies as they renew products [27] [28] [29] [30] [31] [32], in particular, expanded use of aluminum, high-strength steel, and ultra high-strength steel. According to Ducker Worldwide [33], aluminum content in light-duty vehicles is expected to increase by 28% from 2012 to 2015. Novelis and Constellium are expanding aluminum

production capacity in response to the expected increase in demand [34] [35]. Even the use of carbon fiber reinforced polymer is projected to increase significantly as evidenced by a three-fold expansion of carbon fiber capacity by SGL Group [36].

For MY 2015, mass reduction levels are similar to those identified in MY 2014. At the extreme, Ford is claiming a curb weight reduction of 318 kg (700 lb) for its F-150 pickup through the use of aluminum and high-strength steel [27] [37]. For this application, Ford uses aluminum for the body and cargo bed and retained a steel frame. Ford increased the application of high-strength steel in the frame from 23% to 77%, resulting in a weight savings of up to 30 kg (66 lb). In addition to these major structural elements, Ford reduced weight in other subsystems including the following: optimized wheels saving 4.5 kg (10 lb), a bracket-less tire jack saving 1 kg (2.2 lb), and lighter glass [37].

For the MY 2015 Mustang, Ford was able to maintain weight within 2.7 kg (6 lb) of the lightest MY 2014 vehicle, despite extra features and a more powerful engine [38]. While Ford provides no specific values, it achieved weight neutrality through the application of high-strength steels, aluminum hood and fenders, aluminum chassis components, and design optimization.

Honda renewed its Fit for MY 2015 and achieved a 27 kg (59.4 lb) weight reduction in its body structure and closures through greater use of high-strength steels (20 kg, 44 lb) and improved manufacturing processes (7 kg, 15.4 lb) [29]. The Fit chassis mass was reduced through a lighter front sub-frame (2 kg, 4.4 lb) and high-strength steel suspension components. Although Honda did not provide specific values, it claims engine and transmission weight reductions through multiple design changes and material substitution.

Volkswagen shed up to 36 kg (79 lb) on its seventh-generation MY 2015 Golf, which uses its modular transverse matrix vehicle platform (MQB) [31]. The MQB platform increases the use of high-strength steels from 6% to 28%. Combined with the use of ultra high-strength steels and design optimization, Volkswagen was able to reduce the mass of the body structure 23 kg (51 lb). For the engine, Volkswagen made numerous design and material substitution changes including a 32.7 kg (72 lb) lighter thin-cast iron block, polymer oil pan, integrating the exhaust manifold into the cylinder head, reducing crankshaft counterweights, and using aluminum fasteners.

Alfa Romeo introduced its 4C sports car in MY 2015 and is expanding the use of carbon fiber applications through its monocoque design [39]. The rear cell structure, roof reinforcements, and engine mount frame are made from aluminum. The bodywork is sheet mold compound with a claimed weight savings of 20% over steel.

In addition to expanded use and capacity, suppliers and researchers are working to lower the cost of light-weighting. Examples include developing cold forming capabilities of high-strength steels [40], lower cost carbon fiber sheet molding compound [41], and more efficient titanium processing methods [42].

As with mass reduction, current aerodynamic drag and tire rolling resistance reduction strategies will continue to propagate as vehicles are renewed. For MY 2015, passive solutions will continue to be

the main focus, however, the use of active devices is expected to continue to increase as well [43] [44] [45]. As with the current model year findings, actual levels of aerodynamic improvements are rarely stated. Ford has showcased several active aerodynamic features, including active grille shutters, active wheel shutters, and active running boards [46]. While these concepts were targeted for its future pickup trucks, Ford has only announced the use active grille shutters on the MY 2015 F-150 [47].

Among the new vehicle launches for MY 2015 passive aerodynamic improvements through design optimization continues to be the most common approach to reduced aerodynamic drag and, Ford made numerous passive changes for improved aerodynamic drag including front air flow optimization, flush mounted windshield, cab-to-bed gap reduction, inset cargo bed sides to smooth air flow, and a tailgate spoiler to reduce wake [37]. For the MY 2015 Mustang, Ford also focused on passive changes including optimized underhood air flow, front fascia design, reduced frontal area (3%), and improved air flow around the wheels (0.002 to 0.003 Cd improvement) [48]. Finally, tires will continue to receive attention with developments that improve rolling resistance [49] [50].

F. Conclusions

Based on a comprehensive review of MY 2014 light-duty vehicles, automotive manufacturers are deploying a wide range of load reduction strategies and technologies in response to the stricter global standards for fuel efficiency and CO_2 emissions. Improvements are being implemented on all vehicle systems with the most emphasis on mass reduction. Of the 73 strategies identified in MY 2014 vehicles, 61 were mass reduction strategies, with material substitution being the leading focus area. Within the material substitution category, aluminum and high-strength steels are generating the most activity. Reported mass savings generally scale with the mass of the vehicle system. The largest reductions are being reported on the body; however, benefits are also being found in the chassis and powertrain systems. Finally, most manufacturers are pursuing improvements in aerodynamic drag and tire rolling resistance. These non-mass improvements are primarily the result of design optimization.

4. IDENTIFY DATA SOURCES AND COLLECT DATA

To accomplish the analyses required in subsequent tasks, it was necessary to collect, for each vehicle, the attributes associated with mass and non-mass (e.g., aerodynamics) load elements. When these attributes were not available, the information collected allowed for the estimation of these parameters. Additionally, vehicle type and segment information were required for the best-in-class assessments [3, Tasks 4 and 5]. Finally, powertrain and on-board energy storage parameters were necessary to generate the vehicle projections for fuel economy, CO_2 emissions, acceleration performance, and range [3, Task 7]. Consequently, obtaining as much detail as possible was critical to the overall efficacy of the project results.

A. Data Sources

To complete this task, publicly available vehicle and powertrain specifications and features from the manufacturer sources, EPA Verify [51] queries [52] [53], certification documents [54], and third party

sources [55] [56] were aggregated. The manufacturer websites accessed for this task are provided in the reference section.

B. Selection of Vehicle Models

Given the objective and scope of the research, MY 2014 light-duty vehicles were selected as the baseline for non-mass and mass vehicle load reduction potential. Reflecting the need to achieve the national standards for fuel economy and CO_2 emissions [57] [58], the MY 2014 vehicles include a variety of load reduction technologies.

To create the list of MY 2014 light-duty vehicles sold in the US, each manufacturer's website was reviewed to determine the available models and sub-configurations. Key sub-configurations include:

- Power Source (engine options, hybrid options)
- Transmission (e.g., automatic, manual)
- Driveline (e.g., FWD, AWD)
- Passenger Car/Light Truck within a model (e.g., Dodge Journey with 2 row seating vs. 3 row seating)
- Pickup Truck Cab/Cargo Bed
- Body Style within a model (e.g., Honda Accord Sedan/Coupe, Nissan Versa Sedan/Hatch)

The resulting data set includes 1358 vehicle models. By comparison, the MY 2014 fuel economy guide data file published by the Environmental Protection Agency (EPA) [52] includes 1219 vehicles. The additional 139 vehicles in the data set are the variations in body styles, not listed in the EPA guide data, for certain vehicle types. For example, the MY 2014 fuel economy guide data file shows 12 versions of pickup trucks from General Motors (Chevrolet and GMC) while the project data set includes 52. The difference is due to the number of cab and cargo bed combinations. Since cab and cargo bed combinations have a direct impact on vehicle mass and aerodynamic drag, it was necessary to include these configurations given the objective of the study. Similarly, models available with multiple body styles are often shown as a single model in the EPA guide data. The Ford Fiesta, for example, is offered as both a hatchback and a sedan. The project data set includes both versions for a total of 8 sub-configurations while the EPA guide data provide 5 sub-configurations.

C. Data Fields and Data Set Configuration

For this task, 93 variables were deemed necessary to conduct the analyses for this project. The variables collected for the task are provided in Table V with a brief description and source(s) for each. The data set is configured as a 1358-row (vehicle model) and 93-column (vehicle attribute) array.

Table V: Vehicle Attribute Data Fields

Attribute	Description/Notes	Source
Manufacturer	Manufacturer of record	Manufacturer, [52]
Brand		Manufacturer
Model		Manufacturer
Vehicle Platform	Manufacturer's platform name/code	Manufacturer
Product Cycle Year	1 = launch year of model/body configuration, 2 = second year, etc.	Manufacturer, [55]
EPA Classification	Passenger car or light truck	[52], [53]
EPA Vehicle Class	Vehicle class as defined by the EPA (17 classes)	[52]
Consumer Reports Segment	Vehicle segment as defined by Consumer Reports	[55], CONTROLTEC
Ward's Automotive Segment	Vehicle Segment as defined by Ward's Automotive	[56], CONTROLTEC
Vehicle Type	Vehicle type as defined by CONTROLTEC; Sedan, Coupe, Coupe Convertible, Hatchback, Wagon, SUV, Van, Pickup	CONTROLTEC
Number of Occupant Doors		Manufacturer
Cab type	Pickup trucks; regular, extended, crew	Manufacturer
Occupant Seating		Manufacturer
Length		Manufacturer
Width	Overall width without mirrors	Manufacturer
Height	Overall height at default ride height	Manufacturer
Wheelbase		Manufacturer
Front Track		Manufacturer
Rear Track		Manufacturer
Cargo Bed Length	Pickup trucks only	Manufacturer
Road/Ground Clearance	Clearance between road and vehicle underbody or axle	Manufacturer
Fuel Capacity	Capacity of liquid or gaseous fuels	Manufacturer
Battery Capacity	Capacity of the battery for electrified vehicles	Manufacturer
Battery Type/Chemistry	Battery type for electrified vehicles; e.g., Li-ion, Ni-MH	Manufacturer, [52]
Curb Weight	Weight of vehicle with full tank of fuel	Manufacturer, [54], [55]
Equivalent Test Weight	Test weight for fuel economy testing	[53], [54]
Front Weight Distribution	Percent of curb weight on the front tires	Manufacturer, [54]
Rear Weight Distribution	Percent of curb weight on the rear tires	Manufacturer, [54]
3-Term Total Road Load Coefficients	Polynomial coefficients used to describe road load force as a function of vehicle speed. Coefficients represent the constant, the vehicle speed term, and the vehicle speed squared term.	[53], [54]
Aerodynamic Drag Coefficient	Cd, dimensionless	Manufacturer
Aerodynamic Frontal Area	Projected frontal area of the vehicle. Typically ~85% of width x height	Manufacturer
Aerodynamic Effective Frontal Area	CdA. The product of drag coefficient and aerodynamic frontal area.	Manufacturer

Table V: Vehicle Attribute Data Fields (continued)

Attribute	Description/Notes	Source
Front Tire Width	Width of the tread	Manufacturer
Front Tire Aspect Ratio	The ratio of the sidewall to the tread width	Manufacturer
Front Tire Speed Rating	Letter rating representing the tire maximum vehicle speed	Manufacturer
Front Tire Load Rating	Numeric rating for the tire maximum load	Manufacturer
Front Tire Cold Inflation Pressure	Recommended inflation pressure	Manufacturer
Rear Tire Width	Width of the tread	Manufacturer
Rear Tire Aspect Ratio	The ratio of the sidewall to the tread width	Manufacturer
Rear Tire Speed Rating	Letter rating representing the tire maximum vehicle speed	Manufacturer
Rear Tire Load Rating	Numeric rating for the tire maximum load	Manufacturer
Rear Tire Cold Inflation Pressure	Recommended inflation pressure	Manufacturer
Front Wheel Diameter		Manufacturer
Rear Wheel Diameter		Manufacturer
Wheel Material		Manufacturer
Spare Tire Configuration	full-size, compact, run-flat, inflator kit	Manufacturer
Front Brake Type	disc, drum	Manufacturer
Front Brake Size	Diameter of disc or drum	Manufacturer
Rear Brake Type	disc, drum	Manufacturer
Rear Brake Size	Diameter of disc or drum	Manufacturer
Suspension/Chassis Configuration	Description of suspension/chassis	Manufacturer
Power Source Type	Source of tractive power; spark ignition (SI), Compression Ignition (CI), SI-Electric Hybrid (SI-E), Electric (E)	Manufacturer
Number of Engine Cylinders		Manufacturer
Engine Cylinder Arrangement	inline, opposed, V, W	Manufacturer
Engine Displacement		Manufacturer
Cylinder Block Material		Manufacturer
Cylinder Head Material		Manufacturer
Engine Aspiration	natural, turbocharged, supercharged	Manufacturer
Engine Fuel System	port, direct	Manufacturer
Fuel Type	gasoline, Diesel, CNG	Manufacturer
Compression Ratio		Manufacturer
Exhaust Gas Recirculation	yes/no indicator variable	Manufacturer
Lean Combustion	yes/no indicator variable	Manufacturer
Variable Valve Timing	yes/no indicator variable	Manufacturer
Variable Valve Lift	yes/no indicator variable	Manufacturer
Atkinson Cycle	yes/no indicator variable	Manufacturer
Cylinder Deactivation	yes/no indicator variable	Manufacturer
Engine Maximum Power		Manufacturer
Engine Maximum Power Speed		Manufacturer
Engine Maximum Torque		Manufacturer
Engine Maximum Torque Speed		Manufacturer

Table V: Vehicle Attribute Data Fields (continued)

Hybrid Configuration	Basic architecture of the electric hybrid system; e.g., belt starter generator, parallel P2, parallel-series, etc.	Manufacturer
Motor/Generator Rated Power		Manufacturer
Launch Device	torque converter, clutch, motor	Manufacturer
Transmission	traditional automatic, automatic dual clutch, automatic single clutch, belt/pulley CVT, e-CVT, manual single clutch	Manufacturer
Number of Step Ratios	Number of fixed ratios in the transmission. Not applicable to CVTs	Manufacturer
Transmission Configuration	transaxle, transmission	Manufacturer
Drivetrain	FWD, RWD, AWD, 4WD	Manufacturer
Driveline Architecture	Engine and driveline layout; e.g., front engine, front wheel drive, front engine rear wheel drive	Manufacturer
Power Steering Assist	hydraulic, electro-hydraulic, electric	Manufacturer
Stop-Start	yes/no indicator	Manufacturer
Unadjusted Combined Fuel Economy	55%/45% harmonic average of the city (FTP) and highway (HWFET) fuel economy test results	[52]
Unadjusted Combined CO_2	Tailpipe CO_2 emissions computed from the unadjusted combined fuel economy using the appropriate CO_2 volume density values	CONTROLTEC
0-30 mph Acceleration Time	Acceleration to 30 mph from a stop assuming full engine/motor power	Manufacturer
0-60 mph Acceleration Time	Acceleration to 60 mph from a stop assuming full engine/motor power	Manufacturer
¼ mile Acceleration Time	Acceleration to the ¼ mile from a stop assuming full engine/motor power	Manufacturer
¼ mile Acceleration Speed	Vehicle speed at the end of the ¼ mile	Manufacturer
Top Speed	Maximum achievable vehicle speed	Manufacturer
Top Speed Control	Method limiting the maximum achievable vehicle speed; governed, tire-limited, drag-limited, engine speed-limited	Manufacturer
Payload	Maximum added load	Manufacturer
Towing Capacity	Maximum trailer weight without an optional towing package	Manufacturer

D. Data Collection

The data collection began by acquiring all of the available data from the manufacturer's sources. These data included vehicle dimensions, curb weight, powertrain specifications, and vehicle performance (i.e., towing, acceleration, top speed). The reporting frequency varied considerably depending upon the attribute. Nearly every manufacturer provided key dimensions, curb weight, and powertrain specifications while other attributes and performance parameters such as aerodynamic drag and acceleration performance had a reporting frequency of less than 50%.

Next, non-mass vehicle load information, in the form of 3-term road load coefficients, was obtained from the MY 2014 EPA Test Car List [53] and certification documents [54]. In addition to the 3-term road load coefficients, the MY 2014 EPA Test Car List was the key source for equivalent test weight (ETW). The EPA Fuel Economy Guide file [52] was the primary source of information for the

unadjusted fuel economy. Carbon dioxide emissions were calculated from the unadjusted combined fuel consumption data by assuming CO_2 density values of 8887 g/gallon, 10180 g/gallon, and 6765 g/gallon equivalent for gasoline, diesel, and compressed natural gas (CNG), respectively.

Additional information for curb weight, powertrain attributes, and energy storage were obtained from the manufacturer's certification applications [54]. As with the road load information, the reporting was inconsistent among manufacturers. Where available, independent mass measurements were added from Consumer Reports [55] to corroborate the manufacturer reported information. To support the vehicle and subsystem classification assessments the EPA vehicle class, Consumer Reports vehicle segment, and Ward's vehicle segment were mapped to each vehicle.

E. Data Quality Assurance

In addition to conducting manual data entry checks and cross-references, three methods of data quality assurance were employed: plausibility, redundancy, and fundamental correlation. Data found to be out of range were investigated and either corrected or eliminated if an alternate data source was not available.

Plausibility checks are used to determine if any of the variables are beyond a reasonable range, given knowledge of the vehicle and powertrain attributes. The following plausibility checks were performed:

- Road clearance vs. vehicle type
- Aerodynamic drag coefficient (C_d) vs. vehicle type
- Engine displacement per cylinder
- Engine compression ratio vs. combustion type (spark-ignition, compression ignition), aspiration (natural, turbocharged, supercharged), and fuel system (port, direct)
- Engine specific power (power/displacement) vs. combustion type (spark-ignition, compression ignition, aspiration (natural, turbocharged, supercharged), and fuel system (port, direct)
- Engine specific torque (torque/displacement) vs. combustion type (spark-ignition, compression ignition), aspiration (natural, turbocharged, supercharged) and fuel system (port, direct)

Redundancy checks involve comparing two variables that measure or describe the same or related attribute. The variables can be numeric or text. Regarding numeric metrics, these should yield a linear correlation and significant deviation from linearity would indicate suspect data. For this task, the following redundancy checks were performed:

- Front track vs. rear track
- Front brake diameter vs. rear brake diameter
- Front weight distribution vs. rear weight distribution
- Consumer Reports reported curb weight vs. manufacturer reported curb weight
- Curb weight vs. equivalent test weight class
- Equivalent test weight class reported vs. test weight class determined from manufacturer reported curb weight

Fundamental correlations involve plotting two variables that are physically correlated although not necessarily in a linear fashion. In some cases, fundamental correlations are non-linear redundant measures. For this task, the following fundamental correlations were performed:

- Overall width vs. overall length
- Overall height vs. overall length
- Wheelbase vs. overall length
- Vehicle area (length x width) vs. vehicle footprint (wheelbase x average track)
- Curb weight vs. vehicle cubic volume (length x width x height) vs. vehicle type
- Fuel tank capacity vs. curb weight
- Battery capacity vs. curb weight (by hybrid type and electric vehicles)
- Aerodynamic frontal area (C_dA) vs. square frontal area (width x height)
- Tire diameter vs. vehicle cubic volume (length x width x height)
- Tire diameter vs. curb weight
- Tire load rating vs. curb weight
- Road force (at fixed speed) vs. curb weight
- Engine specific power (power/displacement) vs. rated power speed (by aspiration)
- Engine specific power (power/displacement) vs. boost level (turbocharged, supercharged)
- Engine specific torque (torque/displacement) vs. rated torque speed (by aspiration)
- Motor power vs. curb weight (by hybrid type and electric vehicles)
- Acceleration performance vs. curb weight-to-power ratio

The graphical results for each of these quality assessments are provided in Appendix A.

F. Vehicle Data Set

The vehicle data set is available as a separate file using the following naming convention:

Contract_13_313_MY2014_Vehicle_Data_Set_v*x.x_ddmmmyy*.xlsx

where,

vx.x represents the version number (e.g., v1.0)
ddmmmyy represents the date of release (e.g., 01jul14)

The file is provided in a Microsoft Excel file format in both SI and English units.

5. CROSS REFERENCE VEHICLE CONFIGURATION DATA WITH NON-MASS LOAD REDUCTION TECHNOLOGIES

To support the goals of the research project [3], it was necessary to identify those vehicles in the baseline data set that are currently utilizing non-mass load-reduction technologies or designs with specific focus on aerodynamic drag reduction and improved tire rolling resistance.

Vehicles utilizing non-mass load-reduction attributes will be identified by two methods; 1) determining the aerodynamic efficiency and tire rolling resistance for each vehicle and 2) cross-referencing the results of the literature review with the data set. The aerodynamic efficiency and tire rolling resistance provide a method of identifying best-in-class vehicles. The cross-referenced data set will specify the load-reduction technologies and/or characteristics that the best-in-class vehicles are using (e.g., active grille shutters, underbody panels, low rolling resistance tires).

A. Background

Non-mass load is represented by the forces acting on the vehicle at constant speed and include aerodynamic drag, tire rolling resistance, brake drag, and hub drag. These forces account for approximately 60% of the vehicle load over the combined city and highway drive cycles required for certification of tailpipe CO_2 emissions for the United States (US) market.

For purposes of vehicle certification, these non-mass loads are typically determined by coasting the vehicle in neutral and, from the resulting speed-time data, calculating the force as a function of vehicle speed [59] [60]. The road load force resulting from a coastdown test is comprised of forces from the systems noted earlier, plus the drag due to the transmission and driveline (collectively, the drivetrain):

$$F_{total} = F_{aero} + F_{tires} + F_{brakes} + F_{hubs} + F_{drivetrain} \quad (1)$$

The drivetrain drag is not, technically, part of the vehicle's actual road load force; it is present due to the test methodology. The transmission and driveline neutral drag are factored out when the chassis dynamometer set coefficients are established at the time of the fuel economy testing. An example of road load force decomposition is shown graphically in figure 1.

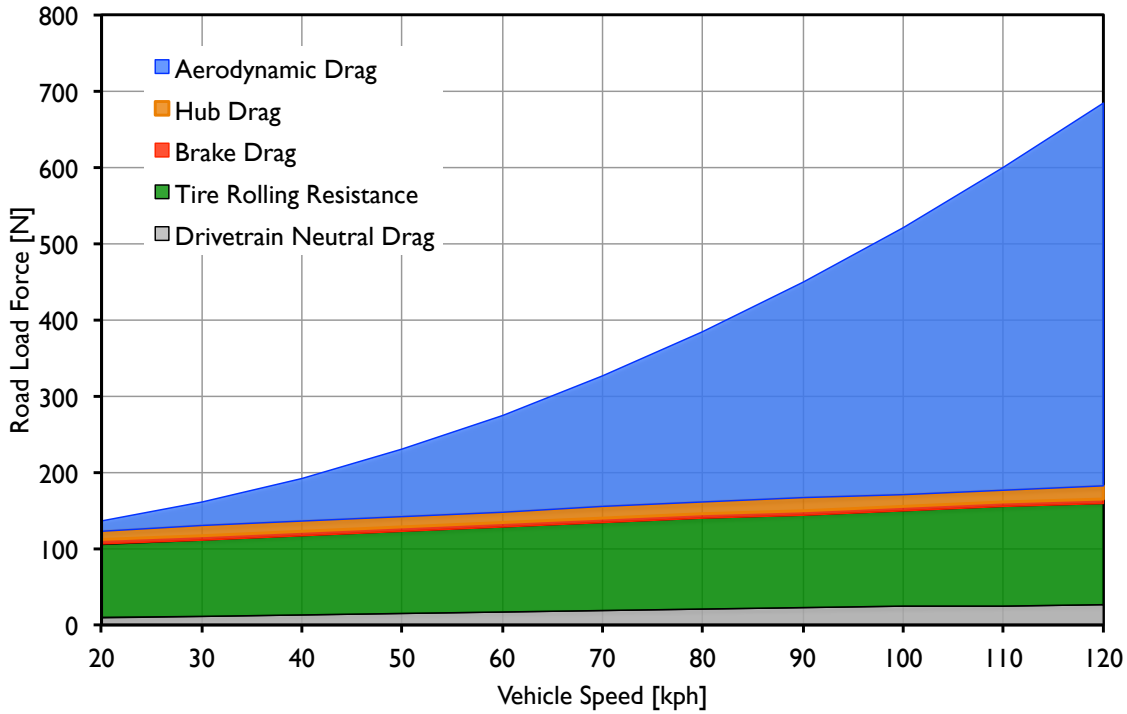

Figure 1: Road Load Force vs. Vehicle Speed.

The road load force resulting from the coastdown test is expressed as a second order polynomial:

$$F_{total} = A + Bv + Cv^2 \quad (2)$$

where:

F_{total} = total road load force
v = vehicle speed
A, B, C = regression coefficients

Road load coefficients are reported in the Environmental Protection Agency (EPA) Test Car List [53] and certification applications [54] and can be used to estimate the individual road load elements. The method of decomposing this data for the current research is described in the following sections.

While the basis of the road load values are assumed to be from a coastdown test, a manufacturer may use any method that yields an equivalent result [61] [62]. Consequently, due to the large number of configurations that can be represented on a single model, a fraction of road load values are likely a combination of test bench, aerodynamic drag, and actual coastdown data or are analytically derived without coastdown testing. The EPA uses the SAE International (SAE) J2263 standard [60] for confirmatory coastdown testing [62].

B. Aerodynamic Drag

Aerodynamic drag represents approximately 20% of the vehicle load for the US city cycle (FTP 75) and approximately 50% of the vehicle load for the US highway cycle (HWFET). The force contribution of the aerodynamic drag is expressed as:

$$F_{aero} = \frac{1}{2} \rho C_d A v^2 \quad (3)$$

where:

ρ = air density
C_d = coefficient of drag of the vehicle
A = frontal area of the vehicle
v = vehicle speed

From this equation, the product of the coefficient of drag (C_d) and frontal area, C_dA, is often used to express the aerodynamic drag of a vehicle. The frontal area is the orthogonal projection of the vehicle including tires and suspension components onto a plane perpendicular to the longitudinal axis of the vehicle [59]. The frontal area is a function of the width and height of the vehicle and is influenced by vehicle task (e.g., van, sedan) and design cues. The coefficient of drag is a measure of aerodynamic efficiency and is, therefore, the most appropriate metric for the current research.

Approximately 50% of the vehicle models had a C_d value reported by the manufacturer. These values are shown graphically in figure 2 as a function of vehicle type. Additionally, table VI provides key statistics for manufacturer-reported C_d. The C_d is dependent upon a number of factors, most of which are not quantifiable by vehicle specifications alone. The C_d can be determined from fluid dynamics modeling, full-scale and fractional-scale wind tunnel testing, or evaluation of coastdown data. For the manufacturers that reported C_d, the method to generate the value is not known. However, even if all of the reported C_d values were generated from full-scale wind tunnel testing, the values cannot be directly compared without knowledge of the wind tunnel configurations as facility-to-facility differences will yield different values for the same vehicle [63] [64] [65]. Consequently, for this research, a consistent method is required to estimate the C_d for every vehicle in the data set.

Certification testing for fuel economy and tailpipe CO_2 emissions requires a set of road load coefficients (eq. 2) for every vehicle model and sub-configuration. Therefore, generating the C_d from these coefficients is the only viable option of assessing all of the vehicles in the research data set.

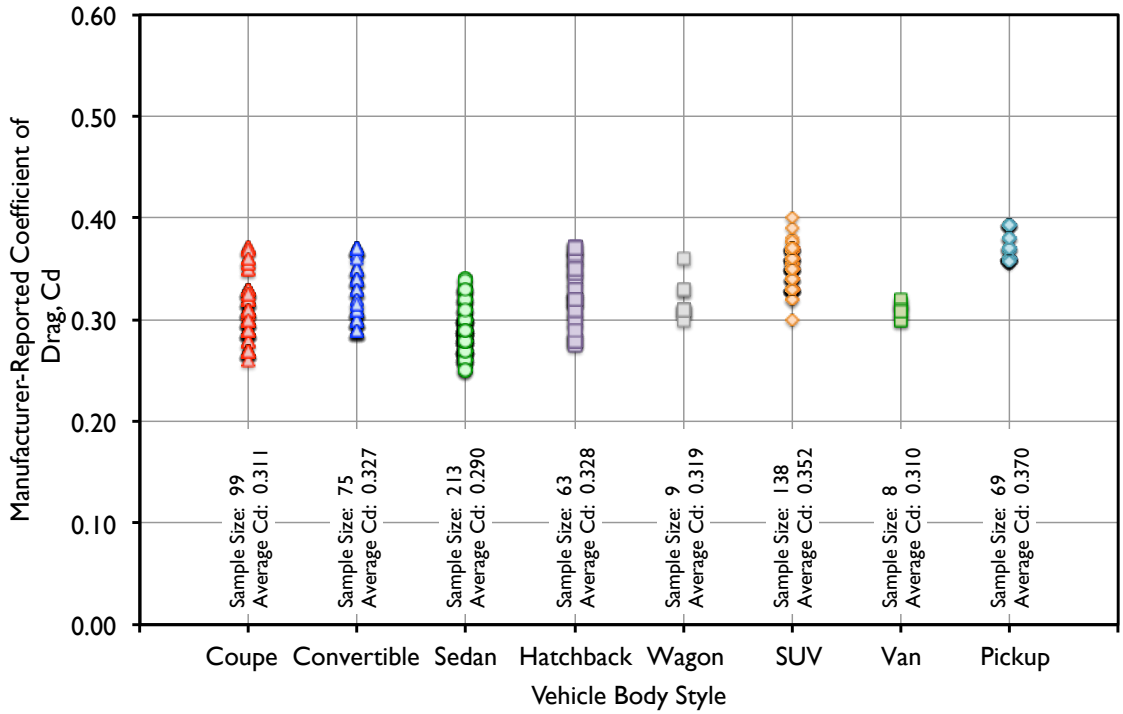

Figure 2: Manufacturer-Reported C_d vs. Vehicle Type.

Table VI: Manufacturer-Reported C_d Statistics vs. Vehicle Type.

Body	Sample Size	Average C_d	Min. C_d	99th Percentile C_d	95th Percentile C_d	90th Percentile C_d	Max. C_d
Coupe	99	0.311	0.260	0.270	0.270	0.270	0.372
Convertible	75	0.327	0.290	0.290	0.290	0.290	0.370
Sedan	213	0.290	0.250	0.250	0.260	0.260	0.340
Hatchback	63	0.328	0.275	0.278	0.280	0.280	0.372
Wagon	9	0.319	0.300	0.301	0.304	0.308	0.360
SUV	138	0.352	0.300	0.320	0.330	0.330	0.400
Van	8	0.310	0.300	0.300	0.300	0.300	0.320
Pickup	69	0.370	0.357	0.357	0.360	0.360	0.394

C. Method of Estimating the Coefficient of Drag

The C_d can be computed by rearranging equation 3:

$$C_d = F_{aero}/(\tfrac{1}{2}\, \rho\, A\, v^2) \qquad (4)$$

To solve for C_d, frontal area and the force due to aerodynamic drag are required. The frontal area is the projected area in the airstream and will be less than the product of width and height. Within the MY 2014 data set, the frontal area was reported for 98 vehicle models (~7%), consequently, an

estimated value is required for this research. Frontal area is commonly estimated as a fraction of the product of width and height:

$$A_{estimated} = c \times W_{vehicle} \times H_{vehicle} \quad (5)$$

where:

$A_{estimated}$ = estimated frontal area
c = multiplier, ≤ 1
$W_{vehicle}$ = vehicle width
$H_{vehicle}$ = vehicle height

The SAE J1263 procedure [59] recommends a value of 0.8 for c when the frontal area is not known. However, this method does not allow for the underbody flow area, which will vary from vehicle-to-vehicle based on ground clearance, track, and tire width. CONTROLTEC has evaluated published values for frontal area and uses the following equation to estimate this attribute:

$$A_{estimated} = c \times [(W_{vehicle} \times H_{vehicle}) - ((T_{front} - W_{tire}) \times H_{road})] \quad (6)$$

where:

$A_{estimated}$ = estimated frontal area
c = multiplier, ≤ 1
$W_{vehicle}$ = vehicle width
$H_{vehicle}$ = vehicle height
T_{front} = front track
W_{tire} = tire width
H_{road} = road clearance

CONTROLTEC uses a multiplier value, c, of 0.918. For the model year 2014 vehicles with a reported frontal area, equation 6 accounted for 98.7% of the variation among the vehicles (i.e., estimated versus actual R^2 = 0.987). As shown in figure 3, CONTROLTEC's method provides a much more accurate value when compared to the SAE J1263 recommendation.

The second variable required for estimating the C_d (eq. 4) is the aerodynamic drag force. This force can be calculated by subtracting the mechanical elements from the total road load force:

$$F_{aero} = F_{total} - (F_{tires} + F_{brakes} + F_{hubs} + F_{drivetrain}) \quad (7)$$

Since the mechanical forces are not known for the vehicles in the data set, CONTROLTEC has developed an alternate method of estimating aerodynamic drag force. Consider the derivative of road load force with vehicle speed:

$$dF_{total}/dv = dF_{aero}/dv + dF_{tires}/dv + dF_{brakes}/dv + dF_{hubs}/dv + dF_{drivetrain}/dv \quad (8)$$

From equation 2:

$$dF_{total}/dv = (B + 2\,Cv) \tag{9}$$

At higher speeds (>100 kph), aerodynamic drag is the largest contributor to the total road load force and dF_{total}/dv is dominated by dF_{aero}/dv. The change in aerodynamic force with vehicle speed is computed from the derivative of equation 3:

$$dF_{aero}/dv = \rho C_d A v \tag{10}$$

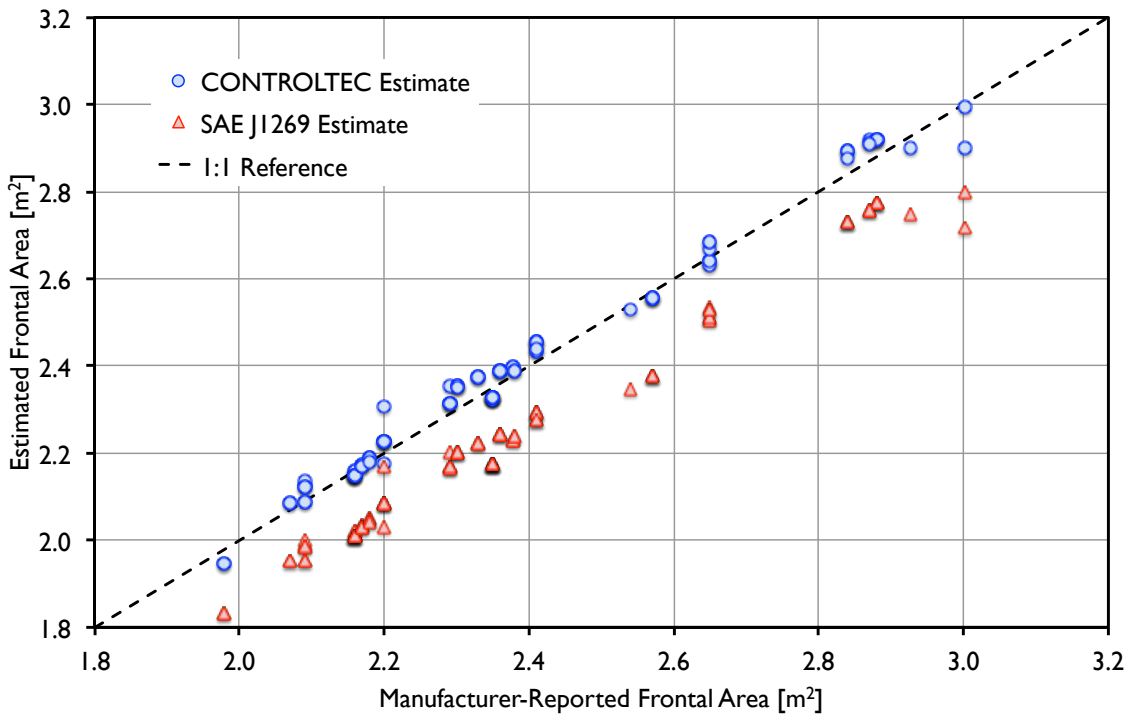

Figure 3: Estimated Frontal Area vs. Manufacturer-Reported Frontal Area.

Tire rolling resistance is the next highest contributor to the total road load force at higher speeds and also increases as a function of speed. The change in tire force with speed can be determined from the SAE procedure J2452 [66]. The result of this procedure is a 5-term equation for rolling resistance as a function of speed, load, and tire pressure:

$$F_{tire} = P^{\alpha}\, L^{\beta} \times (a + bv + cv^2) \tag{11}$$

where:

F_{tire} = tire rolling force
P = tire pressure
α = tire pressure exponent
L = tire load
β = tire load exponent
v = vehicle speed
a, b, c = regression coefficients

Therefore, the derivative of tire force can be expressed as:

$$dF_{tire}/dv = P^{\alpha} L^{\beta} \times (b + 2cv) \quad (12)$$

To evaluate the magnitude of dF_{tire}/dv, SAE J2452 test results are required. While not commonly published, examples are available in technical literature [67] [68].

To compare typical levels of dF_{aero}/dv and dF_{tire}/dv, values were computed for several combinations of mass, C_d, and frontal area at 110 kph. The results are provided in table VII. As shown, dF_{aero}/dv is more than an order of magnitude greater than dF_{tire}/dv.

Table VII: Example of dF_{aero}/dv and dF_{tire}/dv at 110 kph.

Example	Mass [kg]	C_d [-]	A [m^2]	dF_{aero}/dv [N/kph]	dF_{tire}/dv [N/kph]
Mid-size Sedan	1500	0.32	2.3	7.29	0.54
Mid-size SUV	2100	0.38	3.0	11.29	0.76
Large Pickup	2300	0.45	3.2	13.95	0.84

J2452 coefficients: α = -0.4815, β = 1.0051, a = 6.82E-2, b = 2.32E-4, c = 1.20E-6, P =240 kPa [67]

The brake, hub, and driveline drag forces are significantly smaller in magnitude than the aerodynamic drag and tire rolling resistance and, therefore, the derivatives are assumed to be negligible at higher vehicle speeds when compared to dF_{aero}/dv and dF_{tire}/dv. Based on these assumptions, equation 8 becomes:

$$dF_{total}/dv \approx dF_{aero}/dv + dF_{tires}/dv \quad (13)$$

Since dF_{tires}/dv is an order of magnitude smaller than dF_{aero}/dv, then equation 13 can be further simplified to:

$$dF_{aero}/dv \approx c \times (dF_{total}/dv),\ v > 100 \text{ kph} \quad (14)$$

The multiplier, c, will be a value equal to or less than 1 and represents the fraction of dF_{total}/dv associated with dF_{aero}/dv. Combining equations 9, 10, and 14 yields:

$$\rho C_d A v \approx c \times (B + 2\,Cv),\ v > 100 \text{ kph}$$

rearranging,

$$C_d A = c \times (B + 2Cv)/v\rho,\ v > 100 \text{ kph} \qquad (15)$$

For this research, CONTROLTEC used a value of 0.94 for c and evaluated dF_{total}/dv between 105 kph and 115 kph. The value for c was generated from an evaluation similar to that shown in table VII. The potential errors with this approach to estimating C_d include the evaluation of frontal area, dF/dv assumptions, and coastdown test issues [69], however, the only alternative is to measure C_d in the same wind tunnel for every vehicle in the data set, which is beyond the scope of this study.

While the C_d computed from this method may not agree with manufacturer reported values, the authors believe that it is a valid proxy for assessing the aerodynamic drag force contribution to a coastdown test, which is an important element of the vehicle fuel economy and tailpipe emissions certification process.

An alternative, and commonly used approach for estimating C_dA from coastdown testing, is to assume that the C-coefficient (eq. 2) is entirely the result of aerodynamic drag [70] [71]. However, as noted in equation 11, the C-coefficient will also contain v^2 elements associated with tire rolling force. It will be shown in the aerodynamic results section that using the C-coefficient alone to represent aerodynamic drag results in C_d values that are not plausible.

D. Aerodynamic Drag Results

Figure 4 provides the estimated C_d as a function of vehicle type. In general, the lower C_d bound is comparable to figure 2, while the upper C_d bound is higher. This result is not unexpected, as manufacturers may not report vehicles with poor or uncompetitive C_d values.

Figure 5 shows the estimated C_d values as a function of the manufacturer-reported C_d values for 674 vehicles. The estimated C_d values correlate (statistically significant) with the manufacturer-reported values. However, significant variation exists ($R^2 = 0.57$) and the estimated C_d values average 0.016 (~4%) higher than the reported C_d.

Regarding the variation, vehicle manufacturers report the C_d from a variety of sources, which will result in differences in reported levels. As noted earlier, wind tunnel correlations have yielded different C_d values for the same vehicle [63] [64].

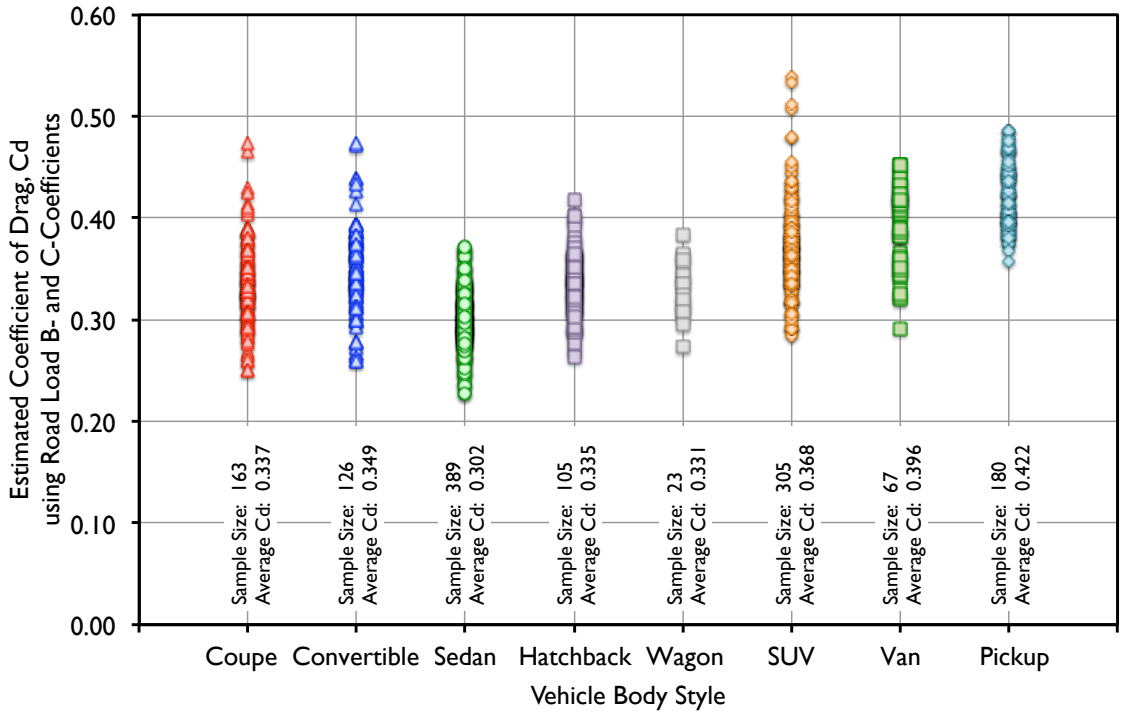

Figure 4: CONTROLTEC Estimated C_d vs. Vehicle Type.

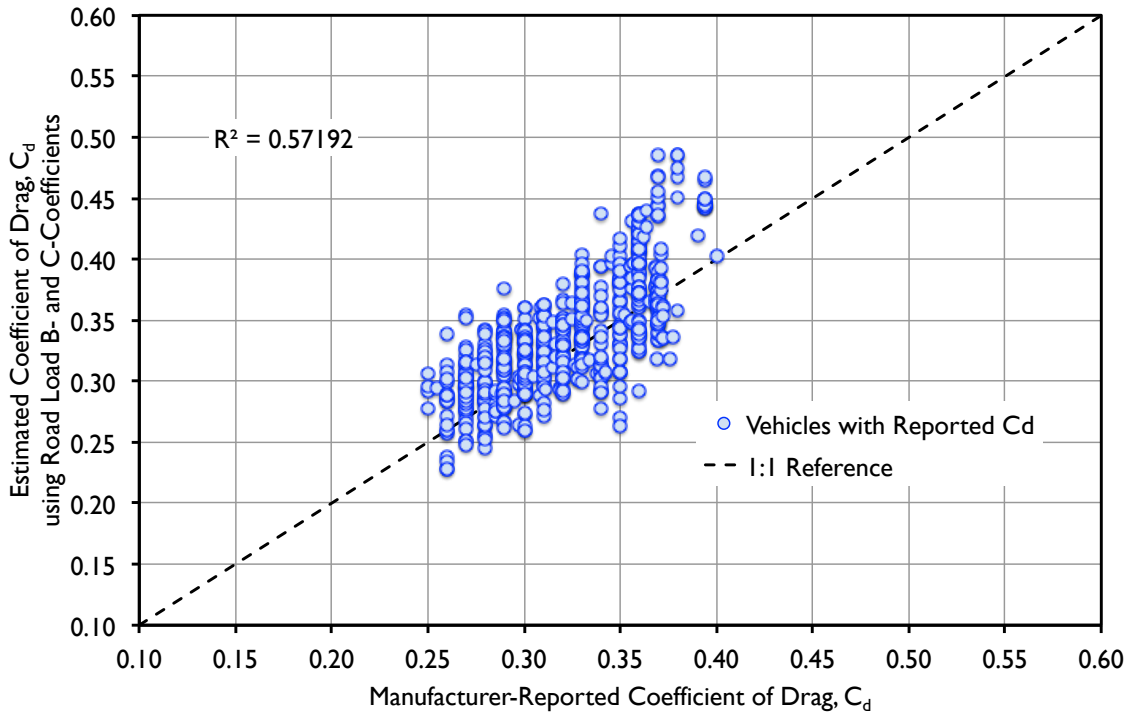

Figure 5: CONTROLTEC Estimated C_d vs. Manufacturer-Reported C_d.

With respect to the offset, the authors believe that this is, in part, due to the dynamic C_d values (rotating tires, vehicle-to-ground speed difference) that will result from the evaluation of a coastdown test. It is expected that the majority of reported C_d values are from static measurements, meaning that the tires are not rotating and the vehicle is not moving relative to the ground. Studies [72] [73] suggest that C_d values generated from a dynamic wind tunnel and on-road tests will be higher than those derived from static wind tunnel testing. Further, road derived C_d may also be influenced by road surface roughness.

As noted earlier, a common method used to estimate C_d is to assume that the C-coefficient from the coastdown test (eq. 2) is entirely the result of aerodynamic drag [70] [71]. As shown in figure 6, applying this assumption yields significantly greater scatter than the CONTROLTEC method, resulting in a lower correlation coefficient (R^2 = 0.38 vs. R^2 = 0.57). Further, this method yields implausible results as indicated by C_d values below 0.20.

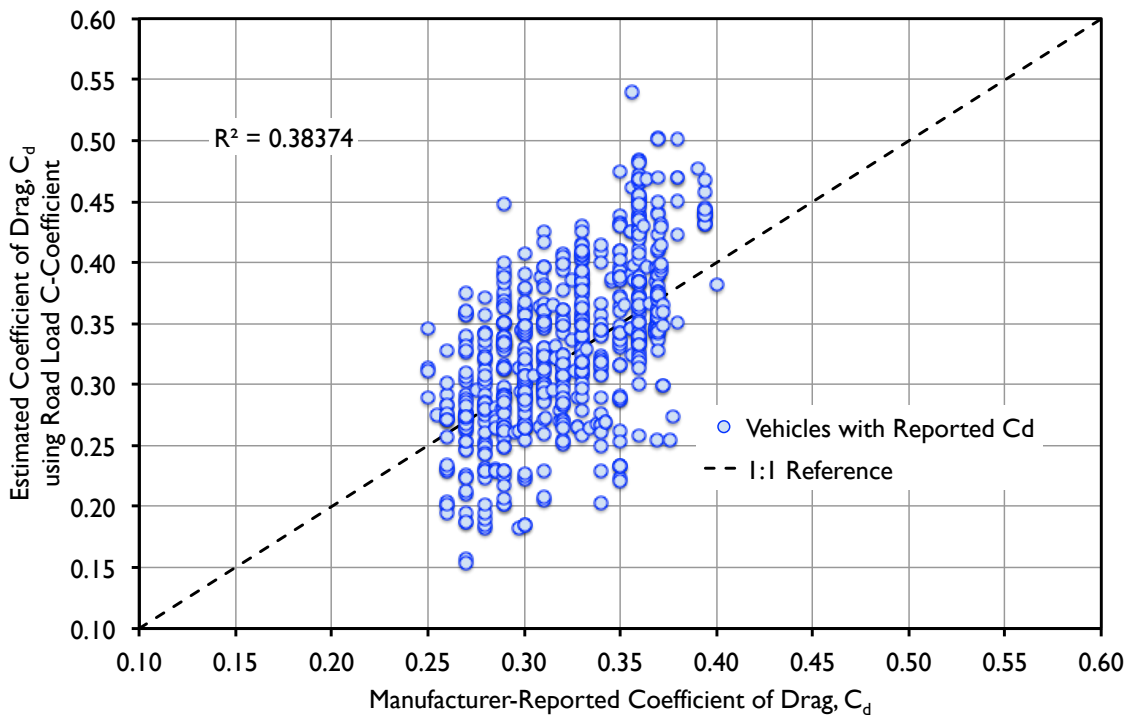

Figure 6: Estimated C_d from Road Load C-Coefficient vs. Manufacturer-Reported C_d.

E. Best-in-Class Aerodynamic Drag

The vehicles in the data set were classified by vehicle body type to determine the best-in-class C_d. Figures 7 through 13 provide the distribution of estimated C_d for each vehicle type. Evaluation of these distributions was necessary to establish the best-in-class criteria.

Within certain vehicle types, it was desirable to sub-categorize by other attributes. In the coupe category the sports-oriented (2 or 2+2 seating) vehicles had an average C_d 0.02 (9%) higher than the standard 4/5-passenger coupes. The very highest C_d values within the coupe class were found on

high performance vehicles. These vehicles likely have aerodynamic features to minimize lift, which can be detrimental to C_d. However, not all of the high performance vehicles had a high C_d. Finally, although the Smart fortwo was classified as a coupe (as does Smart), its shape defies a clear categorization.

As proposed in the research plan, hatchbacks and wagons were to be treated as unique categories. However, as shown in figure 10, their distributions are very similar, suggesting that these two vehicle categories could be combined.

Within the van segment, the full-sized vans had, in all cases, higher C_d, averaging 0.42 while the minivans had an average C_d of just 0.34. This difference may be associated with the commercial focus of the full-size vans. Further, the full-size vans in the MY 2014 data set represent traditional designs that have not changed significantly in recent years. These vans are now being replaced by newer designs and, therefore, may not represent the full-size van class in future years. Two of these newer designs include the Ford Transit and the RAM Promaster. Neither of these vans were available as a light-duty vehicle in MY 2014. The Ford Transit van is now available in MY 2015 as a light-duty vehicle. The RAM Promaster is currently classified as a heavy duty vehicle.

To support the best-in-class proposal for van C_d, the dimensional information and road load coefficients were obtained for multiple configurations of these two vans. The estimated C_d, calculated using the methods described earlier, is 0.358 and 0.370 for the Ford Transit and RAM Promaster, respectively.

For pickup trucks, a review of cab and bed combinations did not yield a clear separation, in part due to the small sample sizes that result when the pickups are sub-divided into the separate cab/bed combinations. However, there was a small shift in the average C_d between rear wheel drive and all/four wheel drive trucks although the overall range of Cd was similar for both configurations as shown in figure 13.

Given the potential errors associated with evaluating the C_d (estimation of frontal area, dF/dv assumptions, and coastdown test issues), using the absolute lowest value to identify best-in-class for each segment is not recommended. Rather, the proposed approach was to select a reasonable subset of the data as best-in-class (e.g., 95th percentile). The percentiles for each vehicle type and sub-category are provided in table VIII. For this analysis, the lowest C_d was assigned to 100th percentile and the highest C_d was assigned the 0th percentile.

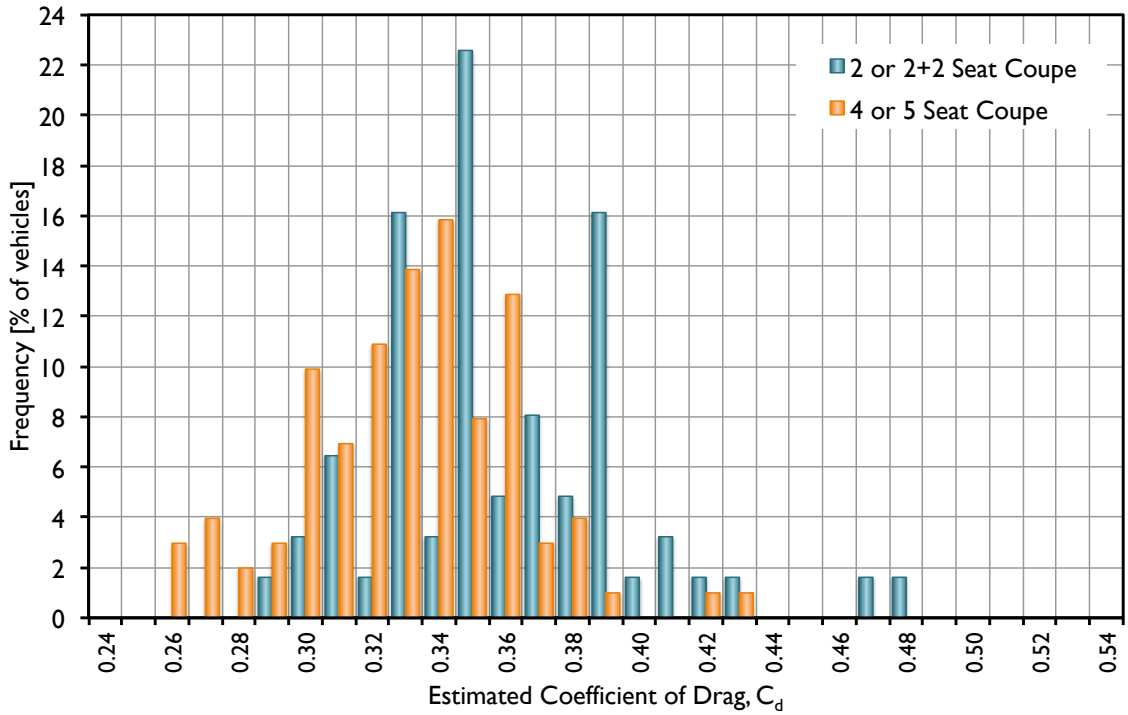

Figure 7: Distribution of Estimated C_d for Coupes.

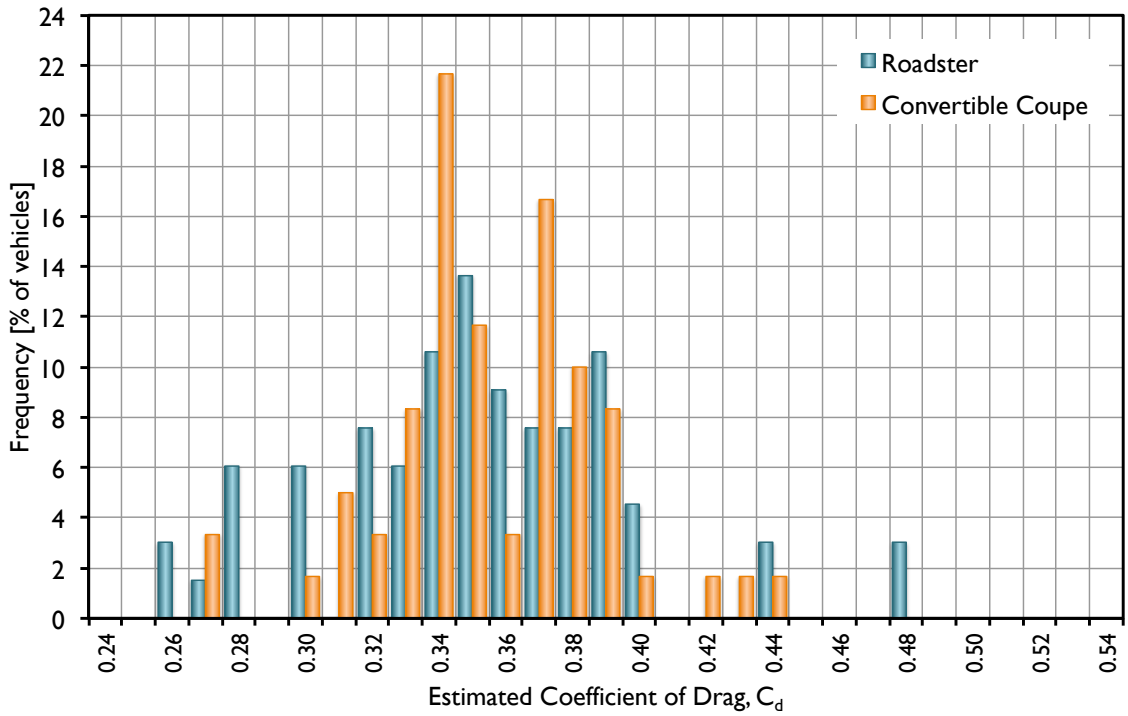

Figure 8: Distribution of Estimated C_d for Convertibles.

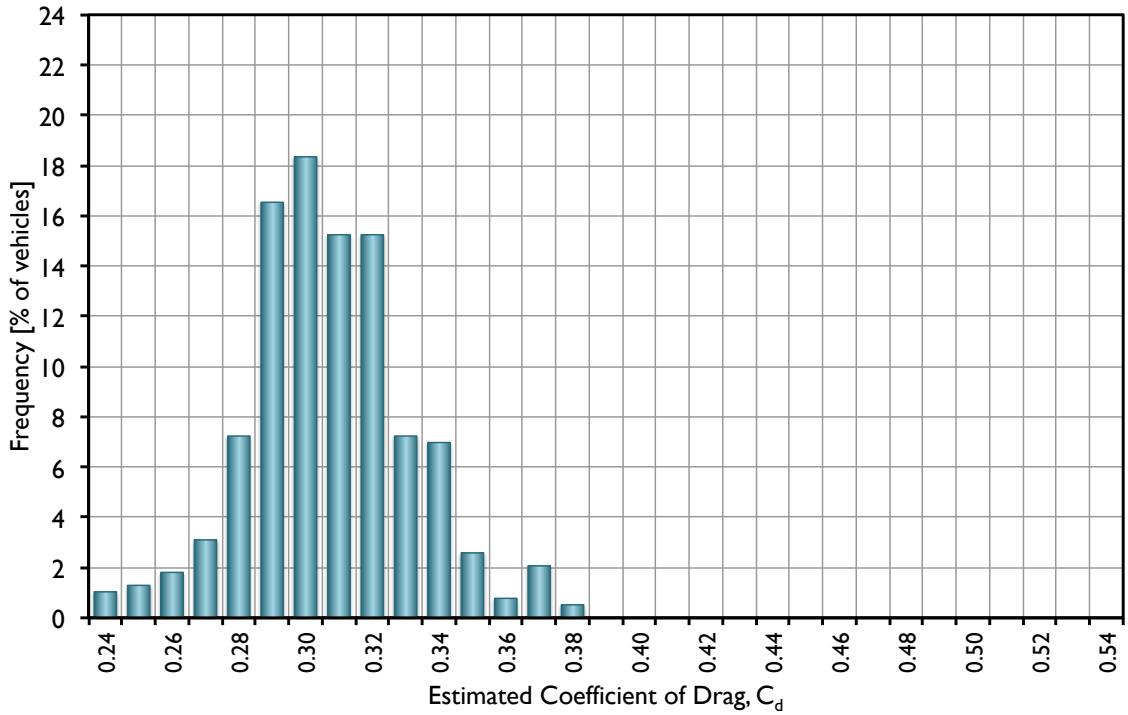

Figure 9: Distribution of Estimated C_d for Sedans.

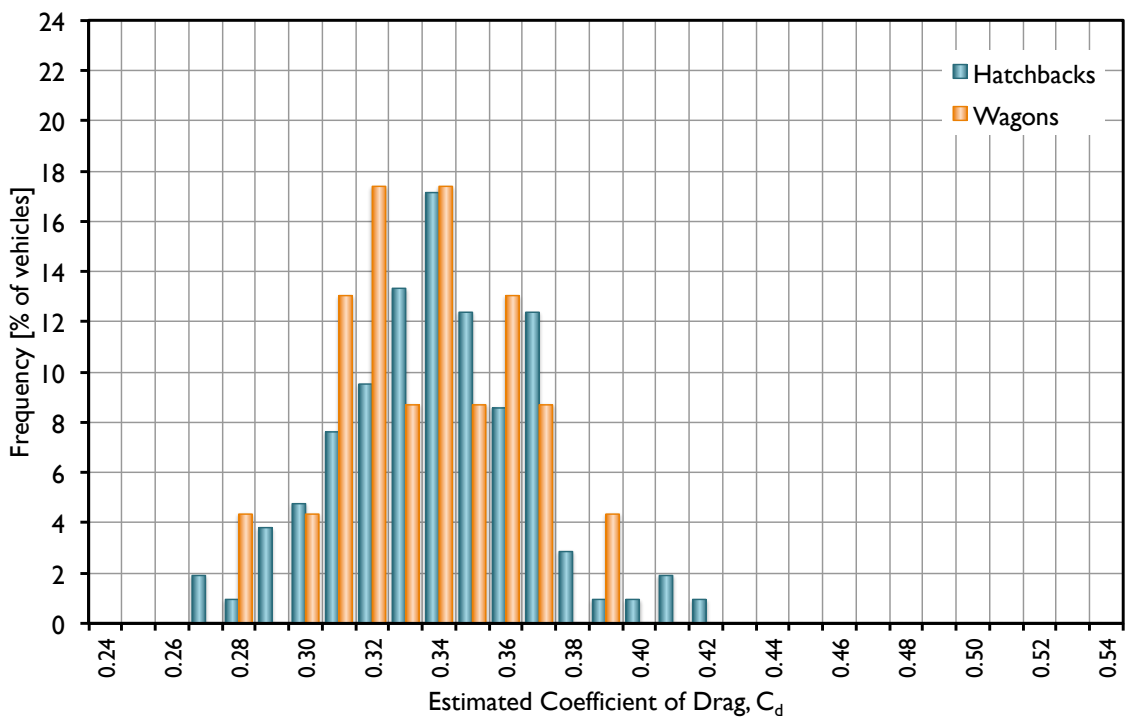

Figure 10: Distribution of Estimated C_d for Hatchbacks and Wagons.

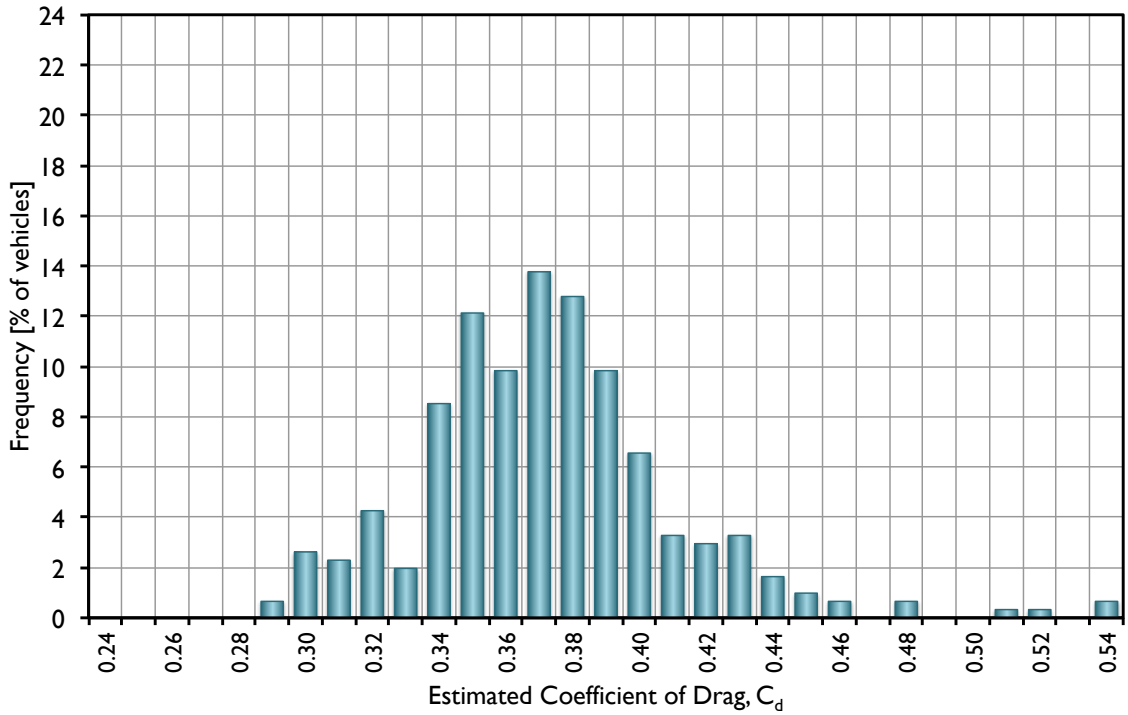

Figure 11: Distribution of Estimated C_d for SUVs.

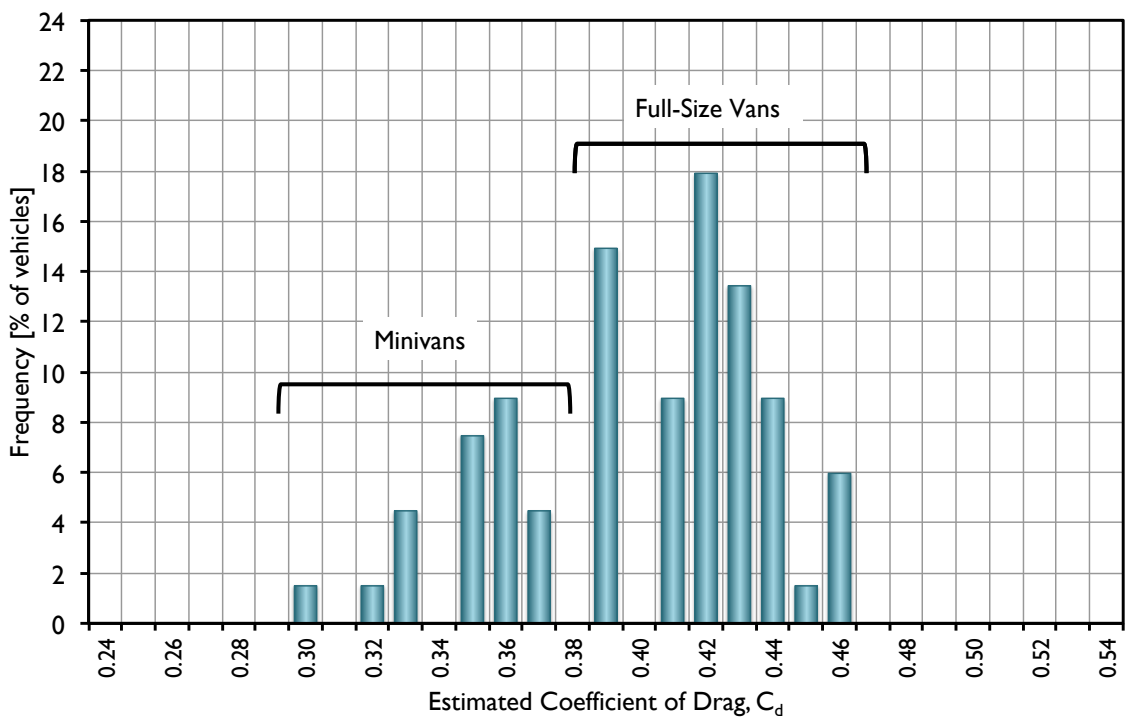

Figure 12: Distribution of Estimated C_d for Vans.

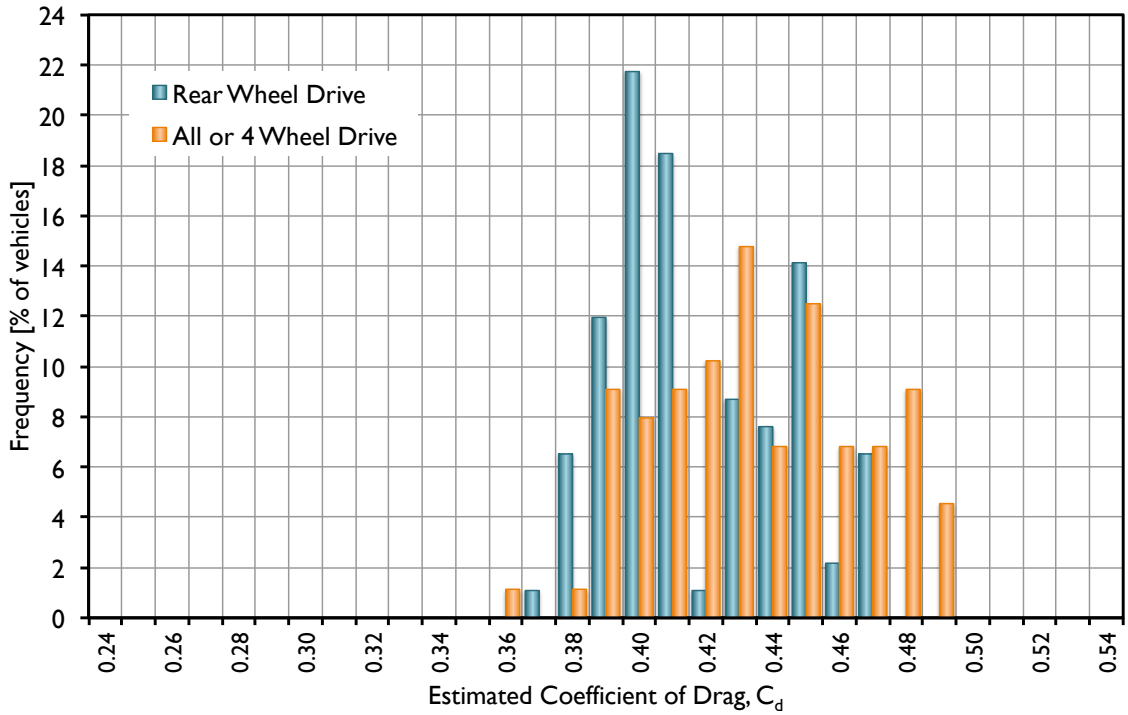

Figure 13: Distribution of Estimated C_d for Pickups.

Table VIII: Estimated C_d Percentiles vs. Vehicle Type and Subcategories.

Body	Sample Size	Average C_d	Min. C_d	99th Percentile C_d	95th Percentile C_d	90th Percentile C_d	Max. C_d
Coupe	163	0.337	0.251	0.256	0.280	0.293	0.474
2/2+2 Seat Coupe	*62*	*0.355*	*0.282*	*0.289*	*0.307*	*0.309*	*0.474*
4/5 Seat Coupe	*101*	*0.326*	*0.251*	*0.251*	*0.267*	*0.286*	*0.430*
Convertible	126	0.349	0.259	0.260	0.277	0.300	0.474
Roadster	*66*	*0.348*	*0.259*	*0.259*	*0.273*	*0.288*	*0.474*
Convertible Coupe	*60*	*0.350*	*0.267*	*0.267*	*0.302*	*0.311*	*0.440*
Sedan	389	0.302	0.228	0.237	0.262	0.274	0.372
Hatchback & Wagon	128	0.334	0.263	0.271	0.289	0.295	0.418
Hatchback	*105*	*0.335*	*0.263*	*0.270*	*0.289*	*0.293*	*0.418*
Wagon	*23*	*0.331*	*0.273*	*0.278*	*0.296*	*0.304*	*0.384*
SUV	305	0.368	0.284	0.291	0.307	0.322	0.539
Van	67	0.396	0.291	0.310	0.327	0.345	0.453
Minivan	*19*	*0.344*	*0.291*	*0.296*	*0.317*	*0.322*	*0.366*
Full-Size	*48*	*0.416*	*0.382*	*0.382*	*0.382*	*0.386*	*0.453*
Pickup	180	0.422	0.357	0.373	0.381	0.385	0.486
4x2 Pickups	*92*	*0.414*	*0.367*	*0.374*	*0.380*	*0.385*	*0.469*
4x4 Pickups	*88*	*0.430*	*0.357*	*0.373*	*0.383*	*0.389*	*0.486*

To assist in establishing an appropriate best-in-class percentile, the top vehicles in each class were reviewed to identify, if available, differences in manufacturer-reported and estimated C_d and the methods and technologies applied to achieve the aerodynamic performance.

The estimated C_d was, in some instances, better than the reported C_d for the most highly ranked vehicles, while poorly ranked vehicles reported C_d levels better than estimated. This is likely due to a combination of potential errors noted earlier, wind tunnel correlation, and the source of the road load coefficients (tested or analytically derived). Given these issues, best-in-class selection will not be lower than the minimum reported value, if available, within a vehicle class.

With respect to cross-referencing technology to aerodynamic performance, no valid trends were observed. Vehicles with median C_d values included features such as active grille shutters and underbody panels while some top performing vehicles had no references to design or features that improve aerodynamic performance.

To determine if there was a trend toward improving aerodynamics with vehicle redesigns, the estimated C_d was assessed as a function of model year of introduction for the two vehicle segments with the most models: sedans and SUVs. For the sedan class, there was no statistically significant trend for C_d as a function of model year introduction. However, the trend was statistically significant, albeit weak, for SUVs as shown in figure 14.

Compared to vehicles with internal combustion engines (ICE), the improved powertrain efficiency and lack of an exhaust system provide electric-powered vehicles with the opportunity to achieve lower C_d through reduced cooling drag and improved underbody flow. To quantify this benefit, the ICE and electric powered configurations were compared for vehicle models that offered both powertrains. The results of the comparison are shown in table IX. The estimated C_d for each powertrain is provided, as well as the difference in C_d. Also noted is if the manufacturer referenced aerodynamic improvements specific to the electric powered model. The difference in estimated C_d varied widely among the seven vehicles assessed, ranging from better to worse. Five of the seven vehicles assessed showed a C_d improvement. These same five vehicles also had manufacturer references to aerodynamic enhancements made to the electric powered version. The Ford Focus was the only ICE powered model that utilized an active grille shutter, consequently, this potential benefit is negated for the electric version. Since manufacturers are already enhancing the aerodynamic performance of their electric-powered vehicles and since ICE powered vehicle can utilize active grille shutters and underbody panels, the proposal does not include a separate best-in-class target for electric vehicles.

Based on the observations noted earlier, the sample size, and a review of the statistics in table VIII, the proposed best-in-class C_d was established as the value equal to the 90th percentile of the estimated C_d for the aerodynamic class. The results are shown in table X for each vehicle class. Using this proposal, the load reduction scenario would assume that the C_d for every vehicle in each segment will improve to be equal to the current top 10%. Those vehicles already in the top 10% would retain their current C_d or a plausible lower limit. The exception to this recommendation is the full-size van class. In this case, the proposal is to use the C_d performance of the new generation vans and, specifically, the average C_d of the MY 2015 Ford Transit.

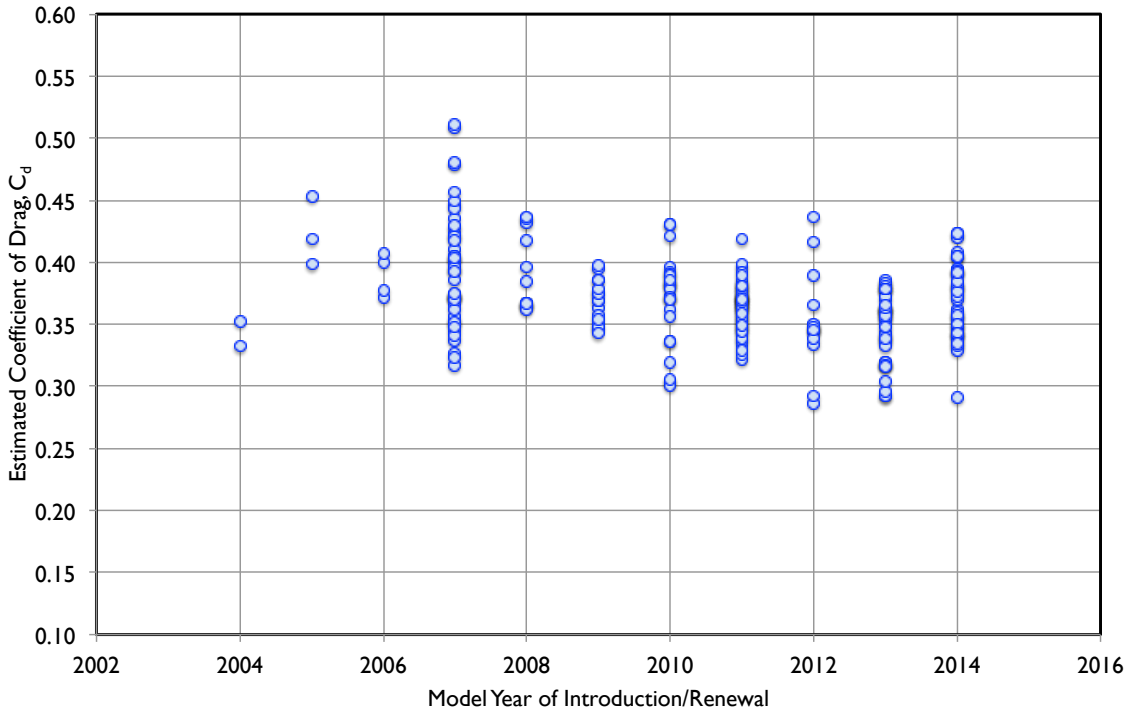

Figure 14: Estimated C_d for SUVs vs. Model Year of Renewal/Introduction.

Table IX: Estimated C_d for ICE and Electric Powered Vehicles.

Model	C_d (ICE)	C_d (electric)	Electric-Specific Aero. Improvements	C_d Change	
	[-]	[-]		[-]	[%]
Chevrolet Spark	0.341	0.314	yes	(0.027)	(7.9)
FIAT 500	0.402	0.293	yes	(0.109)	(27.1)
Ford Focus	0.307	0.336	no	0.029	9.4
Honda Fit[1]	0.363	0.277	yes	(0.086)	(23.7)
Kia Soul[2]	0.370	0.356	yes	(0.014)	(3.8)
Smart fortwo	0.329	0.447	no	0.118	35.9
Toyota RAV4	0.378	0.334	yes	(0.044)	(11.6)

[1] MY 2013 Honda Fit ICE
[2] MY 2015 Kia Soul electric

Table X: Proposed Best-in-Class C_d vs. Vehicle Type and Subcategories.

Body	Sample Size	Current Median C_d	BIC Evaluation C_d	Improvement vs. Median [%]
Coupe	163	0.334	0.293	12
Convertible	126	0.346	0.300	13
Sedan	389	0.301	0.274	9
Hatch & Wagon	128	0.335	0.295	12
SUV	305	0.365	0.322	12
Minivan	19	0.348	0.322	8
Full-Size Van	48	0.418	0.358	14
Pickup	180	0.419	0.385	8

F. Tire Rolling Resistance

Tire rolling resistance represents 25 to 30% of the vehicle load for the US city cycle and the US highway cycle. The force contribution of the tire is expressed as:

$$F_{tire} = RRC\ mg \cos(\Theta) \tag{16}$$

where:

RRC = tire rolling resistance coefficient
m = vehicle mass
g = gravitational constant
Θ = road grade

The rolling resistance coefficient (RRC) is often represented as a single value at a fixed speed, load, and tire pressure. However, tire RRC is a function of load, speed, and tire pressure and standard test procedures for determining RRC [66] [74] define these parameters.

Tire rolling resistance was not reported by any of the manufacturers, although a few report qualitative levels (e.g., low). While there are some government-funded studies [75] [76] that quantified RRC values, these results cannot be directly applied to this research. Therefore, as with the aerodynamic drag, a method of estimating rolling resistance is required.

G. Method of Estimating Tire Rolling Resistance

Using the results from the aerodynamic drag evaluation (eq. 15), the aerodynamic contribution to the road load C-coefficient, C_{aero}, can be generated. Subtracting this value from equation 2 results in an estimated value for the mechanical elements of the road load:

$$F_{mechanical} = A + Bv + (C - C_{aero})v^2 \quad (17)$$

Rearranging equation 7,

$$F_{total} - F_{aero} = F_{tires} + F_{brakes} + F_{hubs} + F_{drivetrain} \quad (18)$$

Combining 17 and 18,

$$F_{tires} + F_{brakes} + F_{hubs} + F_{drivetrain} = A + Bv + (C - C_{aero})v^2 \quad (19)$$

A common first order assessment of tire rolling resistance is to assume F_{brakes}, F_{hubs}, and $F_{drivetrain}$ are negligible which yields:

$$F_{tires} \approx A + Bv + (C - C_{aero})v^2 \quad (20)$$

While this assumption is often viewed as conservative (i.e., the result will be a higher F_{tire} than actual), differences in drag among various transmission and driveline combinations are large enough to affect the results, which will yield incorrect conclusions.

Minimally, the differences in drivetrain drag must be accounted for and, therefore, to estimate tire rolling resistance, equation 19 is rearranged:

$$F_{tires} = A + Bv + (C - C_{aero})v^2 - (F_{brakes} + F_{hubs} + F_{drivetrain}) \quad (21)$$

The challenge with equation 21 is that there is limited information regarding typical values for F_{brakes}, F_{hubs}, and $F_{drivetrain}$. For brake and hub drag, CONTROLTEC uses test results obtained from technical literature [77] [78]. However, there is insufficient information in the technical literature regarding $F_{drivetrain}$ for different combinations of transmission and drivetrain type. Consequently, CONTROLTEC has generated typical values for $F_{drivetrain}$ by evaluating hundreds of coastdown coefficients.

The estimation of tire RRC from a coastdown test cannot be directly compared to the results from standard test procedures as the loads and inflation pressures are not known. The reported value is, therefore, an average RRC at the load on each tire. Similarly, the inflation pressure is specified in the tire test procedure, while the coastdown test procedures requires the tires to be inflated to the manufacturer's recommended cold inflation pressure [59] [60]. For this research, the tire RRC was evaluated at 80 kph (50 mph), as this is a common evaluation speed [74]. However, tire RRC is also a function of speed and, therefore, a two-term equation was assumed when determining the tire force contribution to the total road load:

$$F_{tire} = (A_{RRC} + B_{RRC}v)\ mg\ \cos(\Theta) \quad (22)$$

where:

A_{RRC} = static tire RRC
B_{RRC} = tire RRC offset as a function of vehicle speed

The coefficients for equation 22 were developed by combining the current data set with test results from technical literature [67] [68] [75] [76].

An alternative, and commonly used approach for estimating tire rolling resistance from coastdown testing, is to assume that the A-coefficient (eq. 2) is entirely the result of tire force [70] [71]. However, two issues exist with this assumption; the content of the A-coefficient and the non-linearity of tire rolling resistance. Like the C-coefficient, the A-coefficient is comprised of multiple drag elements. Further, a tire's rolling resistance increases with speed and is typically evaluated at 80 kph, not statically as the A-coefficient represents.

H. Tire Rolling Resistance Results

The distribution of estimated RRC for the vehicles evaluated is shown in figure 15. The average RRC was 9.0 kg/1000 kg while the 90th percentile range was 6.6 to 11.8 kg/1000 kg. Several tires fell below plausible values for RRC, which could be the result of the estimation assumptions, coastdown test reporting issues, or a combination of both. Recent confirmation testing by the EPA has found several coastdown reporting issues [69].

As noted earlier, the mechanical elements of brake, hub, and drivetrain drag must be removed from the coastdown coefficients prior to computing tire RRC. Figure 16 presents the estimated tire RRC if only the aerodynamic contribution is removed from the coastdown coefficients. Without the adjustment, the average RRC is 11.6 kg/1000 kg.

If the A-coefficient is used to estimate the tire rolling resistance, the result is a lower average RRC (8.6 kg/1000 kg) as shown in figure 17. Since tire rolling resistance increases with speed, the lower overall average resulting from the A-coefficient method is expected. However, this method includes the transmission and driveline forces, which increases the evaluated RRC.

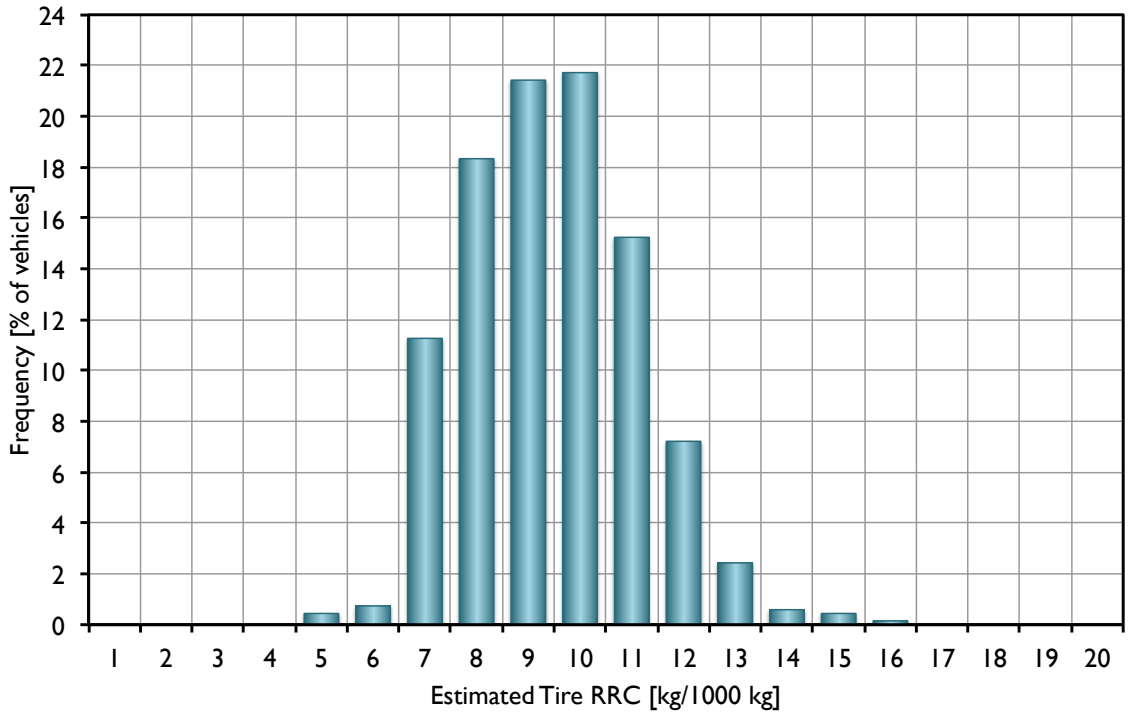

Figure 15: Distribution of Estimated Tire RRC for All Vehicles.

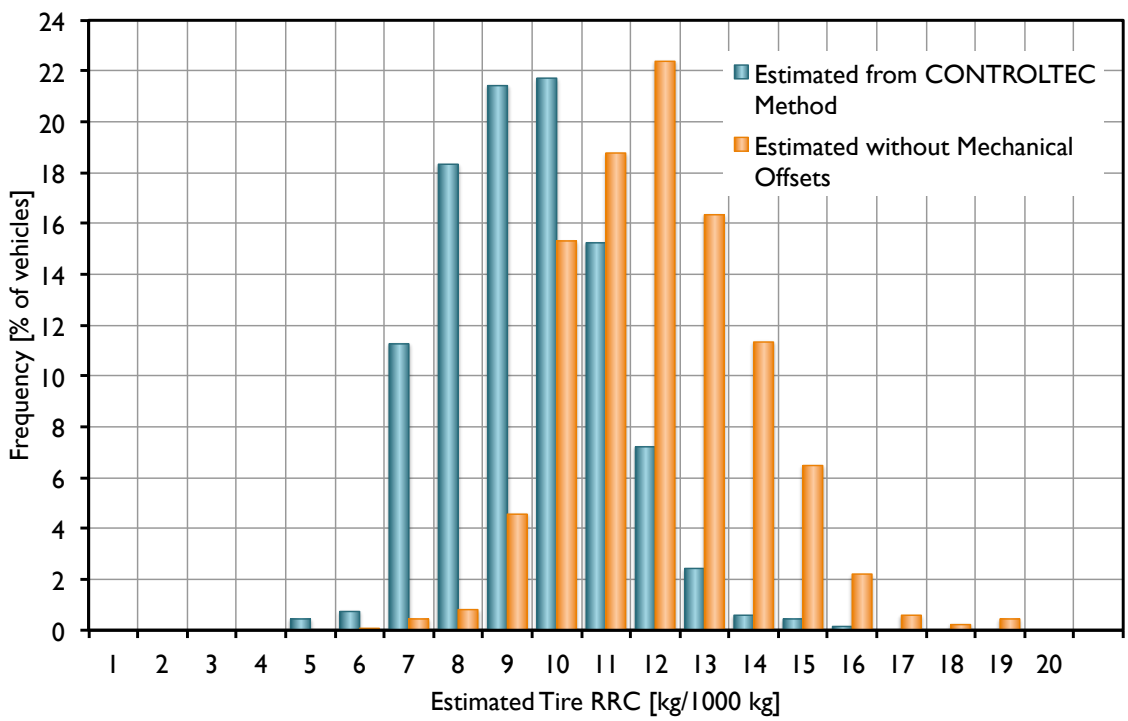

Figure 16: Distribution of Tire RRC vs. Estimation Methodology.

For comparison to available tire RRC data, figure 18 overlays the results of several studies, compiled by the Rubber Manufacturers Association (RMA) [80]. Two groups of tires are shown; original equipment and replacement. Replacement tires generally have higher rolling resistance, as their design must accommodate the needs of many vehicles whereas the original equipment (OE) tires are often designed for a single application. The results of this research are best compared against the original equipment tire set. The average RRC of the OE tire set was 9.2 kg/1000 kg with a 90th percentile range of 7.6 to 10.8 kg/1000 kg. Several factors can contribute to the difference between the OE data set and the estimated RRC from this study. These factors include analysis assumptions, tire load during coastdown versus load during tire testing, inflation pressure during coastdown versus inflation during tire testing, coastdown test reporting issues, tire types represented in the sample, tire break-in, and advancements in tire rolling resistance in the years since the RMA report was issued (2009). It is expected that the latter two items will result in a lower RRC. The wider distribution of the research data set can be explained, in part by the greater diversity of the tires being evaluated. For example, the outside diameter of the tires in the research set ranged from 0.537 to 0.923 m, while the OE set ranged from 0.575 to 0.838 m. Similarly, the tire width in the research data set ranges from 145 mm to 315 mm while the OE data set ranges from 185 mm to 285 mm. Based on this comparison to the RMA OE data set, with the exception of the very low RRC values (<5), the RRC estimates from the MY 2014 data appear to be plausible.

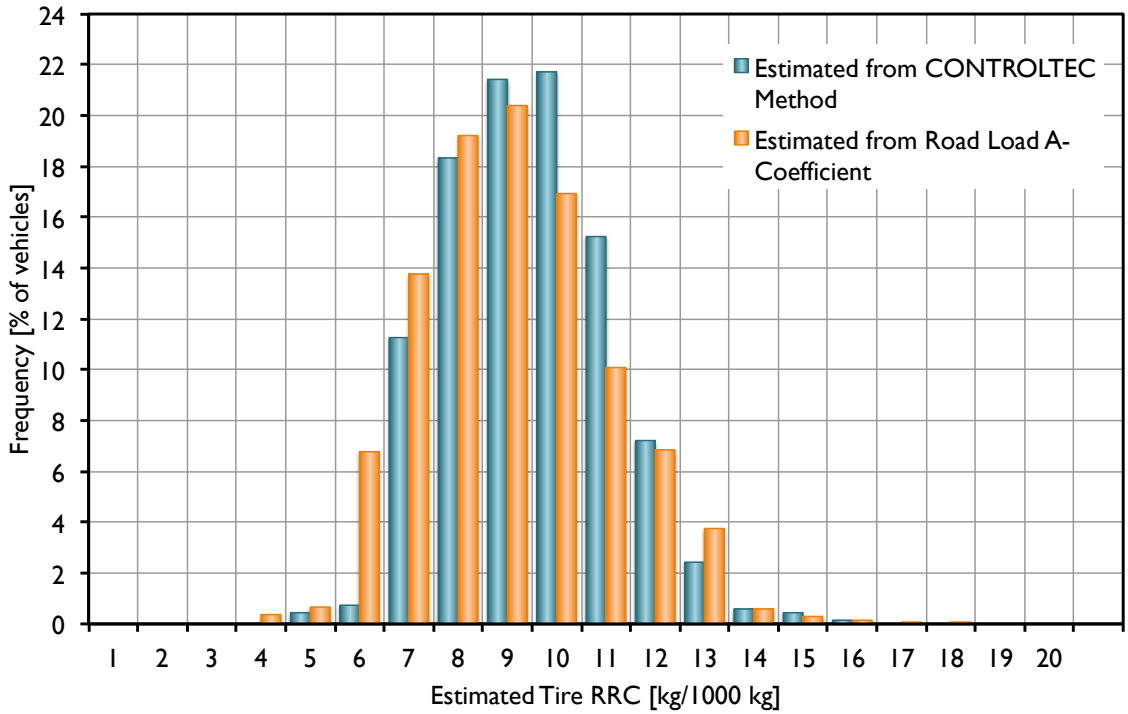

Figure 17: Distribution of Tire RRC vs. Estimation Methodology.

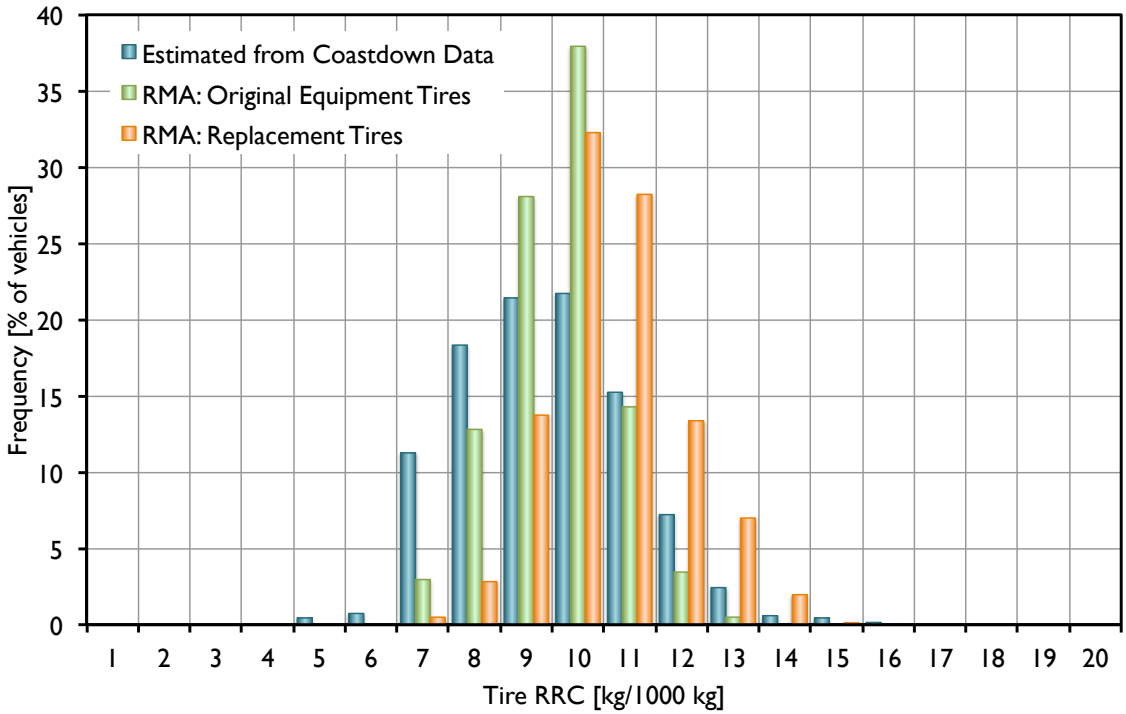

Figure 18: Distribution of Tire RRC for the MY 2014 Data Set and the RMA Analysis [80].

To further qualify the estimates, the results were compared to expected trends. The largest contribution to tire rolling resistance is the repeated deformation of the contact patch [81]. Consequently, rolling resistance will drop with increasing tire diameter, assuming constant tread design and sidewall stiffness. This trend is apparent in the data set as shown in Figure 19. Tire construction appears to be the dominant determinant as evidenced by the spread in RRC at a fixed tire diameter. Estimated tire RRC as a function of width is presented in figure 20. The trend of increasing RRC with width is due to the collinearity of width and traction requirements rather than tire energy fundamentals. Specifically, performance-oriented vehicles tend to have wider tires and also require greater traction.

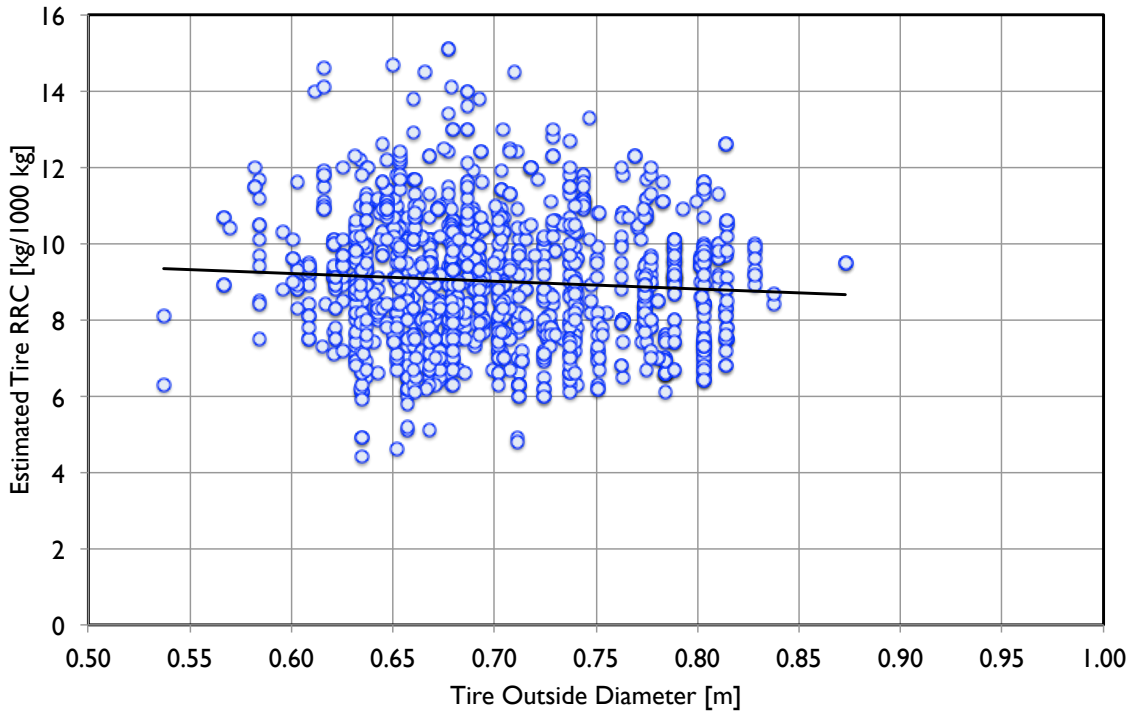

Figure 19: Estimated RRC vs. Tire Outside Diameter.

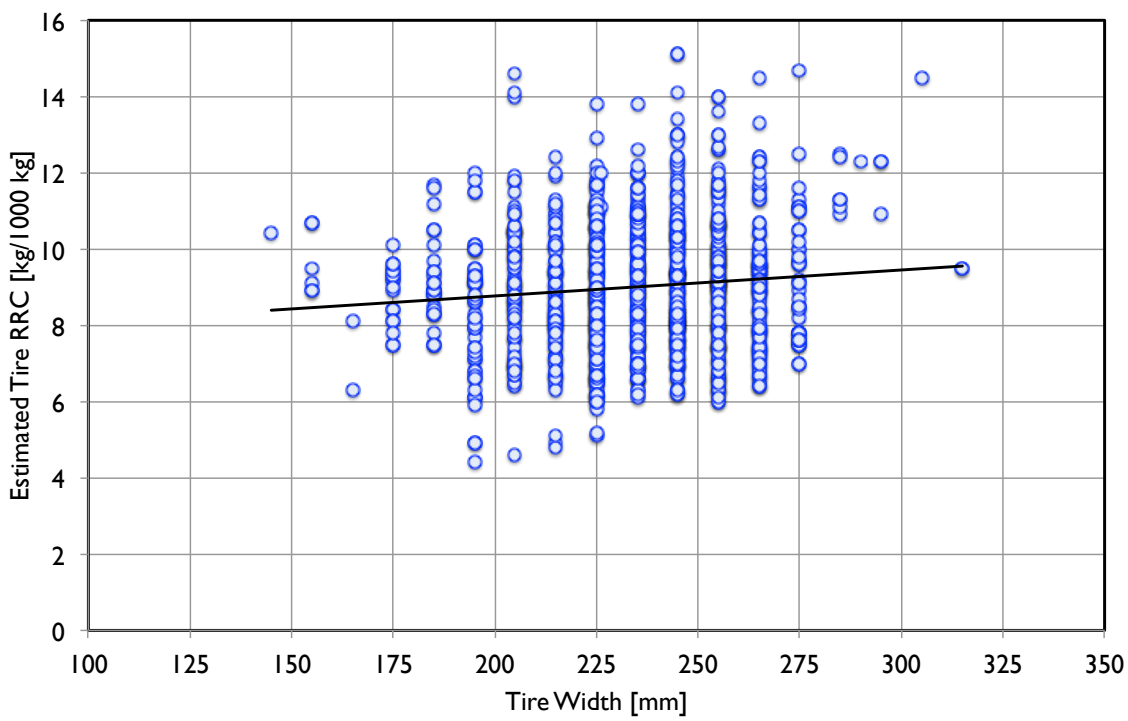

Figure 20: Estimated RRC vs. Tire Width.

I. Best-in-Class Tire Rolling Resistance

The objective of the research is to identify best-in-class rolling resistance and apply the results to all vehicles in the data set. Selection of the tire characteristics for a particular vehicle will depend upon the desired balance of traction, wear, ride-quality, noise, and rolling resistance. Consequently, for this research, the proposal is to classify the vehicles by tire task:

1. Fuel Economy Oriented
2. Balanced
3. Off-road Oriented
4. Performance Oriented

Vehicles selected for fuel economy oriented were those specifically noted by the manufacturer as having either a fuel economy package or fuel economy-oriented vehicles equipped with low rolling resistance tires. Selection of performance and off-road oriented vehicles was somewhat subjective. Performance-oriented vehicles included performance oriented brands (e.g., Ferrari, Lamborghini, Roush) and specialty vehicles within a brand (e.g., Audi R-series, BMW M-series, Chevrolet Corvette, Chrysler-SRT, Mercedes-Benz AMG). While SUVs and trucks are off-road capable, most are equipped with tires biased to on-road duty. Consequently, the vehicles selected as off-road oriented were specialty vehicles within a brand (e.g., Jeep Wrangler, Toyota FJ Cruiser).

Figure 21 provides the RRC results for the four classifications. As expected, the tire RRC correlates to vehicle task. The average RRCs were 8.1 kg/1000 kg for fuel economy oriented, 8.9 kg/1000 kg for balanced, 9.4 kg/1000 kg for off-road oriented, and 10.1 kg/1000 kg for performance oriented.

The similarity of the off-road oriented RRC to the balanced RRC is likely the result of the manufacturer not using the off-road specific tires for fuel economy testing. Consequently, due to the small sample size and similarity to the balanced category, the off-road oriented category was combined with the balanced category.

Similar to the aerodynamic assessment, using the absolute lowest value to identify best-in-class for each segment is not recommended due to the potential errors associated with evaluating the RRC (estimation assumptions, coastdown test reporting). Again, the proposed approach is to select a subset of the data as best-in-class (e.g., 90th percentile). For this analysis, the lowest RRC was assigned the 100th percentile and the highest RRC was assigned the 0th percentile.

While the estimates of RRC are reasonable, they are directly affected by the coastdown coefficients and assumptions for drivetrain drag. Further, unlike C_d, there is no direct comparison to manufacturer-reported values. Additionally, tire rolling resistance must be balanced against other tire attributes such as traction and tread wear. These attributes impact key vehicle performance metrics, including stopping distance and maneuverability, and affect consumer costs and tire disposal. Consequently, less aggressive percentiles were evaluated for best-in-class tire rolling resistance. Table XI presents the RRC results for the 90th (best 10%) and 75th (best 25%) percentiles.

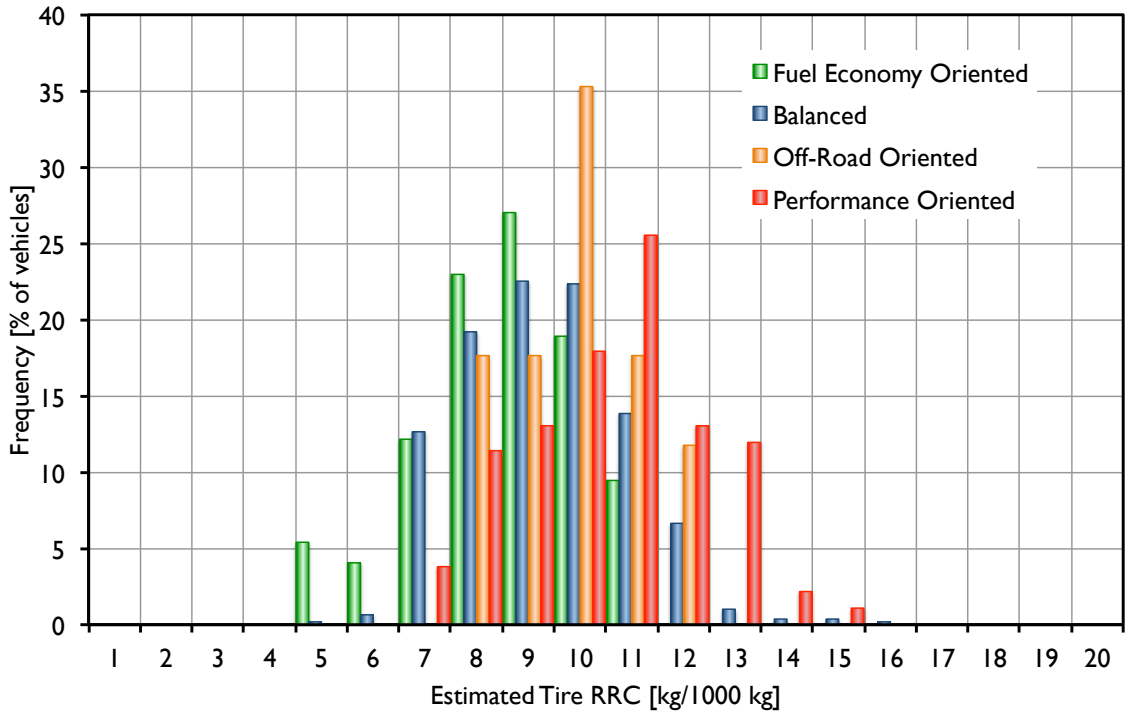

Figure 21: Distribution of Tire RRC vs. Vehicle/Tire Category.

Table XI: Estimated Tire RRC Percentiles vs. Vehicle and Tire Category.

Vehicle/Tire Category	Sample Size	Average RRC	Min. RRC	90th Percentile RRC	75th Percentile RRC	Max. RRC
All Vehicles	1358	9.0	4.4	6.9	7.8	15.1
Fuel Economy Oriented	74	8.1	4.4	6.2	7.4	10.8
Balanced	1083	8.9	4.8	6.9	7.7	15.1
Off-Road Oriented	17	9.4	7.1	7.7	8.3	12.0
Performance Oriented	184	10.1	6.1	7.8	8.9	14.5

Based the evaluation of all data, sample size, and a review of the statistics in table XI, the proposed best-in-class tire RRC was established as equal to the 75th percentile for the vehicle-tire categories shown in table XII. Using this proposal, the load reduction scenario would assume that the tire RRC for every vehicle in each segment would improve to be equal to the current top 25%. Those vehicles already in the top 25% would retain their current RRC or a plausible lower limit.

Table XII: Proposed Best-in-Class Tire RRC vs. Vehicle and Tire Category.

Vehicle/Tire Category	Sample Size	Current Median RRC	Proposed Evaluation RRC	Improvement vs. Median [%]
Fuel Economy Oriented	74	8.3	7.4	11
Balanced	1100	8.9	7.7	14
Performance Oriented	184	10.3	8.9	14

The results of the literature review did not yield specific values for tire RRC, only the use of "low" rolling resistance tires. Vehicles that noted the use of low rolling resistance tires are, with few exceptions, included in the fuel economy-oriented classification. The cross-referenced data set includes a field for low rolling resistance. Within the fuel economy-oriented class, the subset of vehicles identified as having low rolling resistance tires had an average estimated RRC of 8.1 kg/1000 kg, which is the same as the average of all fuel economy-oriented vehicle.

6. DETAILED MASS REDUCTION ANALYSIS METHODOLOGY

To support the goals of the research project, it was desired to develop a mass efficiency metric for vehicles and vehicle subsystems [3, Task 5]. Vehicles utilizing mass reduction technologies and designs will be identified by two methods; 1) determining the mass efficiency for each vehicle and its subsystems and 2) cross-referencing the results of the literature review with the data set. The mass efficiency metric will provide a method of identifying best-in-class vehicles. The cross-referenced data set will identify the load-reduction technologies and/or characteristics that the best-in-class vehicles are using (e.g., material substitution, design optimization).

A. Background

The load associated with the mass of a vehicle includes the kinetic energy due to accelerating the mass and the change in tire rolling resistance as a function of tire load. For a conventional vehicle, much of the kinetic energy can be recovered during coasting. However, in practice, only a portion is recovered during coasting or powered decelerations; much is dissipated as heat through the brakes, pumping losses in the engine, and drag in driveline, hubs, and brakes. The forces associated with vehicle mass are:

$$F_{mass\ related} = ma + mg\sin(\Theta) + RRC\ mg\cos(\Theta) \quad (23)$$

where:

m = vehicle mass
a = vehicle acceleration
g = gravitational constant
Θ = road grade
RRC = tire rolling resistance coefficient

From equation 23, the first term represents the force due to acceleration, the second term is the result of ascending or descending a grade, and the third term represents the tire rolling force. For non-hybrid vehicles, kinetic energy losses represent approximately 40% of the vehicle load for the combined FTP 75 and HWFET cycles. However, kinetic energy can be recovered and stored for later use. Current hybrid powertrain (e.g., spark ignition-electric) and electric vehicles recover and store the kinetic energy through a generator-battery system. Kinetic energy can also be recovered and stored using mechanical systems (e.g., flywheel, hydraulic system).

As noted in the literature review, vehicle mass reduction is a common strategy employed by automotive manufacturers to achieve reduced fuel consumption. However, the benefit of mass reduction depends upon the drive cycle. For the combined city and highway drive cycles required for the certification of tailpipe CO_2 emissions for the US market, a 10% reduction in mass has been estimated reduce the fuel consumption by ~3.5% [82]. If the engine is re-sized to achieve the same performance, the fuel consumption benefit can further improved by another 2 to 3% (~5 to 6.5% total) [82].

These benefits assume that the vehicle was tested at its loaded weight, which is 136 kg (300 lb) greater than the curb weight. For purposes of vehicle certification, vehicles are tested at an equivalent test weight (ETW) [83]. These test weight classes are a function of curb weight and range from 57 kg (125 lb) to 227 kg (500 lb). The mass reduction required to reduce the weight class will depend upon the weight class and position of the vehicle within the class. Figure 22 shows the range of each weight class as a fraction of the class weight. Consequently, from a regulatory perspective, the benefit of mass reduction will vary widely from vehicle-to-vehicle. For example, for a vehicle at the upper end of the 1758 kg (3875 lb) weight class, a mass reduction of just over 3% will shift the vehicle to the next lower ETW. However, for a vehicle at the upper end of the 2722 kg (6000 lb) weight class, a mass reduction of over 8% is required to shift the vehicle to the next lower ETW.

Consider a vehicle at the upper end of the 2722 kg (6000 lb) weight class; the curb weight will need to be reduced by over 8% in order to gain the full benefit of mass reduction. A modeled example of this scenario is provided in figure 23. A 225 kg (495 lb) (8.3%) mass reduction would not change the test weight class and the benefit to tailpipe CO_2 emissions on the regulated drive cycles would be limited to the benefit to tire rolling resistance (~1.1%). If the mass is further reduced by just 4 kg (10 lbs) (8.5% total), the vehicle is shifted into the 2495 kg (5500 lb) weight class and the CO_2 benefit jumps to 3%. If the engine is re-matched in each case, to maintain performance, the total benefit increases to ~3.4% and 5.3% for the 225 kg (495 lb) and 229 kg (505 lb) mass reduction scenarios, respectively.

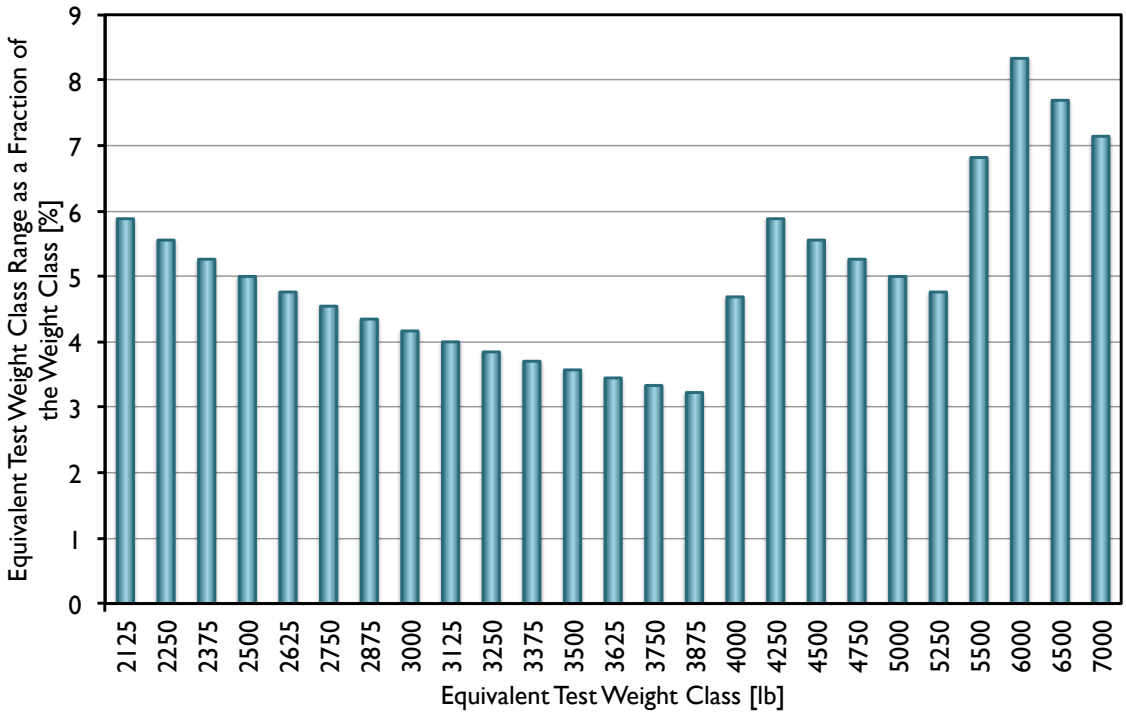

Figure 22: Equivalent Test Weight Class Range vs. Test Weight Class.

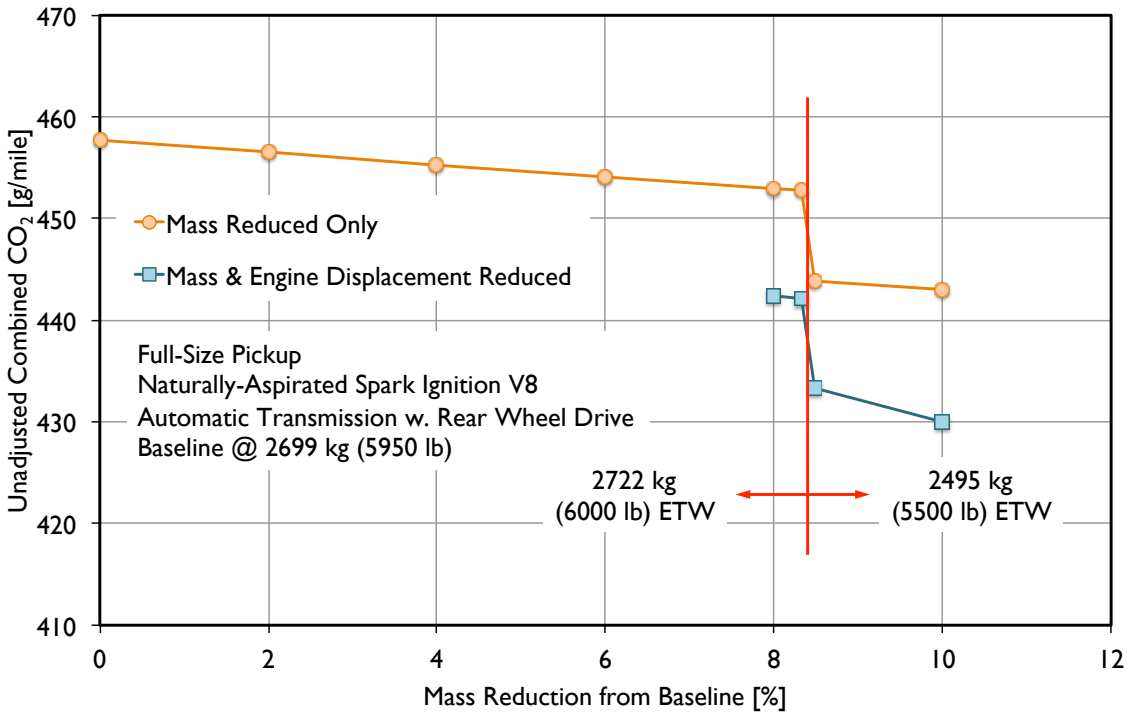

Figure 23: Example of Tailpipe CO_2 Emissions vs. Mass Reduction Scenarios.

B. Curb Weight Reporting

For this research, the curb weight is the weight of the vehicle with all fluids at their maximum level. The reported curb weight can represent multiple values including, but not limited to, a minimally optioned vehicle, a typically equipped vehicle, or a fully optioned vehicle. Curb weight data was collected from one or more manufacturer sources and included their media sites, consumer sites, specifications from brochures, and/or their certification applications. All of the vehicle models and sub-configurations had a curb weight reported from at least one of these four sources. No single source provided curb weights for every vehicle in the data set. In some instances, the manufacturers reported multiple weights representing a range of option levels within a model. Certain manufacturers report significantly lower curb weights on their media sites compared to their certification applications (>8% discrepancy, which is beyond the expectation of options). For the majority of vehicles, the manufacturer does not specify the option level associated with the reported curb weight. In addition to the curb weight, the equivalent test weight, associated with the road load coefficients, was also recorded.

As corroboration, measured weights were collected from three 3rd party sources; Car & Driver [84], Consumer Reports [55], and Motor Trend [85]. In all cases, these publications measure the curb weight of the vehicle as part of their testing procedures. These data were available for only a small percentage of the vehicles in the data set. Additionally, curb weight data was obtained from European Union (EU) homologation data [86]. The difference between the EU and US reporting methods was accounted for when using these values. Based on a review of the EU homologation data, several European manufacturers (e.g., Aston Martin, Ferrari, Porsche) report the EU curb weight, on their media and consumer sites, for the US market vehicles. In some cases, the EU values are significantly lower (>5% discrepancy) than measured by the 3rd party sources.

To verify the reported curb weights, several data quality assessments were conducted. The first assessment was to compare the ETW associated with the road load coefficients to the ETW corresponding to the reported curb weight. If the two equivalent test weights were equal, the lowest manufacturer-reported curb weight was used for subsequent analysis. This condition was satisfied for 87% of the vehicles in the data set.

The reported curb weights that did not satisfy the ETW equivalency condition could be the result of option content, certification flexibilities, the curb weight standard used, or reporting errors. Of the vehicles that reported curb weights associated with options, the average increase was 2.6%, while 75% reported an increase of no greater than 4.2%. Therefore, the reported curb weights were accepted for vehicles failing the ETW equivalency condition but were within 4.2% of the ETW bound associated with the road load coefficients. This condition was satisfied for all but 16 of the 1358 vehicles in the data set. The curb weights for the remaining 16 vehicles were assumed to be from an alternate curb weight standard or simply an erroneous value. For these vehicles, corroborating data from the 3rd party sources [55] [84] [85] was used to generate a plausible curb weight.

C. Vehicle Mass Reduction and Mass Efficiency

As noted in the literature review, there is a significant level of activity towards reducing the mass of light-duty vehicles as one step in achieving the current and future requirements for fuel consumption and tailpipe CO_2 emissions.

The original desire of the research was to develop a mass efficiency metric for vehicle subsystems and apply the weight reductions to every vehicle in the fleet [3, Task 5]. While mass reduction was cited by nearly all manufacturers as a strategy applied to one or more of their current products, there is limited weight data available for individual sub-systems on specific vehicles. Additionally, the substitution of the best available strategy requires that the mass of each subsystem to be replaced is known in order to assign a mass to subtract, prior to adding the best technology. Given the lack of information sufficient to develop and apply sub-system mass efficiency metrics, CONTROLTEC used its mass model to assess vehicle-level mass efficiency.

D. Mass Model

The first order determinant of vehicle mass is its overall size. CONTROLTEC quantifies vehicle size as vehicle cubic volume; the product of length, width, and height. Figure 24 shows the manufacturer-reported curb weight as a function of vehicle cubic volume for the vehicles in the MY 2014 data set. Curb weight correlates well with vehicle cubic volume (R^2 = 0.82). Lines of constant mass density, defined as the ratio of curb weight to vehicle cubic volume, are shown as reference. For the vehicles in the data set, the average mass density is 120 kg/m^3 (7.5 lb/ft^3) but varies from ~100 kg/m^3 (6.2 lb/ft^3) to ~200 kg/m^3 (12.5 lb/ft^3).

The second most important attribute to vehicle mass is the vehicle type and is the single largest contributor to the remaining variation in figure 24. Figure 25 provides the added dimension of vehicle type to the vehicle density function. Using the cubic volume metric, there are the distinct differences in mass density among the various types of vehicles. For example, given the open bed, pickup trucks have a lower cubic mass density than most other vehicles. Convertible coupes, on the other hand, have a higher cubic mass density due to the additional structural and safety requirements associated with not having the benefit of a fixed roof. Accounting for vehicle type improves the overall correlations to over 0.87 R^2.

The remaining variation shown in figure 25 is the result of differences in power source (e.g., spark ignition, compression ignition), power source attributes (e.g., number of engine cylinders, engine aspiration, motor size), transmission type, driveline (e.g., two wheel drive, four wheel drive), drivetrain architecture (e.g., front wheel drive, rear wheel drive), body details (e.g., closures, cargo bed length), on-board energy storage, tires and wheels, seating capacity, option content, design, and material usage.

CONTROLTEC has developed a light-duty vehicle curb weight model as a means of identifying mass efficient vehicles and quantifying opportunities for light-weighting. The model captures most of the remaining sources of vehicle mass variation noted above. The mass model is calibrated with publicly available information.

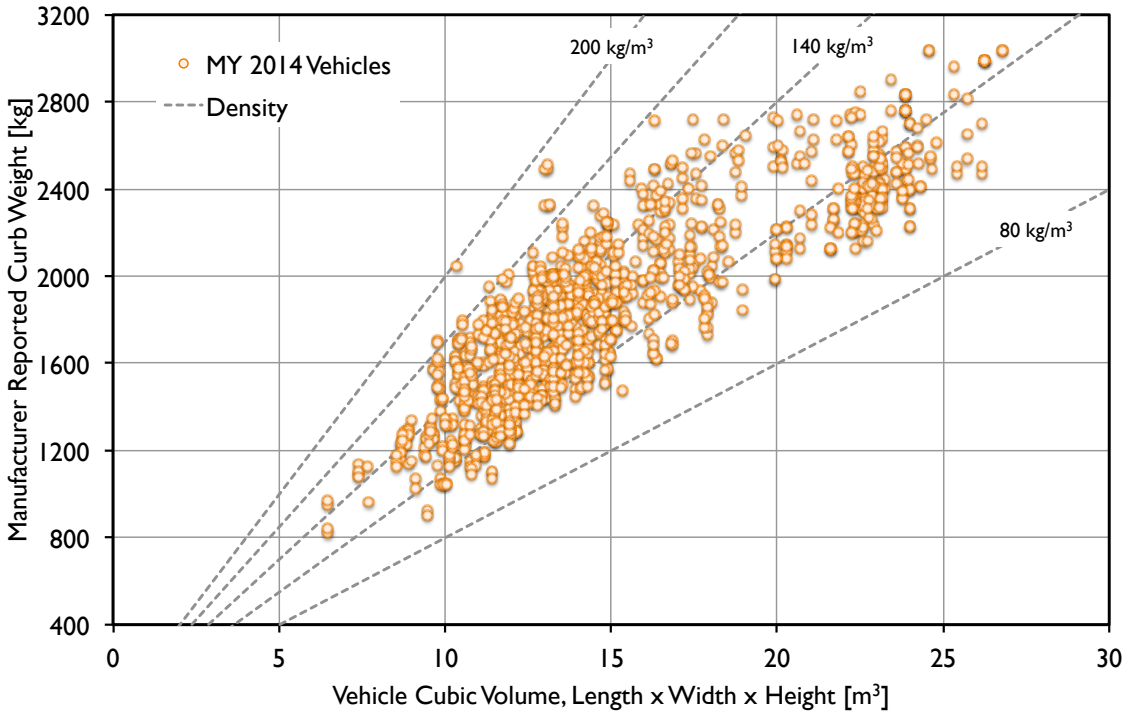

Figure 24: Curb Weight vs. Vehicle Cubic Volume, MY 2014 Vehicles.

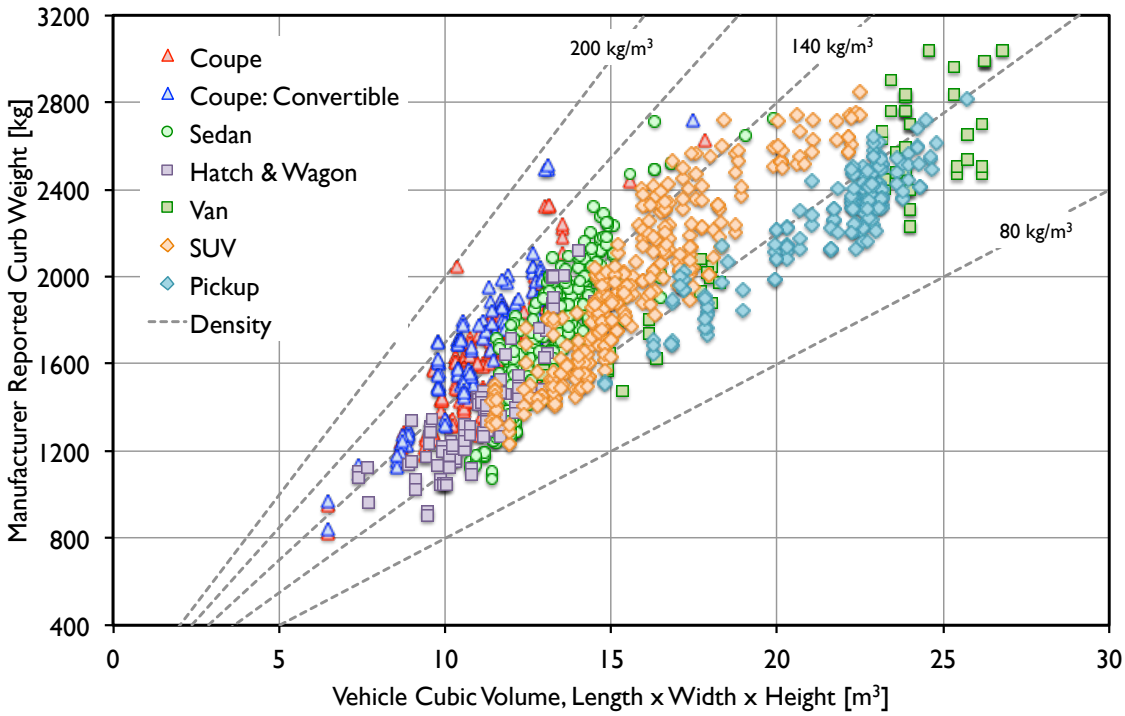

Figure 25: Curb Weight vs. Vehicle Type vs. Vehicle Cubic Volume, MY 2014 Vehicles.

E. Mass Model Elements

CONTROLTEC's proprietary mass model is comprised of four basic elements; 1) base vehicle, 2) power source, 3) transmission, driveline and drivetrain architecture, and 4) on-board energy storage:

$$m_{estimated} = m_b + m_p + m_d + m_e \quad (24)$$

where:

m_b = *f*(vehicle type, length, width, height, cargo bed, tire/wheel size)
m_p = *f*(engine type, cylinders, engine aspiration, hybrid type, motor size)
m_d = *f*(transmission type, driveline, drivetrain architecture)
m_e = *f*(fuel tank capacity, fuel type, battery capacity, battery chemistry)

Each of these four elements is a function of key vehicle or powertrain attributes, all of which are available from the manufacturer's specifications. The elements are comprised of continuous and discrete sub-models. Generating the model coefficients and sub-system mass offsets requires evaluating the reported mass from thousands of vehicles and sub-systems. Since the model is based on the key attributes of the vehicle and powertrain, the model residual (m_{actual} - $m_{estimated}$) then reflects vehicle design and material elements not captured in the basic specifications. Consequently, the actual mass of any vehicle is defined as the sum of the estimated value and the model residual:

$$m_{actual} = m_b + m_p + m_d + m_e + \varepsilon \quad (25)$$

where:

ε = model residual = *f*(materials, design, option content)

Using this mass model, a curb weight is estimated for each vehicle, accounting for the typical mass of key subsystems, which effectively "normalizes" each vehicle based on its attributes. Therefore, if the residual for a particular vehicle is negative, then the vehicle is lighter than projected, suggesting the application of mass reduction technologies and/or a mass efficient design. By correlating the residuals against mass reduction features (e.g., aluminum body-in-white), a mass benefit can be developed for some features, assuming adequate sample size. Additionally, to assess the potential for mass reduction, CONTROLTEC normalizes the residuals:

$$\varepsilon_{norm} = (m_{actual} - m_{estimated})/ m_{estimated} \quad (26)$$

The normalized residual will represent the mass of the vehicle relative to a vehicle with an average execution and the same attributes. For example, an ε_{norm} of -0.10 indicates that the mass is 10% lower than expected, given the vehicle and powertrain features. When ε_{norm} is compared to the same type of vehicle, it becomes a measure of relative mass efficiency. Ranking vehicles by their normalized residuals can be used to understand best-in-class vehicles. It is expected that the mass efficiency will improve each year as manufacturers employ new materials and designs.

F. Mass Model Results

Figure 26 provides the results of the CONTROLTEC mass model applied to the MY 2014 vehicles in the research data set. As shown, the model predicts the mass of a vehicle with an R^2 value of 0.95, meaning that the model captures 95% of the variation of vehicle curb weight within the MY 2014 vehicles evaluated. Of the vehicles in the data set, 95% are within ± 10% of the estimate; 90% are within ± 8% of the estimate. Figure 27 shows the normalized residuals for all vehicle types.

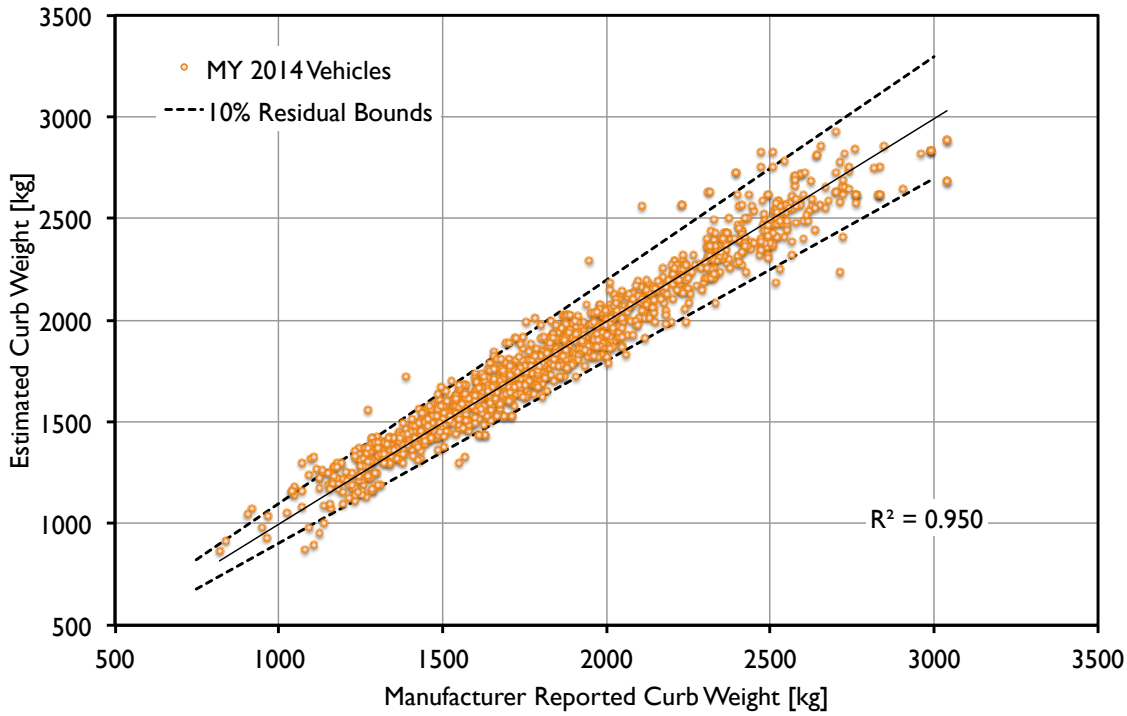

Figure 26: CONTROLTEC Mass Model vs. Manufacturer Reported Curb Weight.

G. Mass Efficiency

Since the mass model captures the key architectural and powertrain elements, then comparing vehicles in the same class provides a method of ranking mass efficiency; those with negative residuals are assumed to be more mass efficient than those with positive residuals. Therefore, the normalized mass model residual can be used as a proxy for mass efficiency. Exploring vehicles with the most negative residuals can reveal successful light-weighting technologies and designs.

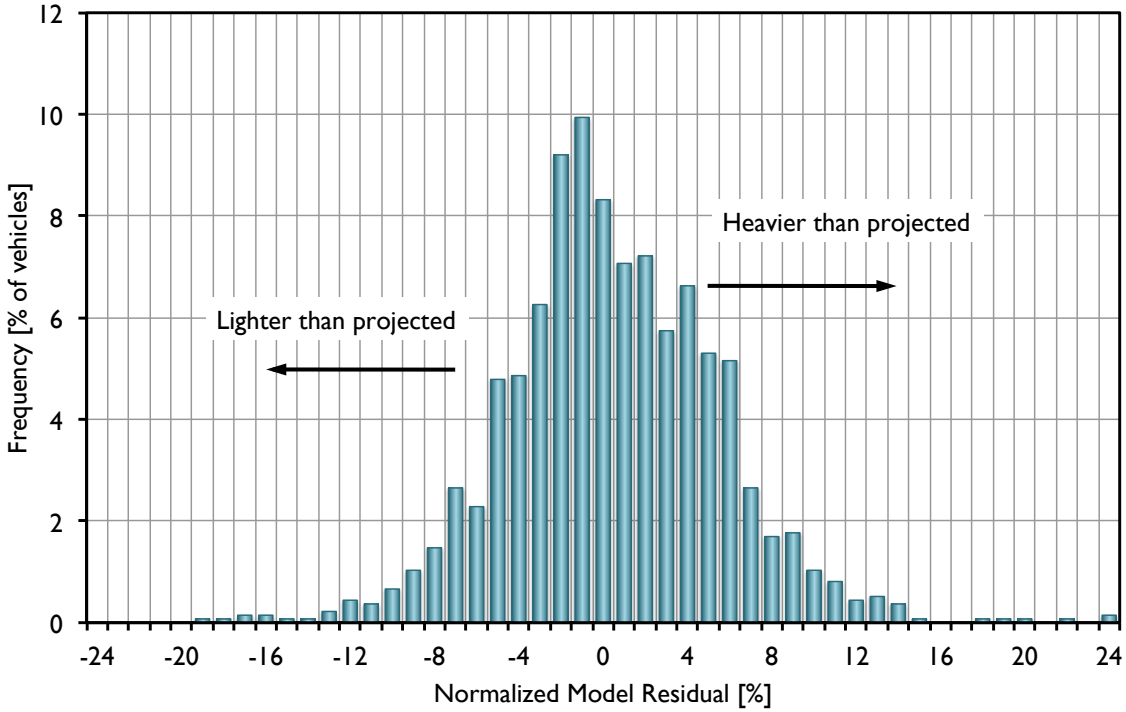

Figure 27: Distribution of Normalized Model Residuals.

To test this proposal, the mass efficiency concept was tested on the MY 2015 Ford F-150. Since manufacturer-reported data were not available at the time of this report, MY 2015 mass reduction was obtained from measurements made by Consumer Reports [55]. This product represents an aggressive light-weighting program and includes an aluminum-intensive body and high-strength steel frame. Since aluminum and high-strength steel intensive vehicles were available in the MY 2014 fleet, CONTROLTEC's expectation is that the MY 2015 F-150 should fall in the lower end of the MY 2014 distribution; this expectation is confirmed as shown in figure 28.

In addition to identifying mass efficient designs, the mass model can also be used to understand the potential to reduce mass by changing vehicle and powertrain attributes. Examples of this include reducing the size of the vehicle, changing the power source from a V6 naturally aspirated engine to an I-4 turbocharged engine, reducing the fuel tank capacity, or changing the battery chemistry. Two examples of this type of analysis were presented in the research plan [87].

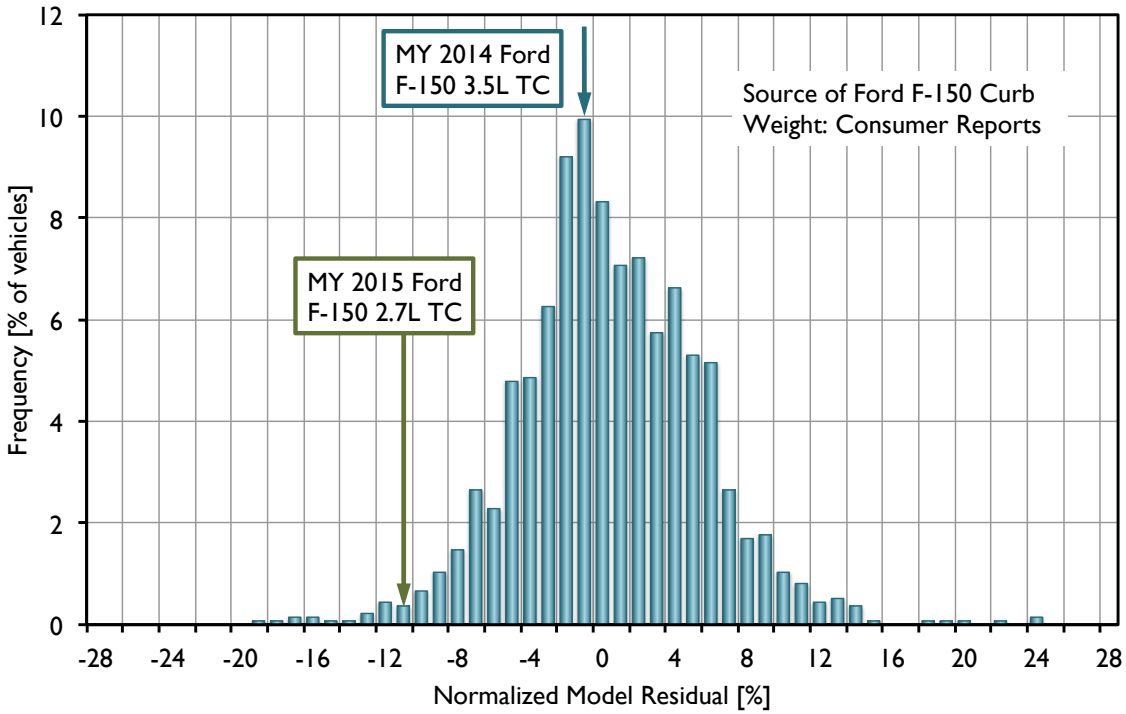

Figure 28: Distribution of Normalized Model Residuals with Ford F-150 Overlays.

H. Best-in-Class Mass Efficiency

The vehicles were classified by type to determine the best-in-class mass efficiency. Figures 29 through 37 provide the distribution of the normalized mass model residuals for each of the major vehicle types. The tabular results are provided in table XIII. For each vehicle type, the lowest mass residual was assigned the 100th percentile and the highest mass residual was assigned the 0th percentile. Evaluation of these distributions was necessary to establish the best-in-class criteria.

With the exception of luxury vehicles, basic vehicles, and pickup trucks, the average and range of the distributions for each vehicle type is similar to the population of all vehicle types, suggesting that the model is type neutral. For luxury sedans, as defined by Ward's Automotive [56], the distribution is shifted 1.6% heavier. Since the base luxury vehicle is typically more heavily optioned than a non-luxury vehicle, the higher weight is expected. In fact the magnitude of this shift is in agreement with the option content analysis noted earlier. The lower end of the luxury sedan distribution includes the aluminum-intensive vehicles from Audi and Jaguar.

As opposed to the luxury vehicles, basic vehicles, defined by Ward's Automotive as lower middle and lower small, are skewed lighter by 2.7% as shown in figure 34. Not only are these vehicles typically equipped with fewer options, they also have less isolation for noise, vibration, and harshness (NVH), which further reduces their weight. Vehicles in this segment are steel-intensive.

In the case of the pickup trucks, the median of the distribution is approximately zero, however, the overall range is narrower and skewed high. The authors believe that this result is due to the

homogeneity of the current pickup truck fleet. Based on the literature review, current pickups are steel intensive with some use of aluminum for closures and other subsystems. By contrast, the population of all vehicles includes a wider array of mass reduction technologies including aluminum-intensive vehicles. Consequently, the best-available mass reduction technologies are expected to shift the pickup truck distribution lower in future years. This is supported by the results shown in figure 28 for the MY 2015 Ford F-150.

Given the variety of curb weight reporting and variations in option content, using the absolute lowest normalized mass model residual to identify best-in-class is not recommended. Rather, the proposed approach is to select a reasonable subset of the data as best-in-class (e.g., 95th percentile).

After an evaluation of all data, sample size, and a review of the statistics in table XIII, the best-in-class mass efficiency was based on the model residuals from the entire vehicle population. For non-luxury vehicles the proposed best-in-class uses the 98th percentile, which is equal to a 10.3% mass reduction relative to the average implementation. For luxury vehicles of all types the proposed best-in-class uses the 90th percentile to account for the increased option content of these vehicles. The 90th percentile corresponds to a 5.9% mass reduction relative to the average vehicle. Using this proposal, the mass-reduced scenario would be generated using the mass model (eq. 24) to compute a new curb weight for each vehicle. Vehicles that fall below the assigned percentile would retain their current mass. Specifically,

$$m_{mass\text{-}reduced} = (m_b + m_p + m_d + m_e) \times (1 + \varepsilon_{norm\ percentile}) \text{ or } m_{actual}\text{, whichever is less.} \quad (27)$$

where:

$\varepsilon_{norm\ percentile}$ = normalized residual at the proposed percentile

Using the current analysis,

$\varepsilon_{norm\ 98}$ = -0.103 (all non-luxury vehicles)
$\varepsilon_{norm\ 90}$ = -0.059 (all luxury vehicles)

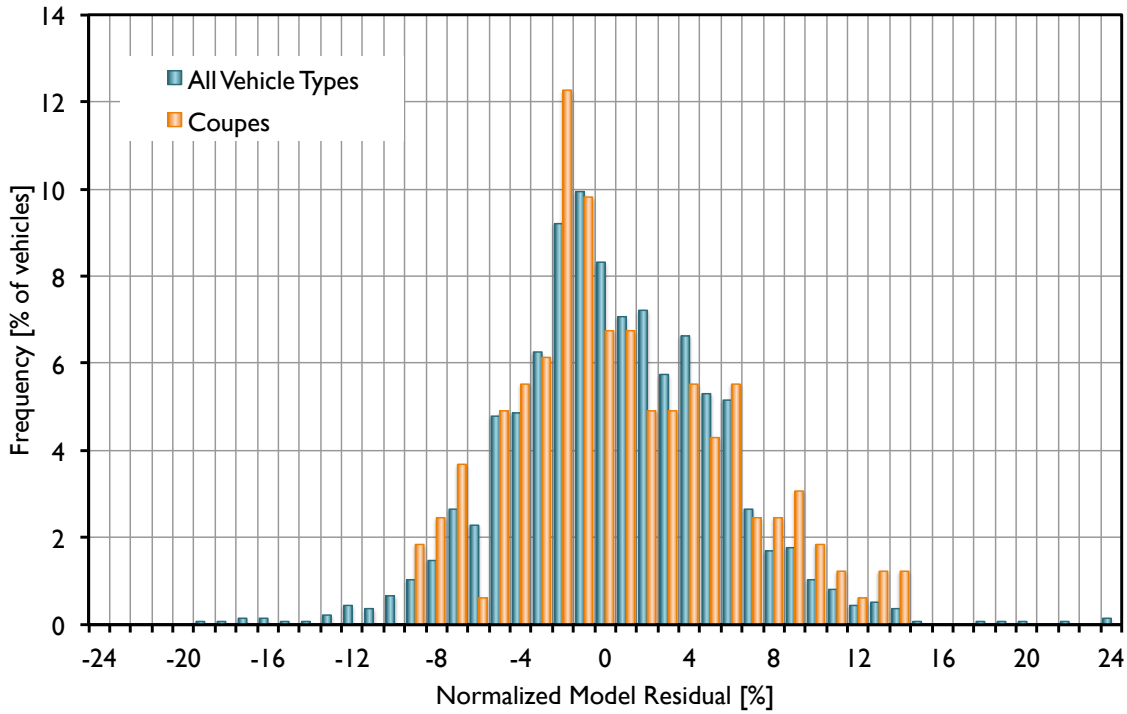

Figure 29: Distribution of Normalized Model Residuals for Coupes.

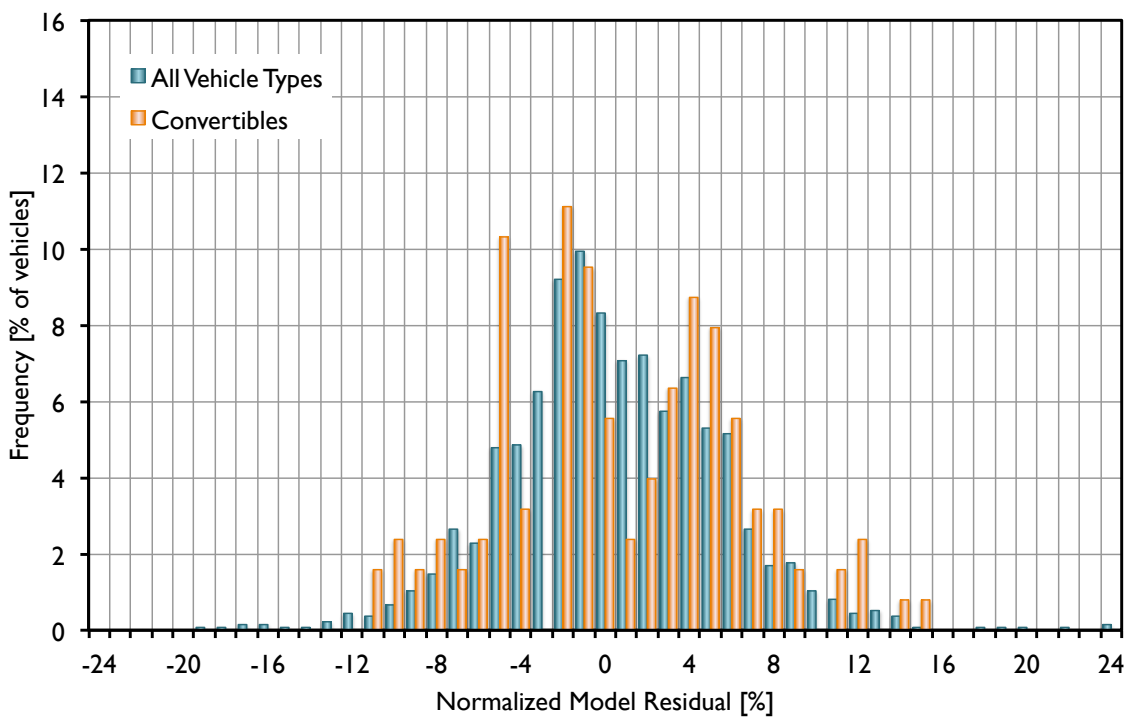

Figure 30: Distribution of Normalized Model Residuals for Convertibles.

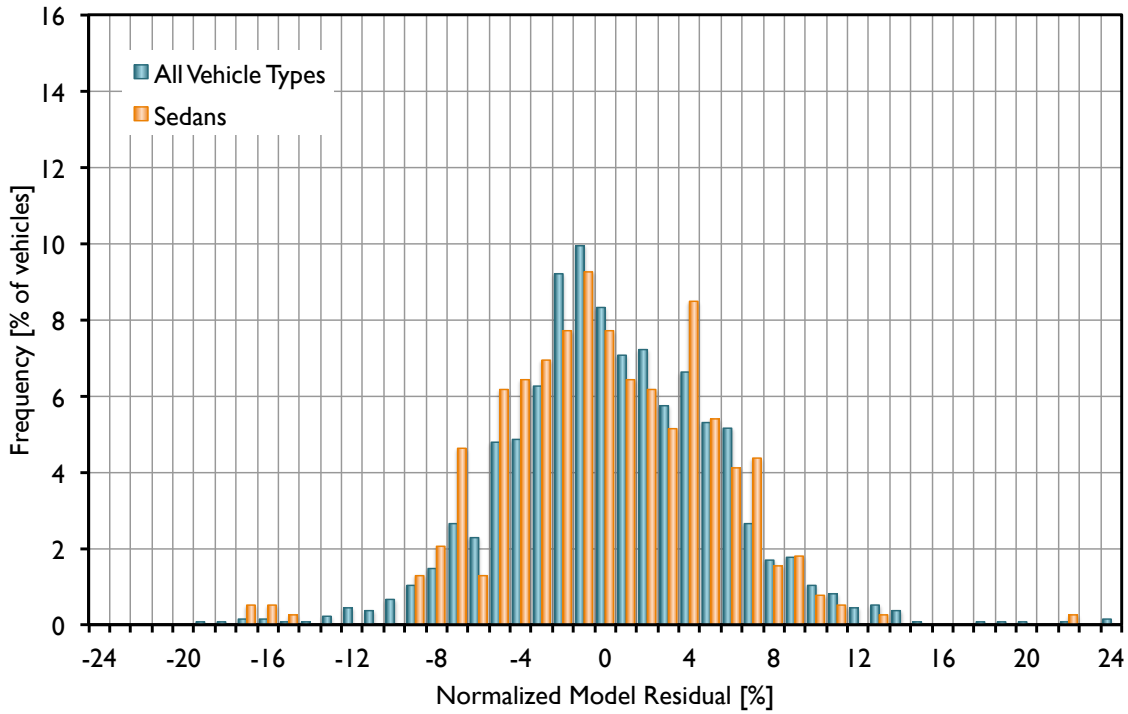

Figure 31: Distribution of Normalized Model Residuals for Sedans.

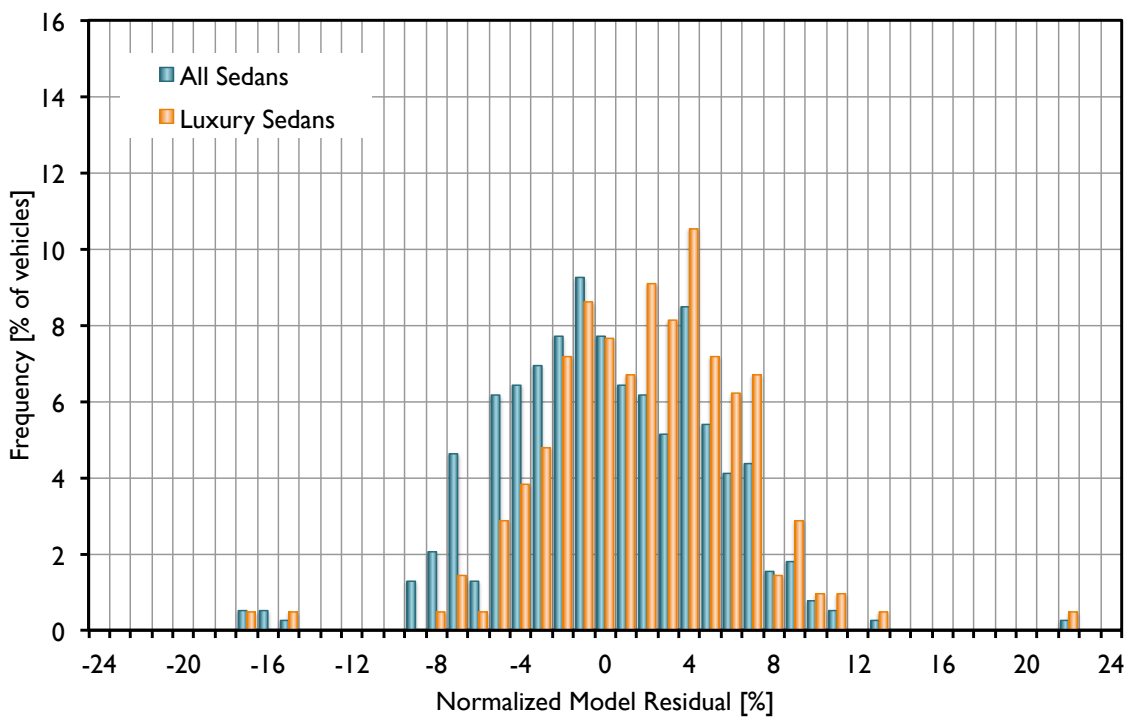

Figure 32: Distribution of Normalized Model Residuals for Non-Luxury and Luxury Sedans.

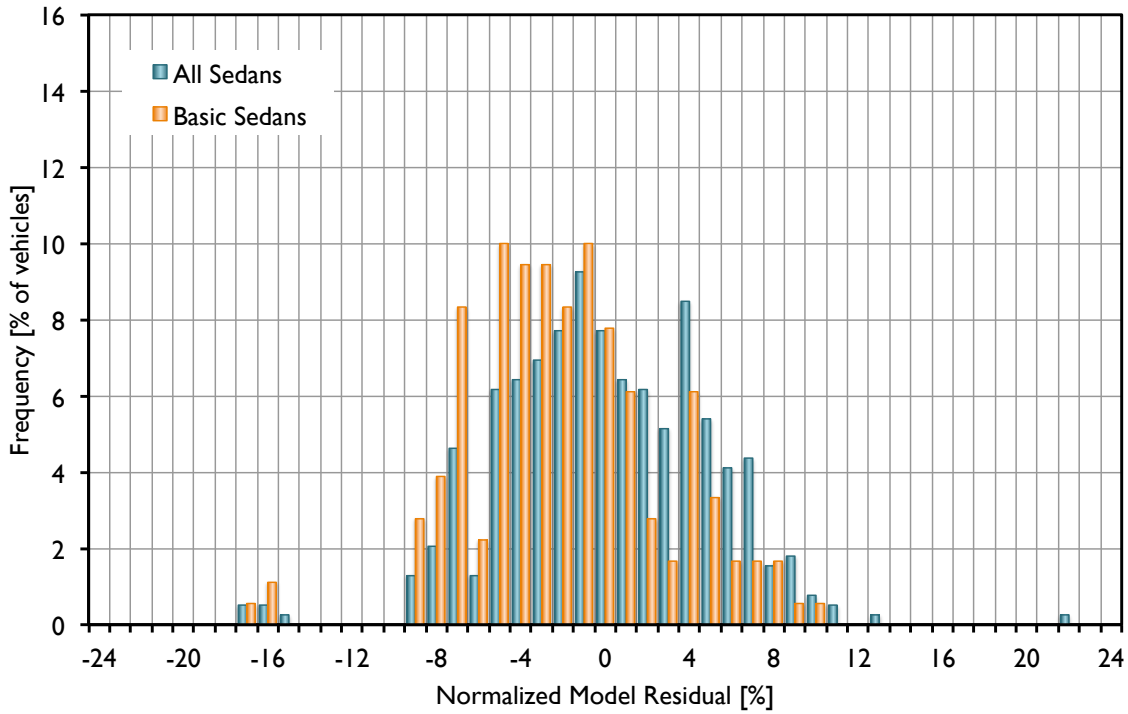

Figure 33: Distribution of Normalized Model Residuals for Basic Sedans.

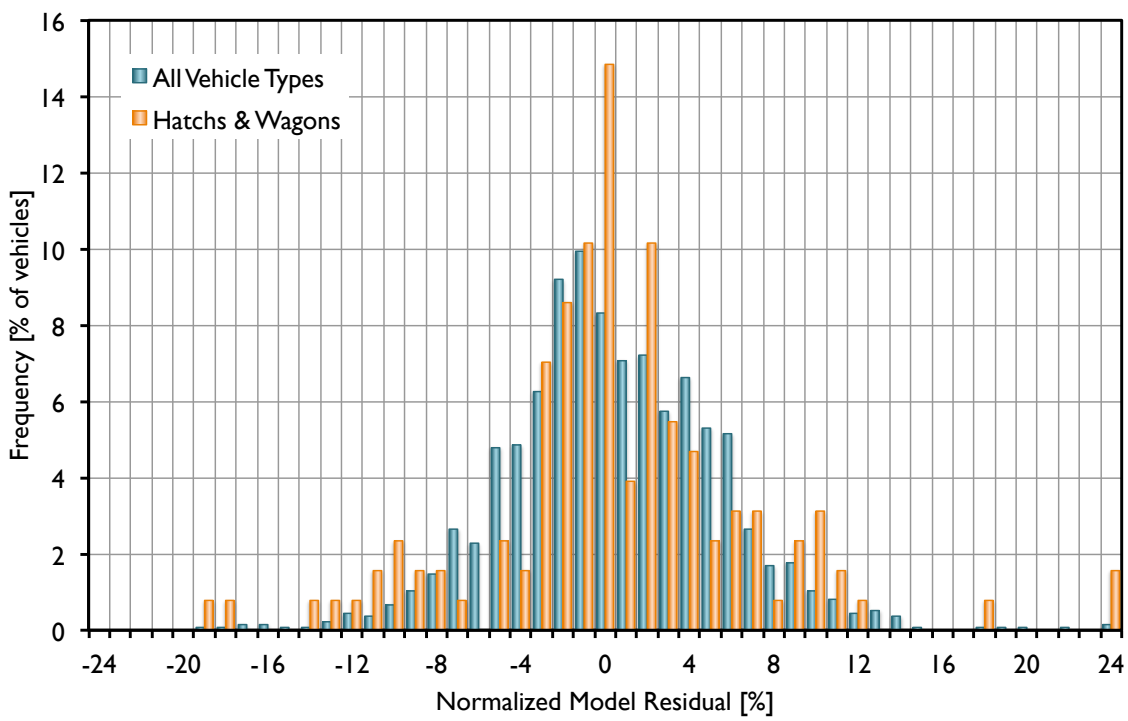

Figure 34: Distribution of Normalized Model Residuals for Hatchbacks & Wagons.

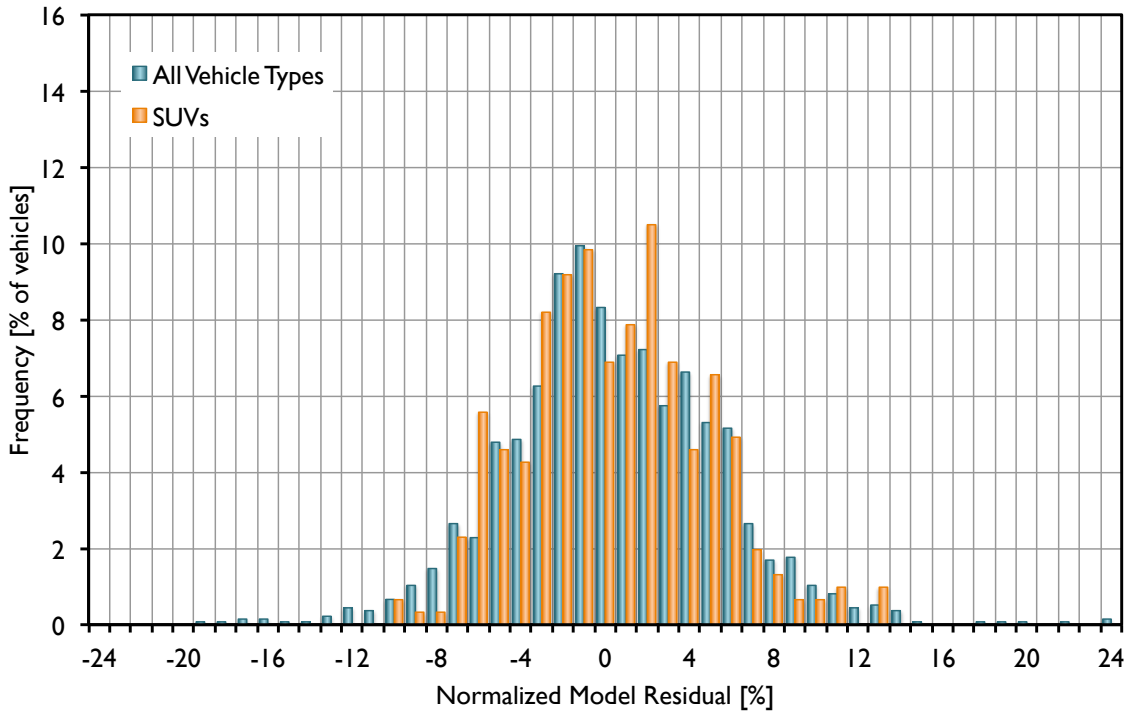

Figure 35: Distribution of Normalized Model Residuals for SUVs.

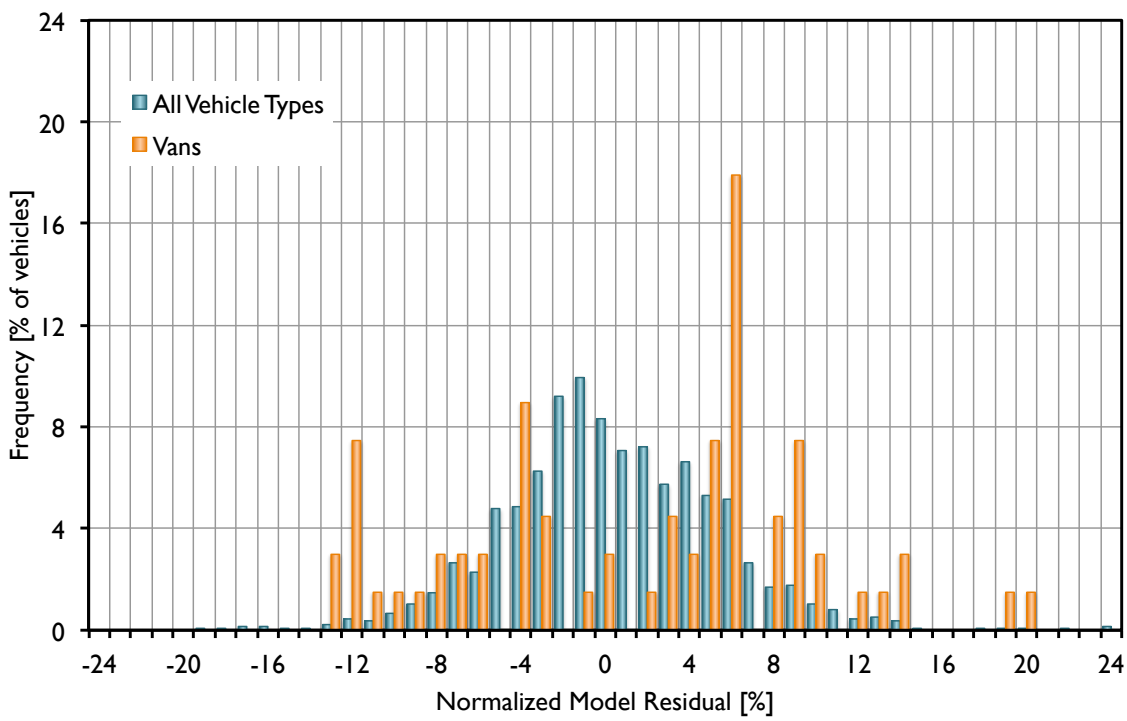

Figure 36: Distribution of Normalized Model Residuals for Vans.

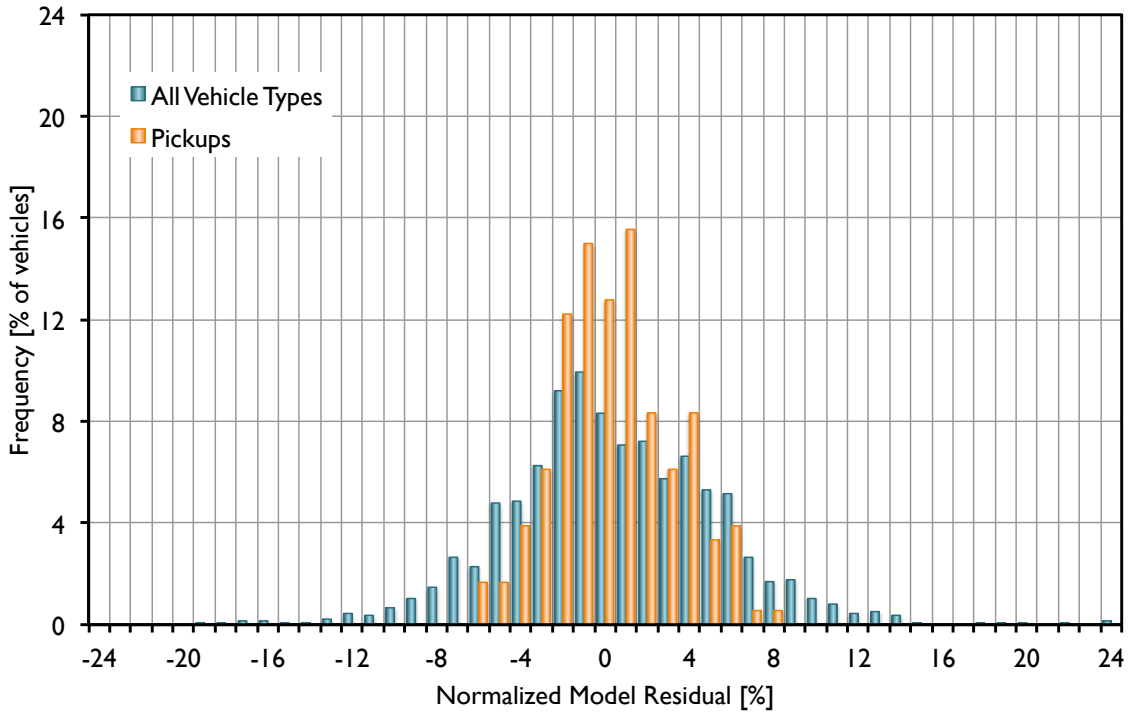

Figure 37: Distribution of Normalized Model Residuals for Pickup Trucks.

Table XIII: Normalized Mass Model Residuals vs. Vehicle Type and Subcategories

Vehicle Type	Sample Size	Median	98th Percentile	95th Percentile	90th Percentile	85th Percentile	75th Percentile
All Types	1358	-0.3	-10.3	-7.9	-5.9	-4.9	-3.1
Coupe	163	-0.4	-8.5	-7.7	-5.8	-4.8	-3.0
Convertible	126	-0.5	-10.4	-9.1	-6.7	-5.3	-3.8
Sedan	389	-0.7	-9.3	-7.8	-6.4	-5.1	-3.7
Basic Sedan	*180*	*-2.7*	*-9.7*	*-8.5*	*-7.6*	*-7.2*	*-5.3*
Luxury Sedan	*209*	*1.6*	*-7.1*	*-5.5*	*-4.0*	*-2.9*	*-1.7*
Hatchback & Wagon	128	-0.3	-14.0	-11.0	-8.4	-4.0	-2.6
SUV	305	-0.3	-7.3	-6.7	-5.8	-4.5	-3.1
Van	67	3.4	-12.9	-12.2	-11.6	-8.8	-4.8
Pickup	180	-0.4	-5.4	-4.6	-3.6	-2.8	-2.1

7. PROJECTION METHODOLOGY

To support the goals of the research project, it was necessary to generate projections for tailpipe CO_2 emissions for the baseline data set of light-duty vehicles and for the same vehicles in a load-reduced configuration. The tools and processes to generate these projections must allow for the evaluation of improved aerodynamics, lower tire rolling resistance, reduced mass, power source re-sizing, and reduced on-board energy storage requirements to maintain driving range [3]. The projection output must include fuel consumption, tailpipe CO_2 emissions, driving range, and acceleration performance. The tailpipe CO_2 emissions will be combined with vehicle sales to generate baseline and load-reduced fleet scenarios.

A. Analysis Software

CT-ENERGY™ [88] was used to compute fuel consumption, tailpipe CO_2 emissions, and acceleration performance for each vehicle. Embedded in the CT-ENERGY™ models are energy conversion efficiency maps for all combinations of engines, engine features, transmissions, drivelines, and motors. Additionally, the energy conversion efficiency maps are automatically modified for attributes such as compression ratio, cylinder surface-to-volume ratio, and high pressure pump losses. Vehicle load elements (weight and road load) can be predicted (based on vehicle parameters) or input by the user. CT-ENERGY™ calculates and stores over 600 variables for each vehicle. For the current research, the critical output variables are provided in Table XIV.

B. Load Scenario Overview

Five scenario iterations were generated to allow an assessment of the individual load changes, requiring approximately 6800 vehicle iterations (1358 vehicles x 5 iterations):

1. Baseline Load
2. Non-mass load reduction to proposed best-in-class aerodynamics and best-in-class tire rolling resistance
3. Scenario 2 + Mass-reduced to proposed best-in-class mass-efficiency plus non-mass load reduction
4. Scenario 3 + Power source re-sizing
5. Scenario 4 + On-board energy storage re-sizing

For each iteration, fuel consumption, tailpipe CO_2 emissions, driving range, and acceleration performance were projected for each vehicle. Specific details are provided in the following sections for each load scenario.

Table XIV: CT-ENERGY™ Output Variables to Support the Research Plan.

Attribute	Description/Notes
Vehicle Energy Intensity	Vehicle energy required due to mass (kinetic) and road load (aerodynamics, tires, brakes, hubs). Reported for city (FTP), highway (HWFET), and combined (55%/45% harmonic average of FTP and HWFET) as MJ/km and MJ/mile
Energy Conversion Efficiency	Energy conversion efficiency of the powertrain, including parasitic losses. Reported as a percentage for FTP, HWFET, and combined.
Energy Supplied	Energy (fuel and/or electrical) required by the powertrain. Reported as a MJ/km or MJ/mile for FTP, HWFET, and combined.
Fuel Consumption	Energy supplied reported as fuel volume or electrical energy per unit distance.
Fuel Economy	Energy supplied reported as distance per unit fuel volume.
CO_2 Emissions	Tailpipe CO_2 emissions. Reported as g/km and g/mile for FTP, HWFET, and combined.
Range	The distance that can be traveled using the on-board energy storage (fuel and/or electrical energy). The value will be based on the combined fuel economy.
Acceleration Performance	Acceleration performance at full power from a stop. Reported as time to 30 mph and 60 mph.

C. Baseline Load Scenario

For most of the vehicles in the data set, the baseline road load coefficients were those provided in the MY 2014 vehicle data set. However, there are three cases that required adjustments to the values in the data set:

1. When the estimated aerodynamic drag coefficient was implausible (too low), a best-in-class C_d will be assigned, and the change in the aerodynamic C-coefficient will be added to the manufacturer-reported road load.
2. When the estimated tire rolling resistance coefficient was implausible (too low), a best-in-class tire rolling resistance coefficient will be assigned, and the increase will be added to the manufacturer-reported road load coefficients.
3. When the equivalent test weight computed from the curb weight does not match the ETW associated with the manufacturer-reported road load coefficients, the tire rolling force contribution will be computed and subtracted or added to the manufacturer-reported road load coefficients.

To validate the baseline, the vehicle energy intensity (defined in Table XV) was computed for the manufacturer-reported ETW and road load coefficients and the adjusted ETW and road load coefficients. The baseline fuel consumption, tailpipe CO_2 emissions, and acceleration were computed and compared to the reported values.

D. Non-Mass Load Reduction Scenario

Starting from the baseline road load coefficients, coefficients for the non-mass load reduced scenarios were generated for vehicles that have a C_d and/or a tire RRC that are higher than the assigned best-in-class.

When a vehicle's baseline C_d was lower (better) than the best-in-class value, no aerodynamic adjustments were applied to the baseline road load coefficients. For vehicles with an estimated C_d that was higher than the best-in-class value, a new aerodynamic C-coefficient was computed and applied to the baseline road load coefficients. If a vehicle's baseline tire RRC was lower (better) than the best-in-class value, no tire RRC adjustments were applied to the baseline road load coefficients. For vehicles with an estimated tire RRC that was higher than the best-in-class value, new tire road load coefficients were computed and applied to the baseline road load coefficients.

To quantify the vehicle load benefit of the non-mass load reduction scenario, the vehicle energy intensity was computed from the load-reduced road load coefficients and baseline ETW. The fuel consumption, tailpipe CO_2 emissions, and acceleration were then computed and the results compared to the baseline scenario.

E. Mass-Reduced plus Non-Mass Load Reduction Scenario

For vehicles with a mass efficiency that is worse than best-in-class, a new curb weight was computed using equation 27. A new ETW was applied if required.

Since a reduction in vehicle weight will lower the tire rolling force, the force reduction was computed and subtracted from the non-mass load reduced road load coefficients. This contribution was computed assuming the tire RRC from the previous step.

To quantify the vehicle load benefit of the mass-reduced plus non-mass load reduction scenario, the vehicle energy intensity was computed from the load-reduced road load coefficients and mass-reduced ETW. The fuel consumption, tailpipe CO_2 emissions, and acceleration were then computed and the results compared to the baseline and non-mass load reduced scenarios.

F. Power Source Resizing

Acceleration performance will improve for the mass-reduced vehicles. Consequently, the power source can be re-sized to maintain the baseline performance. Therefore, the engine displacement (or motor size for electric vehicles) was reduced until the acceleration performance was similar to the performance projected during the baseline scenario. The 0-30 mph and 0-60 mph times were used as the proxy for overall performance. The fuel consumption, tailpipe CO_2 emissions, and acceleration were then computed and the results compared to the baseline and load reduced scenarios.

G. On-board Energy Storage Resizing

The driving range is a product of the on-board energy storage capacity and the fuel/electric consumption rate. The combination of the reduced vehicle load and re-sized power source will result in an extension of the driving range. Therefore, the on-board energy storage was re-sized to achieve the baseline range. The resulting mass reduction was subtracted from the mass-reduced curb weight and the road load coefficients were updated to reflect the change in tire rolling force. The fuel consumption, tailpipe CO_2 emissions, and acceleration were then computed and the results compared to the baseline, load reduced, and re-sized power source scenarios.

H. Fleet Scenario

With each of the above vehicle-load iterations, sales-weighted unadjusted combined tailpipe CO_2 emissions (g/mile) were computed for a California light-duty fleet, using sales volumes provided by CARB. Additionally, sales-weighted reductions in mass, aerodynamics, tire rolling resistance, and vehicle energy intensity were computed as a method of quantifying the total changes in vehicle load. Likewise, sales-weighted engine displacement, motor size, and on-board energy storage capacity were computed to quantify those changes.

8. RESULTS

The results of the analysis are provided in three sections. The first section describes the changes in the load attributes: aerodynamic drag, tire rolling resistance, and mass. The second section presents the reduction of vehicle energy intensity that results from the change in the load attributes. Vehicle energy intensity is the most important metric of the evaluation as it combines the changes in aerodynamic drag, tire rolling resistance, and mass into a single metric that is directly correlated to the change in CO_2 emissions. Finally, the energy conversion efficiency, fuel consumption, and tailpipe CO_2 emission projections are provided in the third section. Tabular results are provided in Appendix B.

The results are presented as both un-weighted and sales-weighted averages. However, the sales-weighted average is the more important metric as it provides a better estimate of the impact of the load attribute changes on the entire population of new light-duty vehicles.

A. Load Attributes

As shown in figure 38, the sales-weighted average C_d of the baseline fleet is estimated to be 0.333. Applying the best-in-class aerodynamic drag to each vehicle (or maintaining the C_d if better than the best-in-class value) resulted in a sales-weighted C_d of 0.298, representing a 10.6% reduction. As discussed earlier, the proposed best-in-class values for C_d were 8% to 12% lower than the median value; consequently the result is not unexpected. The un-weighted average C_d was higher than the sales-weighted C_d, indicating that the sales are biased toward vehicle classes with lower drag, such as sedans and coupes.

The tire rolling resistance results are provided in figure 39. Applying best-in-class tire RRC (or maintaining the RRC if better than the best-in-class value) resulted in the sales-weighted average tire RRC dropping from 8.2 kg/1000 kg to 7.2 kg/1000 kg, an 11.4% reduction. The sales-weighted average value is lower than the best-in-class values because approximately 20% of the vehicles had an estimated RRC value that was already lower and, therefore, did not change. As noted earlier, the proposed best-in-class values for tire RRC were 11% to 14% lower than the median value; consequently the result is expected. The average tire RRC was higher than the sales-weighted tire RRC, indicating that the sales are biased toward vehicles with lower tire rolling resistance.

The sales-weighted average curb weight of the fleet is estimated at 1633 kg (3600 lb) as shown in figure 40. Applying best-in-class mass efficiency resulted in a 7.8% reduction of sales-weighted curb weight to 1505 kg (3318 lb) for a total mass reduction of 128 kg (282 lb). The sales-weighted equivalent test weight was reduced from 1771 kg (3904 lb) to 1642 kg (3620 lb) or 7.3% as shown in figure 41. The absolute change in curb weight and ETW was approximately the same. The lower percent reduction associated with ETW is due to the larger value. The ETW represents the loaded vehicle condition and is, therefore, a more important value for this study. Sales-weighted values for mass were lower than the un-weighted average indicating that the sales are biased toward lighter vehicles, such as sedans and coupes, rather than large SUVs and pickup trucks.

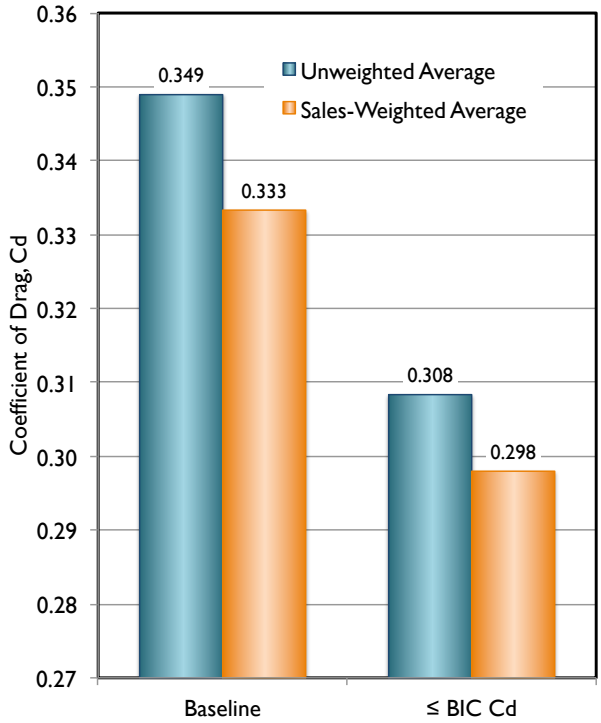

Figure 38: Un-Weighted and Sales-Weighted C_d vs. Baseline and Best-in-Class (BIC)

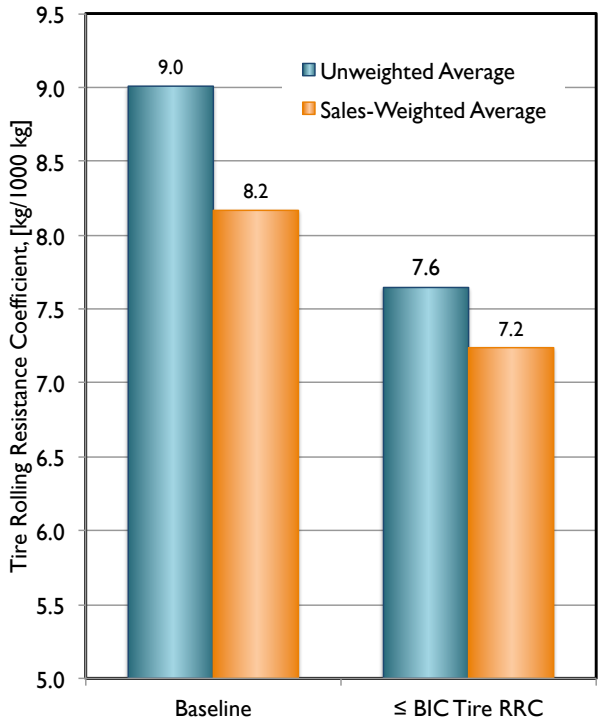

Figure 39: Un-Weighted and Sales-Weighted Tire RRC vs. Baseline and Best-in-Class (BIC)

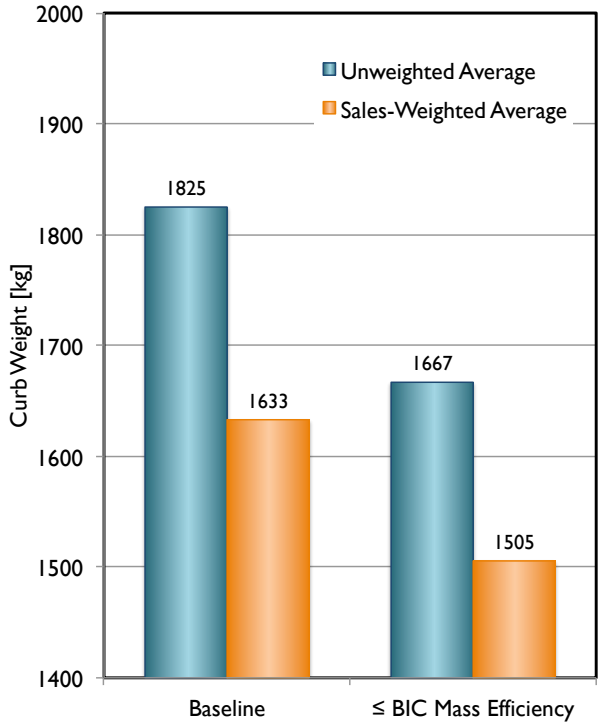

Figure 40: Un-Weighted and Sales-Weighted Curb Weight vs. Baseline and Best-in-Class (BIC)

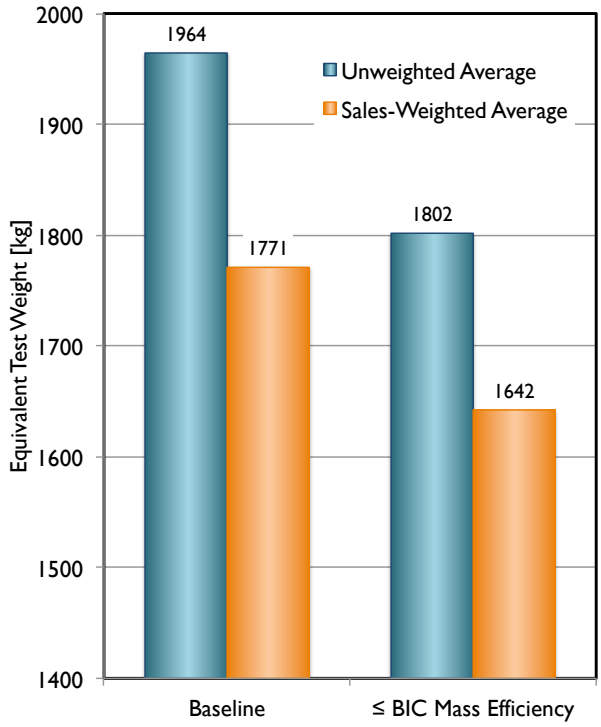

Figure 41: Un-Weighted and Sales-Weighted ETW vs. Baseline and Best-in-Class (BIC)

The secondary benefit of lower weight is a reduction of tire rolling force, which is the product of mass and rolling resistance coefficient as shown in equation 23. This result is provided in figure 42. The combination of best-in-class tire RRC and mass efficiency yielded a 17.8% reduction of sales-weighted tire rolling force at 80 kph, from 142 N to 117 N. The lower mass contributed to a 6.4% reduction (36% of the total) in tire rolling force.

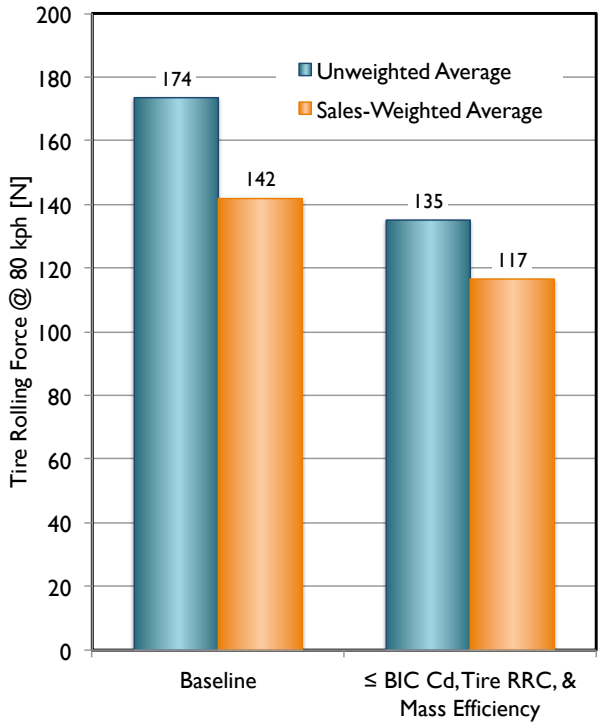

Figure 42: Un-Weighted and Sales-Weighted Tire Rolling Force vs. Baseline and Best-in-Class (BIC)

B. Vehicle Energy Intensity

The change in the load attributes described in the previous section is not directly correlated to a reduction in vehicle energy (e.g., a 10% reduction in aerodynamic drag does not result in a 10% reduction in vehicle energy). Each attribute has a different effect on vehicle energy and, therefore, CO_2 emissions, depending upon the drive cycle. For this research, one of the most important metrics from the analysis is the vehicle energy intensity over the combined cycle (defined in table XIV).

To visualize the range of vehicle energy intensity among the vehicles in the fleet, the results for the main load reduction scenarios are presented in figures 43 through 45. For each chart, the baseline vehicle energy intensity is represented on the horizontal axis while the load-reduced vehicle energy intensity is represented by the vertical axis. A data point represents each of the 1358 vehicles. Vehicles that are the furthest below the baseline reference line were the most impacted by the load reduction. The correlation (y = cx) shown is indicative of the average load reduction.

Applying best-in-class C_d, resulted in an average load reduction of ~3½% for the combined cycle. However, the energy level for some individual vehicles was reduced by over 15%. Adding best-in-class tire RRC increased the average load reduction to a total of ~7½%, while the maximum load reduction for some individual vehicles exceeded 20%. Finally, adding best-in-class mass efficiency further reduced the average load reduction to a total of ~12½% with the load reduction for individual vehicles reaching 30%.

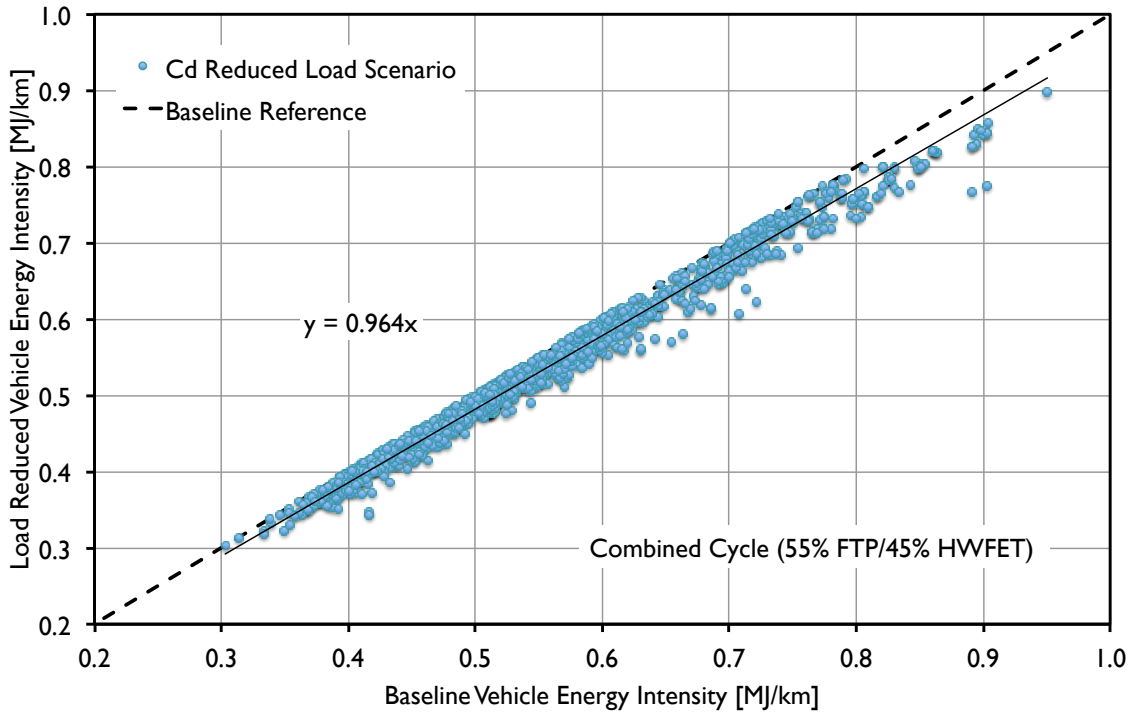

Figure 43: Vehicle Energy Intensity for the Best-in-Class C_d Load Scenario

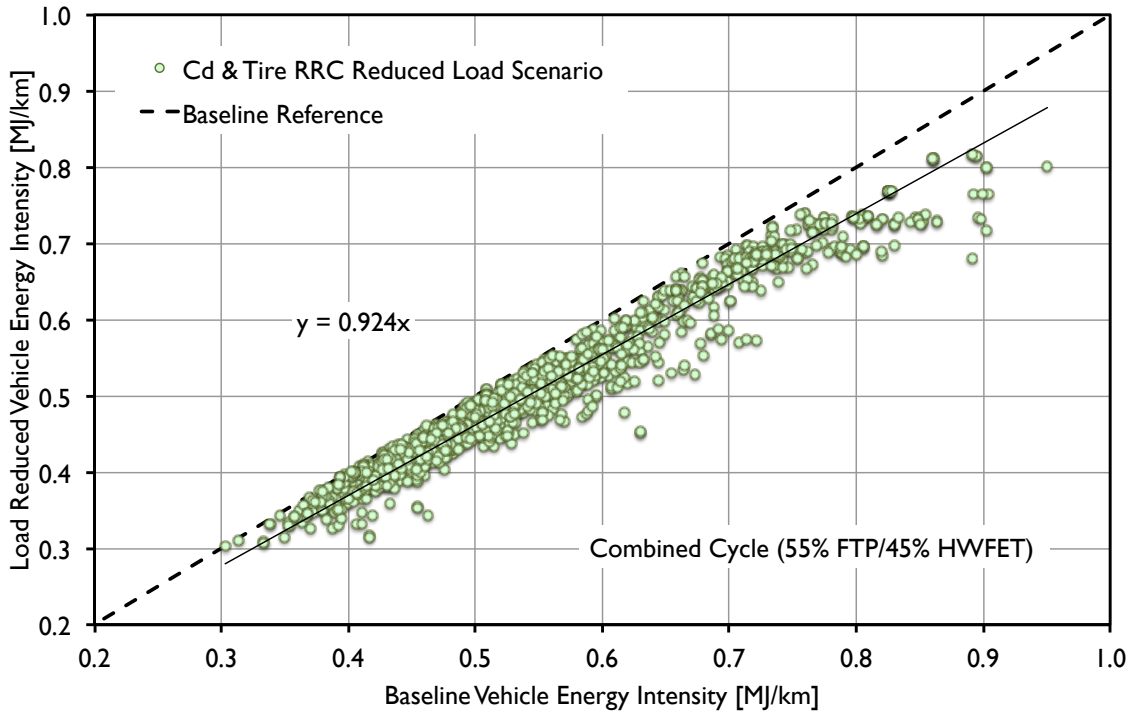

Figure 44: Vehicle Energy Intensity for the Best-in-Class C_d and Tire RRC Load Scenario

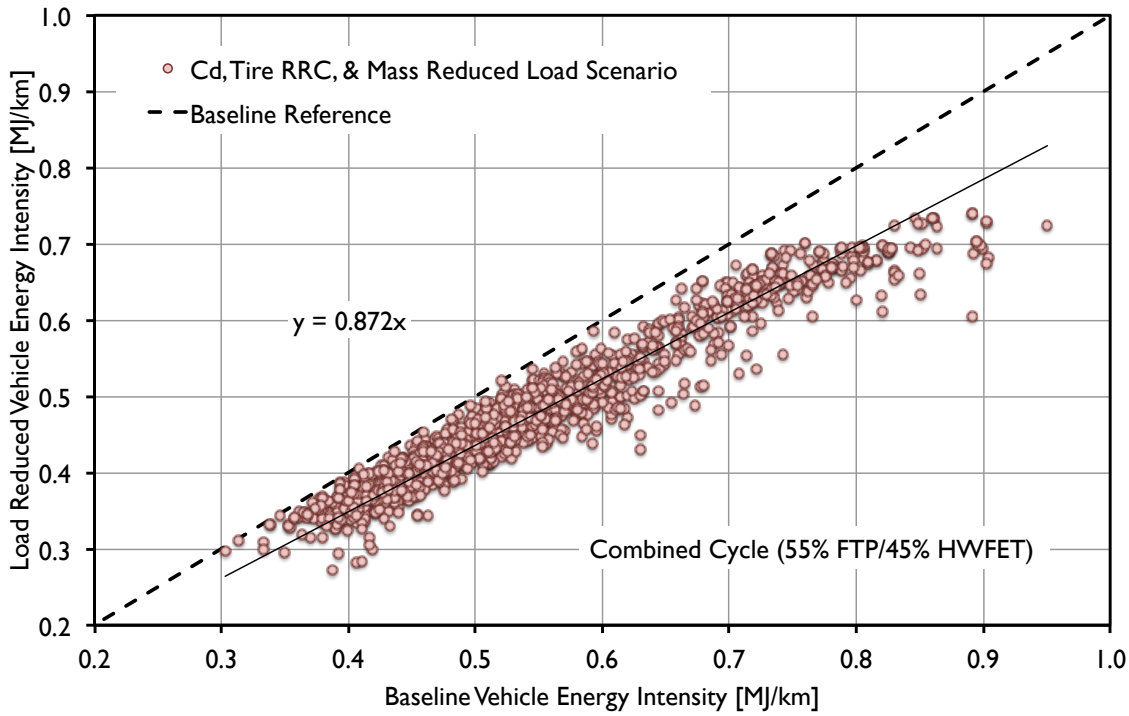

Figure 45: Vehicle Energy Intensity for the Best-in-Class C_d, Tire RRC, and Mass Efficiency Load Scenario

The un-weighted and sales-weighted averages for vehicle energy intensity are provided in figure 46 for each of the six load scenarios. The sales-weighted energy intensity of the baseline fleet is estimated at 0.488 MJ/km. The combination of reduced aerodynamic drag, lower tire rolling resistance, and improved mass efficiency yielded a sales-weighted vehicle energy intensity of 0.436 MJ/km; a reduction of 10.6%. Reducing the on-board energy storage had minimal impact on the overall weight, bringing the total energy reduction to 10.7%.

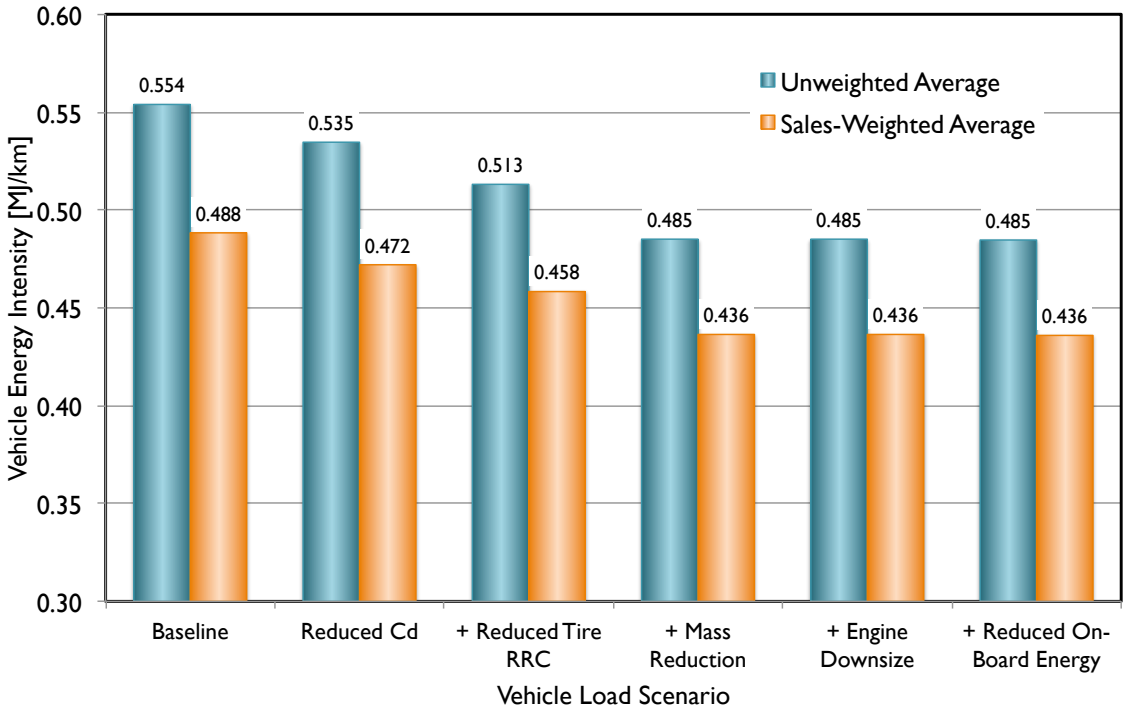

Figure 46: Average Vehicle Energy Intensity vs. Load Scenario

By computing the ratio of the reduction in load attribute to the reduction in vehicle energy intensity, average values can be generated to support the discussion of other load reduction scenarios. The energy-to-attribute ratios from this study are provided in table XV.

Table XV: Vehicle Energy Intensity-to-Load Attribute Ratios.

Load Attribute	Vehicle Energy Intensity Change
Aerodynamic Drag	3.1% per 10% change in Cd
Tire Rolling Resistance	2.6% per 10% change in RRC
Curb Weight	5.8% per 10% change in Mass

C. Energy Conversion Efficiency, Fuel Consumption, and Carbon Dioxide Emissions

The reported and projected fuel economy and tailpipe CO_2 emissions are provided in figures 47 and 48 for the baseline condition. As shown, the projections provided good agreement with the reported values. Multiple unknowns during the simulation process limit the ability to generate the same fuel economy and CO_2 emissions values as reported. These unknowns include the unique energy efficiency maps and control system settings (e.g., transmission shift schedules) for each of the hundreds of powertrain combinations in the vehicle data set. Additionally, due to the certification and fuel economy labeling process, it is not possible to precisely align, for every vehicle, the published fuel economy result with the available equivalent test weight and road load coefficients. The published fuel economy is often the result of multiple tests, can cover multiple vehicle configurations, or can represent an analytically derived value. Finally, facility-to-facility, vehicle-to-vehicle, test-to-test, and driver-to-driver variations that are present in the reported values contribute to the variation.

All powertrain elements (i.e., engine, motor, transmission, driveline) become less efficient as the operating load is reduced. Consequently, as a result of the reduced aerodynamic drag, tire rolling resistance, and curb weight, the projected sales-weighted powertrain efficiency dropped from 22.0% to 21.1% (4.3% loss). This is shown in figure 49. The result of this efficiency loss is to limit the full benefit of the reduction in vehicle energy intensity. Reducing the size of the power source to maintain acceleration performance increased the projected efficiency to 21.5%. While downsizing the power source to maintain acceleration performance recovers some of the lost efficiency, the powertrain system would need to be fully optimized to return to the baseline efficiency. Determining the details of such a powertrain re-optimization is out of the scope of this study, however, it is reasonable to assume that the average baseline efficiency (22%) could be recovered.

As shown in figure 50, fuel/electrical energy intensity was reduced by 6.6% by applying the proposed best-in-class aerodynamic drag, tire rolling resistance, and mass efficiency. Recovering some of the lost powertrain efficiency through power source downsizing improved the sales-weighted fuel consumption reduction to 8.3%. The reduced on-board energy storage, to maintain range, had minimal effect. The improvement in fuel economy followed the reduction in fuel consumption. A sales-weighted improvement of 3.0 mpg (9.1%) was projected if best-in-class aerodynamic drag, tire rolling resistance, and mass efficiency were applied and the power source was downsized to maintain acceleration performance as shown in figure 52.

The reduction of tailpipe CO_2 emissions followed the fuel consumption trends as presented in figure 52. More specifically, the 10.6% lower C_d provided a 5 g/mile benefit to CO_2 emissions. The addition of lower rolling resistance tires provided an additional 5 g CO_2/mile benefit and the 128 kg (282 lb) mass reduction further reduced CO_2 emissions by 7 g/mile. A sales-weighted reduction of 22 g CO_2/mile (8.3%) was projected if best-in-class aerodynamic drag, tire rolling resistance, and mass efficiency were applied and the power source was downsized to maintain acceleration performance.

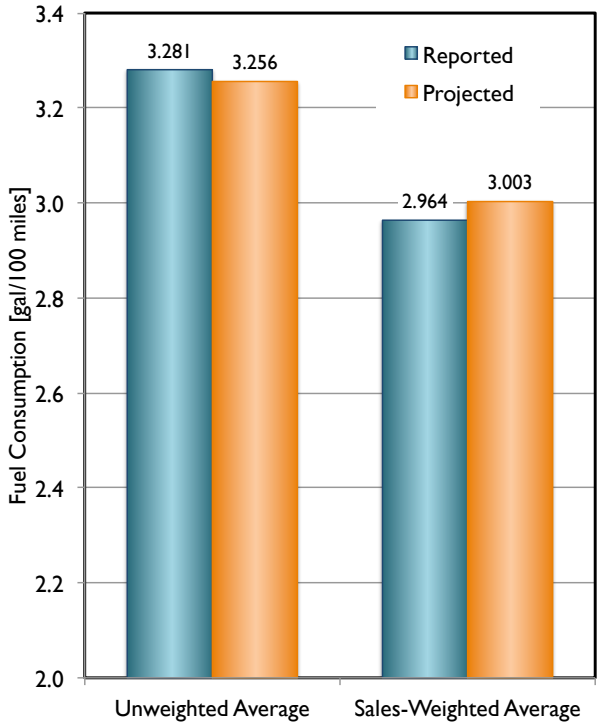

Figure 47: Reported vs. Projected Fuel Consumption (Combined Cycle) for the Baseline Condition

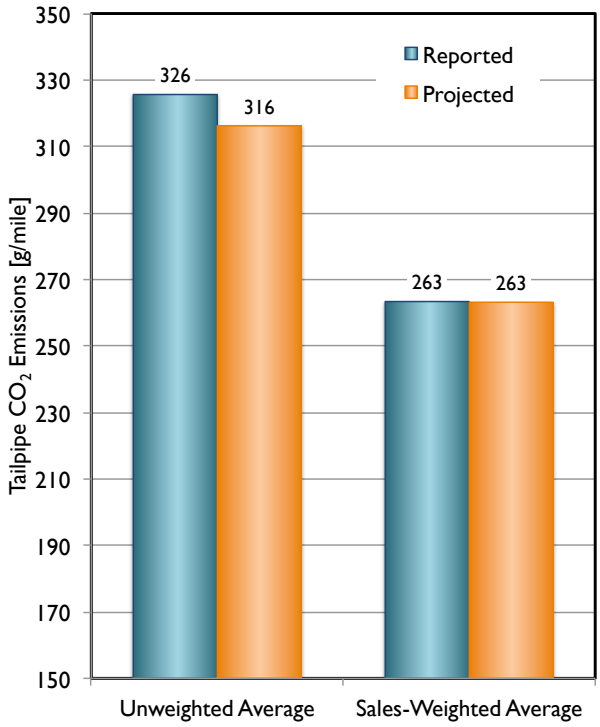

Figure 48: Reported vs. Projected Tailpipe CO_2 Emissions (Combined Cycle) for the Baseline Condition

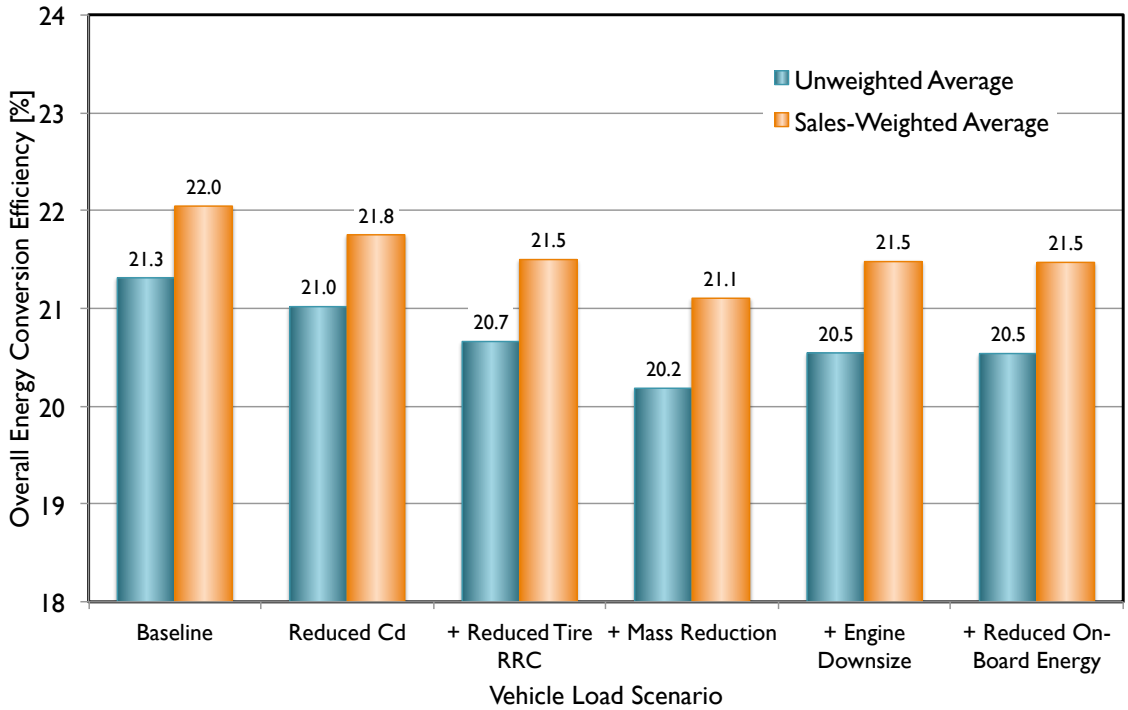

Figure 49: Average Energy Conversion Efficiency vs. Load Scenario

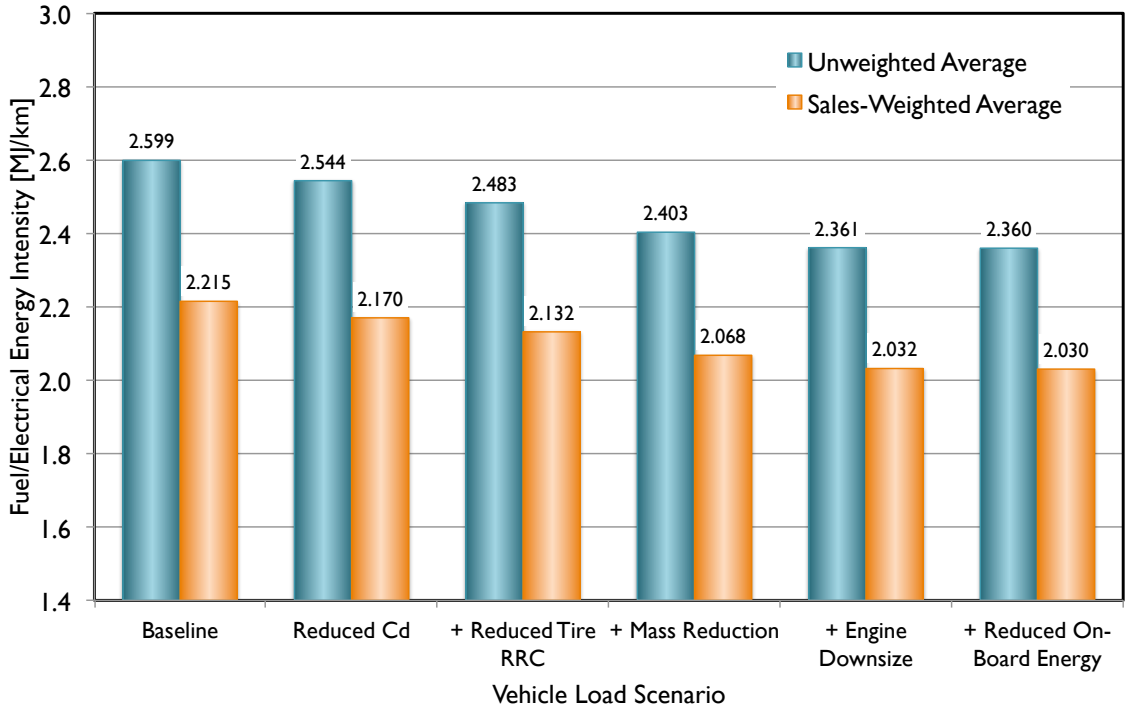

Figure 50: Average Fuel/Electric Energy Intensity vs. Load Scenario

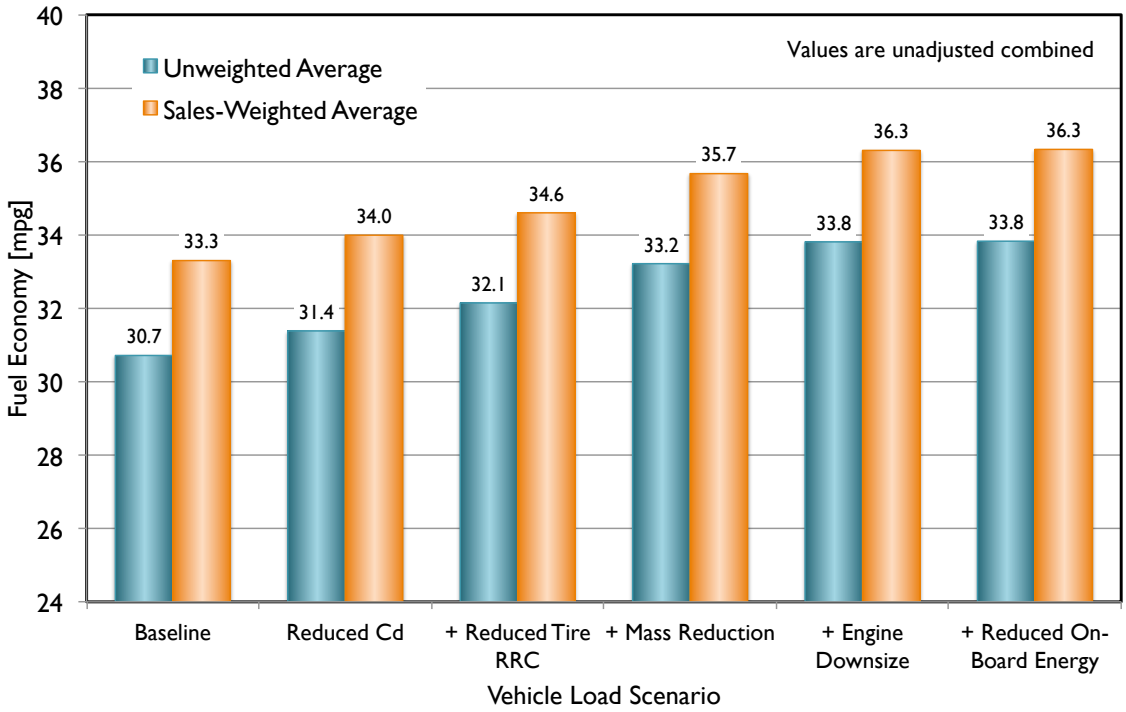

Figure 51: Average Fuel Economy vs. Load Scenario (Combined Cycle)

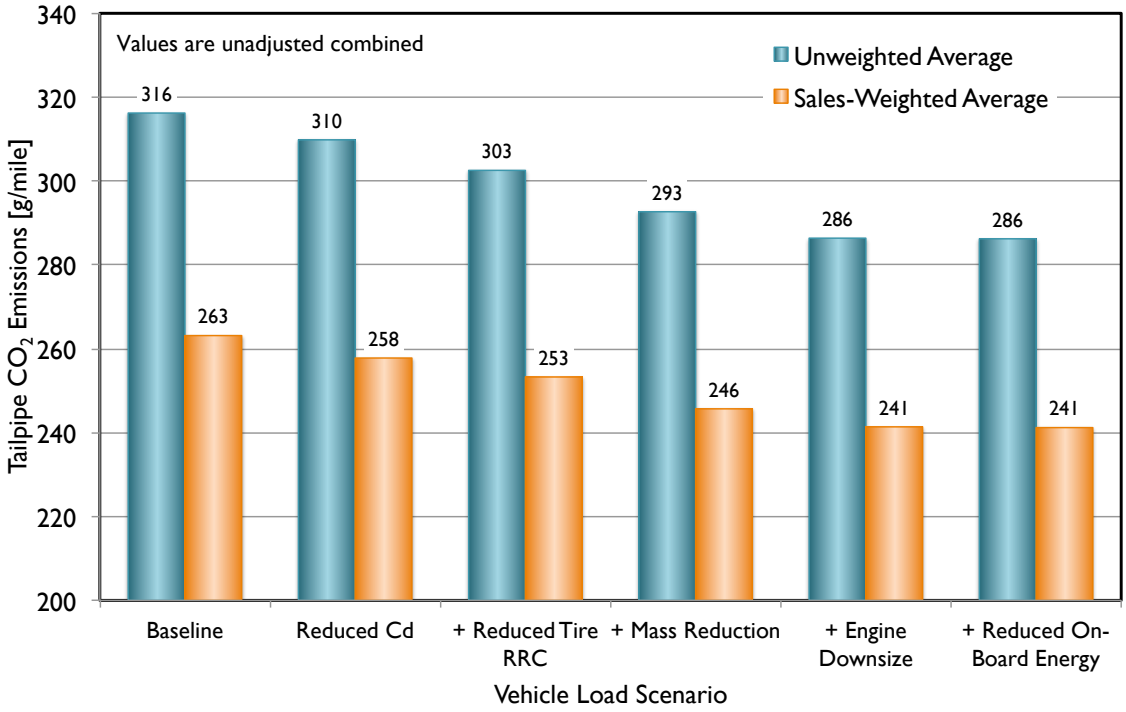

Figure 52: Average Tailpipe CO_2 Emission vs. Load Scenario (Combined Cycle)

9. SUMMARY AND CONCLUSIONS

Based on a comprehensive review of vehicle load attributes and load reduction technologies, the MY 2014 light-duty vehicle fleet includes a variety of load reducing technologies and strategies. The results of this study suggest that there is opportunity to reduce the vehicle energy intensity of the fleet by over 10% by fully applying aerodynamic drag, tire rolling resistance, and mass technologies and strategies that exist in production vehicles today. Consequently, it is reasonable to suggest that these changes could be readily applied, along with powertrain re-matching, during vehicle redesigns over the next decade in support of the MY 2025 standards for GHG emissions.

Reducing vehicle loads through these reductions in aerodynamic drag, tire rolling resistance, and mass efficiency, along with re-sizing the powertrain system to maintain equivalent performance, could reduce mobile source tailpipe CO_2 emissions by 8.3%. The benefit to CO_2 emissions was not commensurate with the load reduction due to a loss in energy conversion efficiency. To recover all of the lost efficiency, the powertrain system would need to be fully re-optimized. While determining the details of such a re-optimization is out of the scope of this study, it is reasonable to assume that the average baseline efficiency (22.0%) could be attained. If the baseline efficiency were to be fully recovered, the potential CO_2 emission reduction could increase to 10.4%. The majority (64%) of this CO_2 emissions benefit is the direct result of the reduced vehicle load. Re-matching the powertrain to take advantage of the lower loads provides the remaining benefit. The potential improvement of CO_2 emissions represents nearly one third of the 34% reduction required to support California's Advanced Clean Cars program.

Assuming the current fleet mix, powertrain technology, and deployment of road load reduction technologies already in production across the entire fleet, the potential reduction of mobile source CO_2 emissions is between 22 g/mile (8.3%) and 27 g/mile (10.4%). Given the current new vehicle fleet of 1.83 million units per year, the potential reduction in mobile source GHG load is between 40 and 50 metric tons per mile traveled. Future changes to fleet mix and powertrain technology deployment will change the absolute levels (i.e., g/mile) of potential mobile source CO_2 emissions reduction, however, the fractional benefit (~10%) is expected to remain as long as the internal combustion engine is the dominant light-duty vehicle power source.

10. RECOMMENDATIONS

The research could be updated at a regular cadence to understand both the trends of the industry as well as the performance of emerging technologies and strategies that are introduced in subsequent model years. Additionally, a similar assessment can be applied to the heavy-duty vehicle fleet. Finally, the evaluation could be expanded to better assess the real world benefit of vehicle load reduction rather than the benefit estimated solely from the urban and highway certification cycles used for certification.

REFERENCES

[1] California Air Resources Board, "California's Advanced Clean Cars program," http://www.arb.ca.gov/msprog/consumer_info/advanced_clean_cars/consumer_acc.htm.

[2] Environmental Protection Agency, "EPA and NHTSA Set Standards to Reduce Greenhouse Gases and Improve Fuel Economy for Model Years 2017-2025 Cars and Light Trucks," EPA-420-F-12-051, August 2012.

[3] California Air Resources Board, "Technical Analysis of Vehicle Load-Reduction Potential for Advanced Clean Cars," Request for Proposal No. 13-313, July 30, 2013.

[4] Jaguar Land Rover, "2014 Range Rover Sport Press Kit (US)," http://newsroom.jaguarlandrover.com/en-us/land-rover/press-kits/2013/11/2014-land-rover-press-kit_us/2014-range-rover-sport-press-kit/

[5] Porsche, http://press.porsche.com/vehicles/2014/Press%20Information-%20Porsche_Cayenne_US.pdf

[6] Mitsubishi, "2014 Mitsubishi Outlander – Smartly Styled and Engineered," http://media.mitsubishicars.com/releases/8e82ebb6-573a-4c76-9203-66e8ca23509f, March 19, 2013.

[7] Nissan, "2014 Nissan Versa Note Press Kit," http://nissannews.com/en-US/nissan/usa/presskits/us-2014-nissan-versa-note-press-kit

[8] BMW, "Introducing The All-New 6th Generation BMW 3 Series Sedan Dynamic, Efficient and Luxurious," http://www.bmwusanews.com/newsrelease.do?id=935&mid=, February 10, 2012.

[9] BMW, "The All-New BMW 4 Series Convertible," http://www.bmwusanews.com/newsrelease.do?id=1862&mid=, October 12, 2013.

[10] BMW, "The All-New BMW 4 Series Coupe," http://www.bmwusanews.com/newsrelease.do?id=1727&mid =, June 14, 2014.

[11] Honda, "2012 Acura TL – Chassis," http://www.hondanews.com/channels/acura-automobiles-tl/releases/2012-acura-tl-chassis, March 9, 2011.

[12] Porsche, "The New Porsche 911," http://press.porsche.com/vehicles/12_press_kits/pdf/2012_911_Product_Info.pdf

[13] Society of Automotive Engineers, "Audi tackles 'huge challenge' of lightweighting the A3," http://articles.sae.org/11121/, June 18, 2012.

[14] General Motors, "2014 GMC SIERRA 1500 BRINGS BOLD REFINEMENT TO FULL-SIZE TRUCKS," http://media.gm.com/media/us/en/gmc/vehicles/sierra/2014.html, November 11, 2013.

[15] Honda, "2014 Acura RLX Sport Hybrid SH-AWD: Body," http://www.hondanews.com/channels/acura-automobiles-rlx-technical/releases/2014-acura-rlx-sport-hybrid-sh-awd-body, March 9, 2011.

[16] Society of Automotive Engineers, "Nissan develops high-volume, fully recyclable composite liftgate," http://articles.sae.org/13346/, July 14, 2014.

[17] Chrysler, "The All-new 2013 Dodge Dart Redefines Performance," http://media.chrysler.com/newsrelease.do?id=11878&fIId=11857&mid=324, April 28, 2012.

[18] Honda, "2014 Honda Accord Hybrid: Body," http://www.hondanews.com/channels/honda-automobiles-accord-press-kit/releases/2014-honda-accord-hybrid-sedan-body, October 10, 2013.

[19] General Motors, "2014 CHEVROLET CAMARO Z/28 IS THE MOST TRACK-CAPABLE EVER," http://media.gm.com/media/us/en/chevrolet/vehicles/camaro-z28/2014.html

[20] General Motors, 2014 CADILLAC XTS OFFERS TWIN-TURBO V-6, AUTOMATIC PARKING ASSIST," http://media.gm.com/media/us/en/cadillac/vehicles/xts/2014.html

[21] Volkswagen, "2014 VOLKSWAGEN TOUAREG: SPORT UTILITY LUXURY THAT'S PRICED WITHIN REACH," http://media.vw.com/model/pack/57/

[22] Bugatti, "Lightweight Construction Concept," http://www.bugatti.com/en/veyron/technology/structure.html

[23] Honda, "2012 Honda Civic - Body and Chassis," http://www.hondanews.com/channels/Civic-Press-Kit/releases/2012-honda-civic-body-and-chassis, April 20, 2011.

[24] Audi, "2014 Audi Q7 Press Kit," http://www.audiusanews.com/pressrelease/3460/2014-Audi-Q7-Press-Kit, June 20, 2013.

[25] Honda, "2012 Honda Civic - Overview," http://www.hondanews.com/channels/Civic-Press-Kit/releases/2012-honda-civic-overview, April 20, 2011.

[26] Porsche, "Press Information," http://press.porsche.com/vehicles/2013/Boxster_Press_Information.pdf

[27] Ford Motor Company, "Ford Uses High-Strength Steel Plus High Strength Aluminum Alloys on Toughest F-150 Ever," https://media.ford.com/content/fordmedia/fna/us/en/news/2014/01/13/ford-uses-high-strength-steel-plus-high-strength--aluminum-alloy.html, January 13, 2014

[28] General Motors Company, "Engineering, Advanced Materials Help Slim Down Colorado", http://media.gm.com/media/us/en/gm/news.detail.html/content/Pages/news/us/en/2014/mar/0311-colorado.html.

[29] Honda, "2015 Honda Fit – Body," www.hondanews.com/channels/honda-automobiles-fit/releases/2015-honda-fit-body, April 9, 2014.

[30] Kia Motors, "ALL-NEW 2015 KIA SEDONA MAKES GLOBAL DEBUT IN CONJUNCTION WITH THE NEW YORK INTERNATIONAL AUTO SHOW," http://www.kiamedia.com/us/en/models/sedona/2015, April 14, 2104.

[31] Volkswagen, "2015 VOLKSWAGEN GOLF: THE BEST HATCHBACK JUST GOT EVEN BETTER," http://media.vw.com/release/749/, May 12, 2014.

[32] Volvo Car Group, "New Scalable Product Architecture enables Volvo Car Group to move faster towards a crash-free future," https://www.media.volvocars.com/global/en-gb/media/pressreleases/136653/new-scalable-product-architecture-enables-volvo-car-group-to-move-faster-towards-a-crash-free-future, December 12, 2013.

[33] Ducker Worldwide, "2015 North American Light Vehicle Aluminum Content Study," http://www.drivealuminum.org/research-resources/PDF/Research/2014/2014-ducker-report, June 2014.

[34] Novelis, "Novelis Announces $205 Million Investment to Further Expand Global Automotive Aluminum Capacity to 900,000 Tons Annually," http://www.novelis.com/en-us/Pages/News-Releases.aspx, December 17, 2013.

[35] Constellium, "Constellium and UACJ announce plan to create Joint Venture in the United States to produce Body-in-White aluminium sheet for the automotive industry," http://www.constellium.com/media/news-and-press-releases, January 23, 2014.

[36] SGL Group, "BMW Group and SGL Group to triple production capacities at Moses Lake carbon fiber plant," http://www.sglgroup.com/cms/international/press-lounge/news/2014/05/05092014_p.html?__locale=en, May 9, 2014.

[37] Ford Motor Company, "Most Capable" https://media.ford.com/content/fordmedia/fna/us/en/products/trucks/f-150/2015-f150/most-capable.pdf

[38] Ford Motor Company, "Agile Ford Mustang Features All-New Suspension; Performance pack Raises Bar for Handling and Braking" https://media.ford.com/content/dam/fordmedia/North%20America/US/2014/08/21/mustang/15mustang-kit.pdf, July 17, 2014

[39] FCA, "Press Kit: 2015 Alfa Romeo 4C Coupe", http://www.media.chrysler.com/newsrelease.do?id=15725&mid=447, April 16, 2014

[40] Society of Automotive Engineers, "High-strength steel that bends," http://articles.sae.org/12968/, May 22, 2014.

[41] Society of Automotive Engineers, "Carbon-fiber sheet molding compound," http://articles.sae.org/12041/, April 22, 2013.

[42] Society of Automotive Engineers, "Titanium auto parts 3D-printed from low-cost metal powders," http://articles.sae.org/12687/, January 14, 2014.

[43] Honda, "2015 Honda Fit – Exterior," www.hondanews.com/channels/honda-automobiles-fit/releases/2015-honda-fit-exterior, April 9, 2014.

[44] Nissan, "2015 Nissan Murano – 10 Fast Facts," http://nissannews.com/media_storage/downloads/2015-Nissan-Murano-Fast-Facts-NYIAS-4-14.pdf, July 8, 2014.

[45] Society of Automotive Engineers, "Advanced aerodynamics features applied to Mustang," http://articles.sae.org/12878/, March 3, 2014

[46] Society of Automotive Engineers, "Active wheel shutters show Ford's aero focus for 2015 F-150," http://articles.sae.org/11731/, January 15, 2013

[47] Ford Motor Company, "ALL-NEW FORD F-150 REDEFINES FULL-SIZE TRUCKS AS THE TOUGHEST, SMARTEST, MOST CAPABLE F-150 EVER," https://media.ford.com/content/fordmedia/fna/us/en/news/2014/01/13/all-new-ford-f-150-redefines-full-size-trucks.html, January 13, 2014.

[48] Ford Motor Company, "More Aerodynamic Testing Helps the All-New Ford Mustang Slice Through the Air Efficiently and Stay Planted" https://media.ford.com/content/dam/fordmedia/North%20America/US/2014/08/21/mustang/15mustang-kit.pdf, March 26, 2014

[49] Tire Technology International, "Tall story; Bridgestone's Emilio Tiberio reveals the story behind the development of the award-winning 'ologic' technology," Tire Technology International Magazine, March 2014

[50] Rubber News.com, "Goodyear previews tire innovations," http://www.rubbernews.com/article/20140307/NEWS/140309961, March 7, 2014

[51] Environmental Protection Agency, "Verify: Engine and Vehicle Compliance System," epa.gov/otaq/verify.

[52] Environmental Protection Agency, 2014 FEGuide-for DOE1-release dates before 6-14-2014-no-sales-6-13-2014public.xls, June 2014

[53] Environmental Protection Agency, "Test Car List Data Files," epa.gov/otaq/tcldata.htm.

[54] Environmental Protection Agency, "Light-Duty Vehicle and Engine Emission Certification," epa.gov/otaq/cert.htm.

[55] Consumer Reports, consumerreports.org

[56] Ward's Auto, wardsauto.com

[57] Environmental Protection Agency and National Highway Traffic Safety Administration, "Light-Duty Vehicle Greenhouse Gas Emission Standards and Corporate Average Fuel Economy Standards; Final Rule," Federal Register, Volume 75, May 7, 2010.

[58] Environmental Protection Agency and National Highway Traffic Safety Administration, "2017 and Later Model Year Light-Duty Vehicle Greenhouse Gas Emissions and Corporate Average Fuel Economy Standard," Federal Register, Volume 77, October 15, 2012.

[59] SAE International, "Road Load Measurement and Dynamometer Simulation Using Coastdown Techniques," J1263, March 2010.

[60] SAE International, "Road Load Measurement Using Onboard Anemometry and Coastdown Techniques," J2263, December 2008.

[61] Environmental Protection Agency, "Determination and Use of Alternative Dynamometer Power Absorber Settings," OMS Advisory Circular, December 12, 1986.

[62] Environmental Protection Agency, "Single Roll Dynamometer Adjustment and Road Force Determination," VPDC-98-16, December 21, 1998.

[63] Le Good, G., Howell, J., Passmore, M., and Garry, K., "On-Road Aerodynamic Drag Measurements Compared with Wind Tunnel Data," SAE International Technical Paper 950627, February 1995.

[64] Tortosa, N., Meinert, F., Schenkel, F., Lounsberry, T., Gleason, M., Koester, W., and Walter, J., "A Correlation Study between the Full Scale Wind Tunnels of Chrysler, Ford, and General Motors," SAE International Technical Paper 2008-01-1205, April 2008.

[65] Sherman, Don, "Drag Queens," Car & Driver Magazine, June 2014, pages 86-92.

[66] SAE International, "Stepwise Coastdown Methodology for Measuring Tire Rolling Resistance," J2452, June 1999.

[67] Kelly, Kenneth, "Modeling Tools for Predicting the Impact of Rolling Resistance on Energy Usage and Fuel Efficiency for Realistic Driving Cycles," International Tire Exhibition Technical Paper 31C, 2002.

[68] Wen, B., Rogerson, G., and Hartkey, A., "Correlation Analysis of Rolling Resistance Test Results from SAEJ1269 and J2452," SAE International Technical Paper 2014-01-0066, April 2014.

[69] Environmental Protection Agency, "Fuel Economy Label: Updates," epa.gov/fueleconomy/updates.htm

[70] Sovran, G. and Blaser, D., "Quantifying the Potential Impacts of Regenerative Braking on a Vehicle's Tractive-Fuel Consumption for U.S., European, and Japanese Driving Schedules," SAE International Technical Paper 2006-01-0664, April 2006.

[71] Lutsey, Nicholas, "A technical analysis of model year 2011 US automobile efficiency," Transportation Research Part D, 17(5): 361-369

[72] Howell, J., Sherwin, C. Passmore, M., and Le Good, G., "Aerodynamic Drag of a Compact SUV as Measured On-Road and in the Wind Tunnel," SAE International Technical Paper 2002-01-0529, March 2002, February 1997.

[73] Wickern, G., Zwicker, K., and Pfadenhauer, M., "Rotating Wheels – Their Impact on Wind Tunnel Test Techniques and on Vehicle Drag Results," SAE International Technical Paper 970133

[74] SAE International, "Rolling Resistance Measurement Procedure for Passenger Car, Light Truck, and Highway Truck and Bus Tires," J1269, September 2006.

[75] Ecos Consulting, Transportation Research Board Data Set, 2002.

[76] California Energy Commission, 2007

[77] Backstrom, Alan, "Brake Drag Fundamentals," SAE International Technical Paper 2011-01-2377, September 2011.

[78] Shevket, C., Ciulla, L., and Re P., "Development of Low Friction and Light Weight Wheel Hub Units to Reduce both the Brake Corner Unsprung Mass and Vehicle CO2 Emission (Part 1 – Friction)," SAE International Technical Paper 2010-01-1706, October 2010.

[80] Rubber Manufacturers Association, "Compilation and Analysis of Data Related to the Rolling Resistance of Passenger Car Tires," Comments to Docket NHTSA-2008-0121, August 21, 2009.

[81] Michelin, "The tyre – Rolling resistance and fuel savings," 2003.

[82] Environmental Protection Agency and National Highway Traffic Safety Administration, "Joint Technical Support Document: Final Rulemaking for 2017-2025 Light-Duty Vehicle Greenhouse Gas Emission Standards and Corporate Average Fuel Economy Standards," EPA-420-R-12-901, p 3-234, August 2012.

[83] Code of Federal Regulation, Title 40, Subpart 1, 1066.805.

[84] Car & Driver, www.caranddriver.com.

[85] Motor Trend, www.motortrend.com.

[86] Deutsche Automobil Treuhand, "Leitfaden über den Kraftstoffverbrauch, die CO2-Emissionen und den Stromverbrauch," 1st quarter 2014.

[87] CONTROLTEC, LLC, "Technical Analysis of Vehicle Load Reduction Potential For Advanced Clean Cars, Research Plan," version 1.3, April 22, 2014.

[88] CONTROLTEC, LLC, CT-ENERGY, www.control-tec.com/product/ct-energy.

REFERENCES: MANUFACTURER WEBSITES

Manufacturer	Brand	Type	Uniform Resource Locator (URL)
Aston Martin	Aston Martin	Consumer	astonmartin.com
BMW	BMW	Consumer	bmwusa.com
BMW	BMW	Media	bmwusanews.com
BMW	Mini	Consumer	miniusa.com/content/miniusa/en.html
BMW	Rolls Royce	Consumer	rolls-roycemotorcars.com
BMW	Rolls Royce	Media	press.rolls-roycemotorcars.com/rolls-royce-motor-cars-pressclub
Chrysler	Chrysler	Consumer	chrysler.com
Chrysler	Dodge	Consumer	dodge.com
Chrysler	FIAT	Consumer	fiatusa.com
Chrysler	Jeep	Consumer	jeep.com/en
Chrysler	RAM	Consumer	ramtrucks.com
Chrysler		Media	media.chrysler.com
Ferrari	Ferrari	Consumer	ferrari.com
Ford Motor Company	Ford	Consumer	ford.com
Ford Motor Company	Ford	Media	media.ford.com
Ford Motor Company	Lincoln	Consumer	lincoln.com
Ford Motor Company	Lincoln	Media	media.lincoln.com
General Motors	Buick	Consumer	buick.com
General Motors	Buick	Media	media.gm.com/media/us/en/buick/vehicles.html
General Motors	Cadillac	Consumer	cadillac.com
General Motors	Cadillac	Media	media.gm.com/media/us/en/cadillac/vehicles.html
General Motors	Chevrolet	Consumer	chevrolet.com
General Motors	Chevrolet	Media	media.gm.com/media/us/en/chevrolet/vehicles.html
General Motors	GMC	Consumer	gmc.com
General Motors	GMC	Media	media.gm.com/media/us/en/gmc/vehicles.html
Honda	Acura	Consumer	acura.com
Honda	Acura	Media	hondanews.com/channels/acura-automobiles
Honda	Honda	Consumer	automobiles.honda.com
Honda	Honda	Media	hondanews.com/channels/honda-automobiles
Hyundai	Hyundai	Consumer	hyundaiusa.com
Hyundai	Hyundai	Media	hyundainews.com/us/en-us/2014
Jaguar Land Rover	Jaguar	Consumer	jaguarusa.com
Jaguar Land Rover	Jaguar	Media	newsroom.jaguarlandrover.com/en-us/jaguar
Jaguar Land Rover	Land Rover	Consumer	landrover.com/us/en
Jaguar Land Rover	Land Rover	Media	newsroom.jaguarlandrover.com/en-us/land-rover
Kia	Kia	Consumer	kia.com/us/en
Kia	Kia	Media	kiamedia.com/us/en
Lotus	Lotus	Consumer	lotuscars.com
Maserati	Maserati	Consumer	maserati.us/maserati/us/en/index.html
Mazda	Mazda	Consumer	mazdausa.com
Mazda	Mazda	Media	mazdausamedia.com
Mercedes-Benz	Mercedes-Benz	Consumer	mbusa.com
Mercedes-Benz	Smart	Consumer	smartusa.com
Mitsubishi	Mitsubishi	Consumer	mitsubishicars.com
Mitsubishi	Mitsubishi	Media	media.mitsubishicars.com
Nissan	Infiniti	Consumer	infinitiusa.com
Nissan	Infiniti	Media	infinitinews.com/en-US/infiniti/usa

Nissan	Nissan	Consumer	nissanusa.com
Nissan	Nissan	Media	nissannews.com/en-US/nissan/usa
Porsche	Porsche	Consumer	porsche.com/usa
Porsche	Porsche	Media	press.porsche.com/models
Subaru	Subaru	Consumer	subaru.com
Subaru	Subaru	Media	media.subaru.com
Toyota	Lexus	Consumer	lexus.com
Toyota	Lexus	Media	pressroom.lexus.com
Toyota	Scion	Consumer	scion.com
Toyota	Scion	Media	pressroom.scion.com
Toyota	Toyota	Consumer	toyota.com
Toyota	Toyota	Media	toyotanews.pressroom.toyota.com
Volkswagen	Audi	Consumer	audiusa.com
Volkswagen	Audi	Media	audiusanews.com
Volkswagen	Bentley	Consumer	bentleymotors.com
Volkswagen	Bentley	Media	bentleymedia.com
Volkswagen	Bugatti	Consumer	bugatti.com/en/home.html
Volkswagen	Lamborghini	Consumer	lamborghini.com
Volkswagen	Volkswagen	Consumer	vw.com
Volkswagen	Volkswagen	Media	media.vw.com
Volvo	Volvo	Consumer	volvocars.com/us
Volvo	Volvo	Media	media.volvocars.com

APPENDIX A: DATA QUALITY ASSURANCE CHARTS

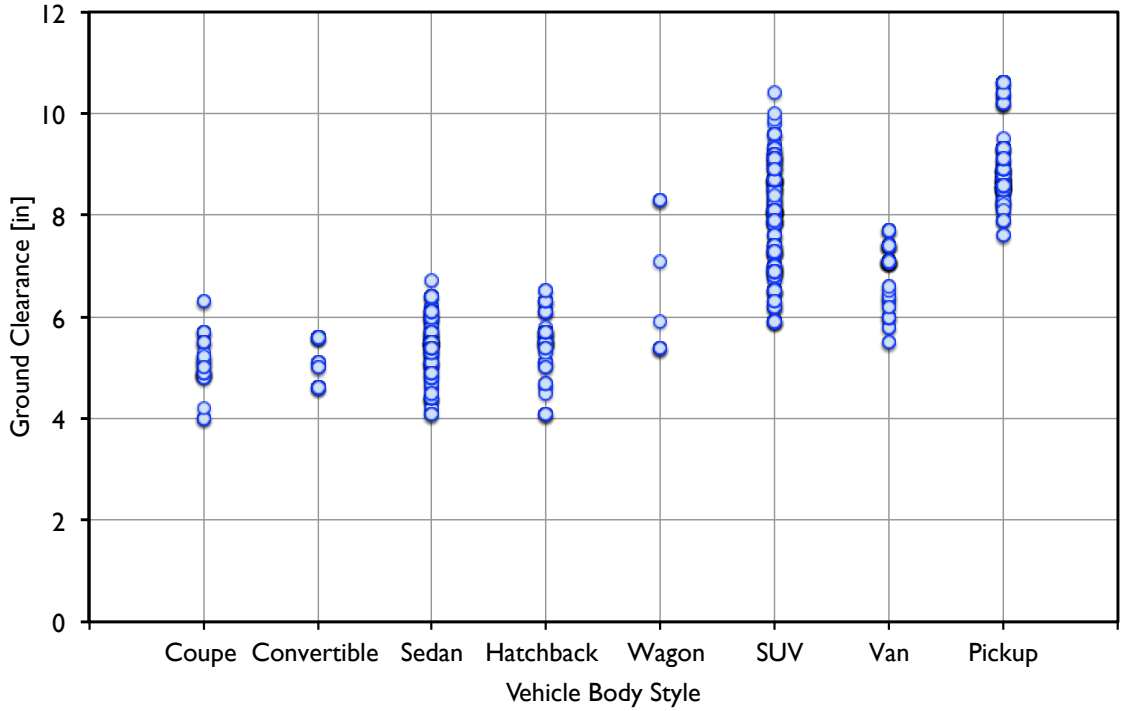

Figure 53: Ground Clearance vs. Vehicle Type

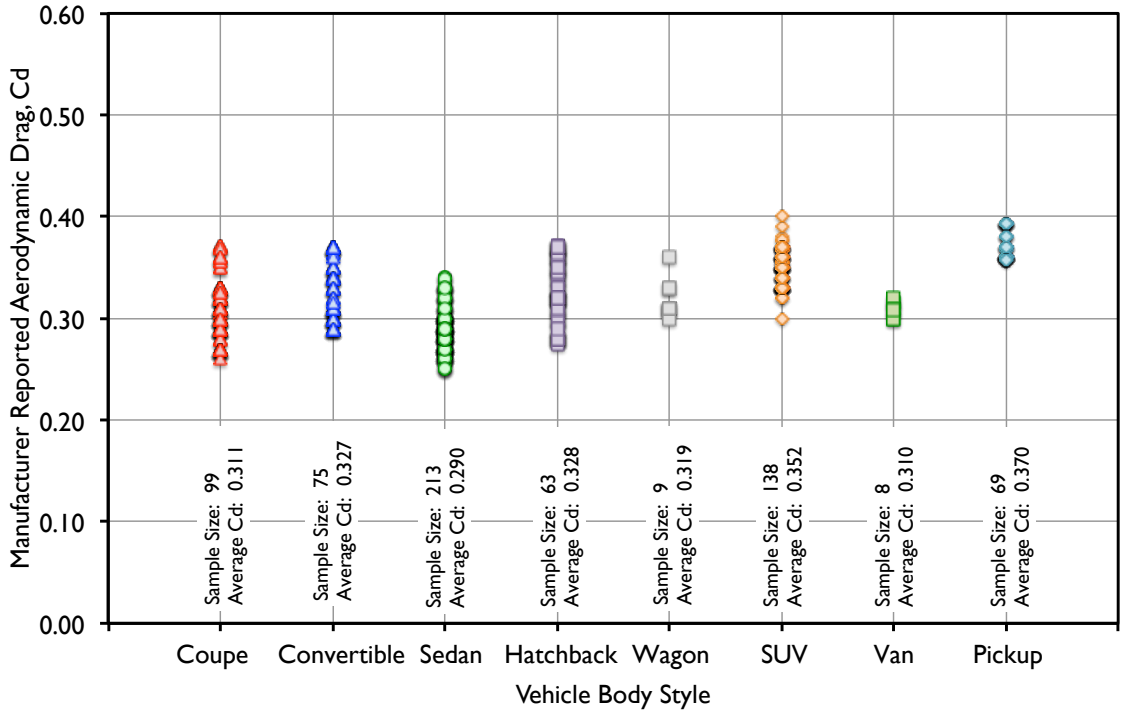

Figure 54: Aerodynamic Drag Coefficient (C_d) vs. Vehicle Type

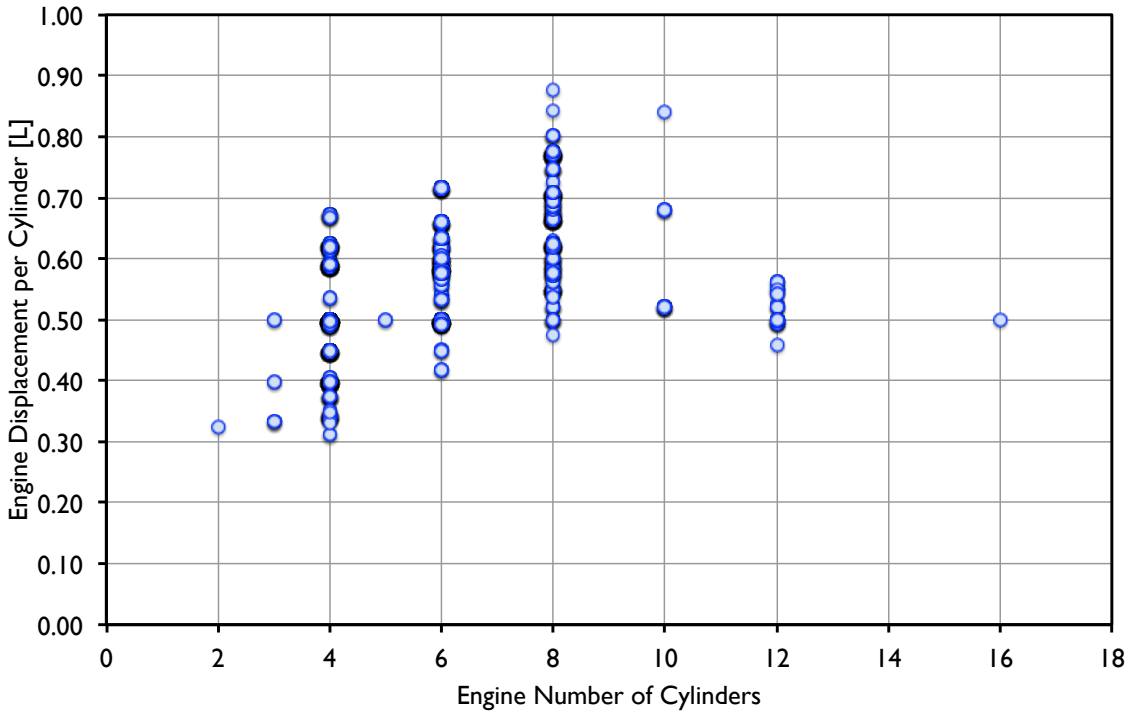

Figure 55: Engine Displacement per Cylinder

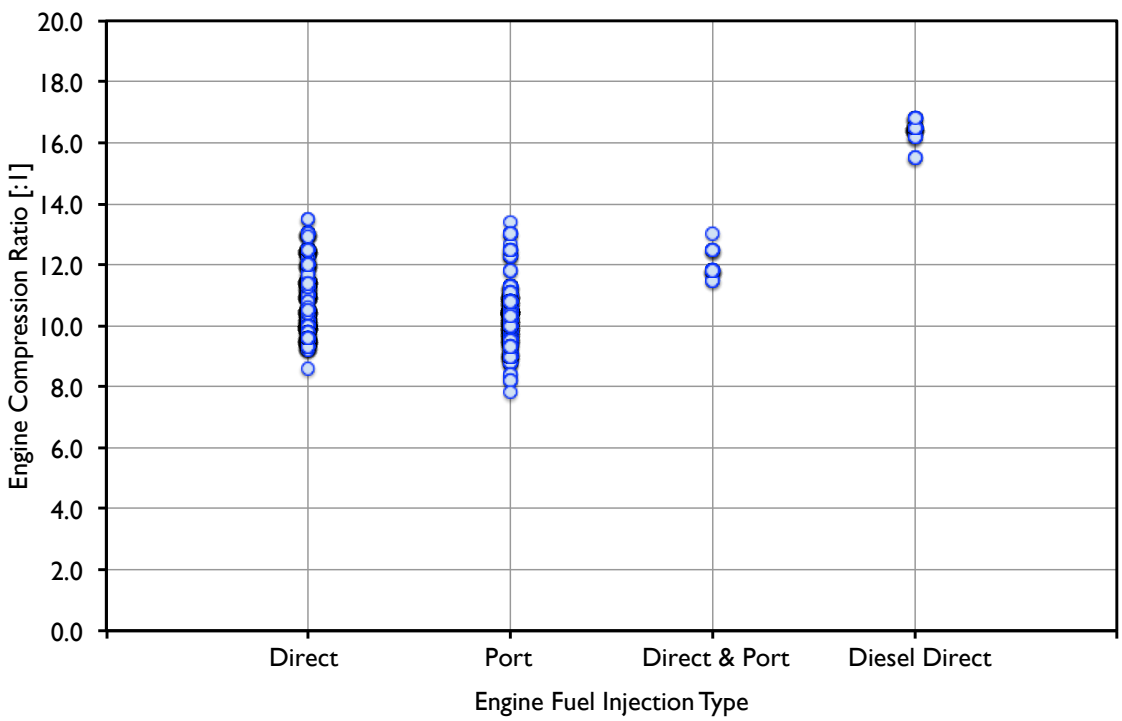

Figure 56: Engine Compression Ratio vs. Fuel System

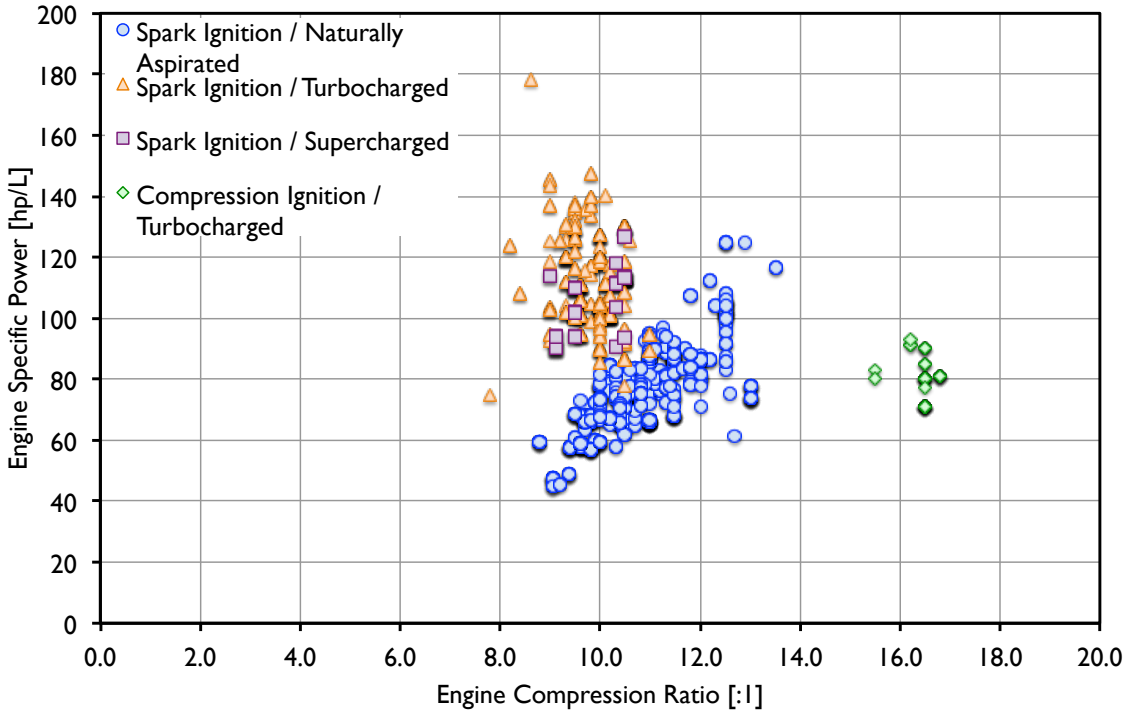

Figure 57: Engine Specific Power vs. Compression Ratio, Power Source and Aspiration

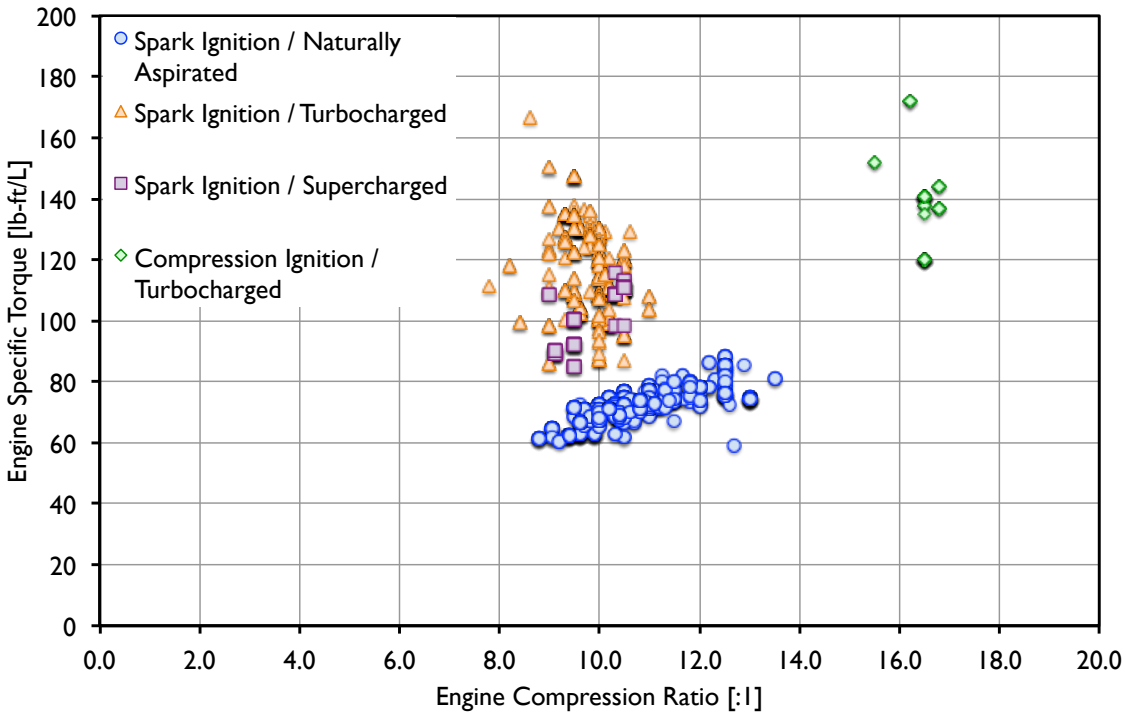

Figure 58: Engine Specific Torque vs. Compression Ratio and Power Source Type

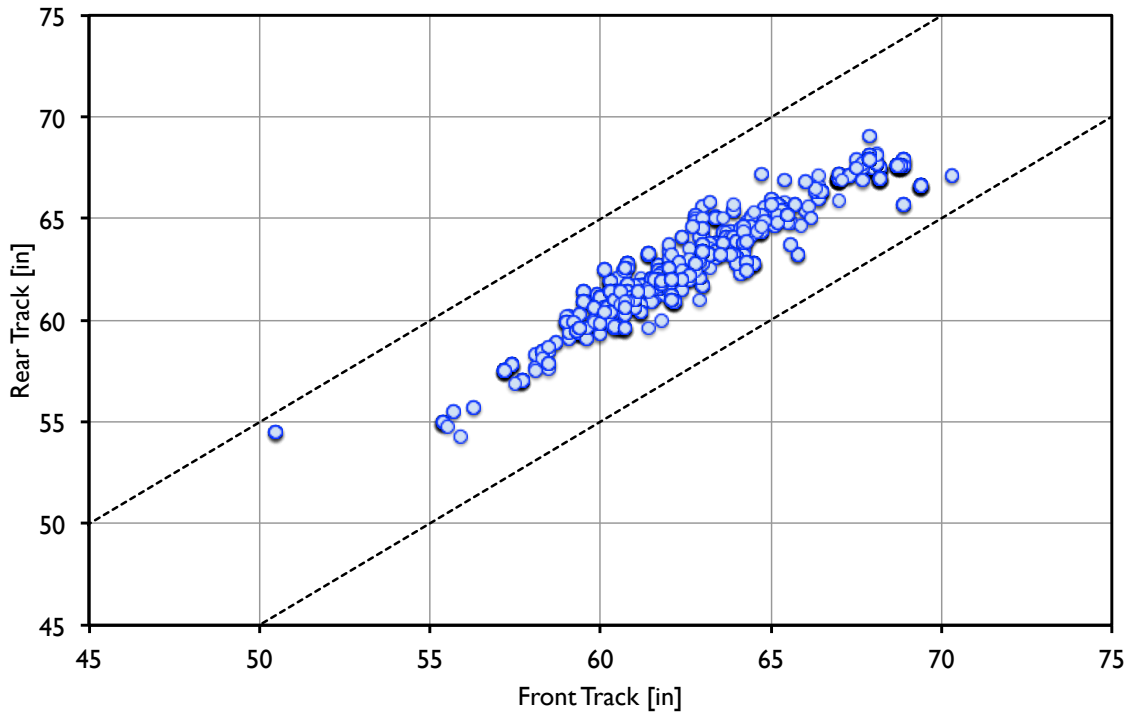

Figure 59: Rear Track vs. Front Track

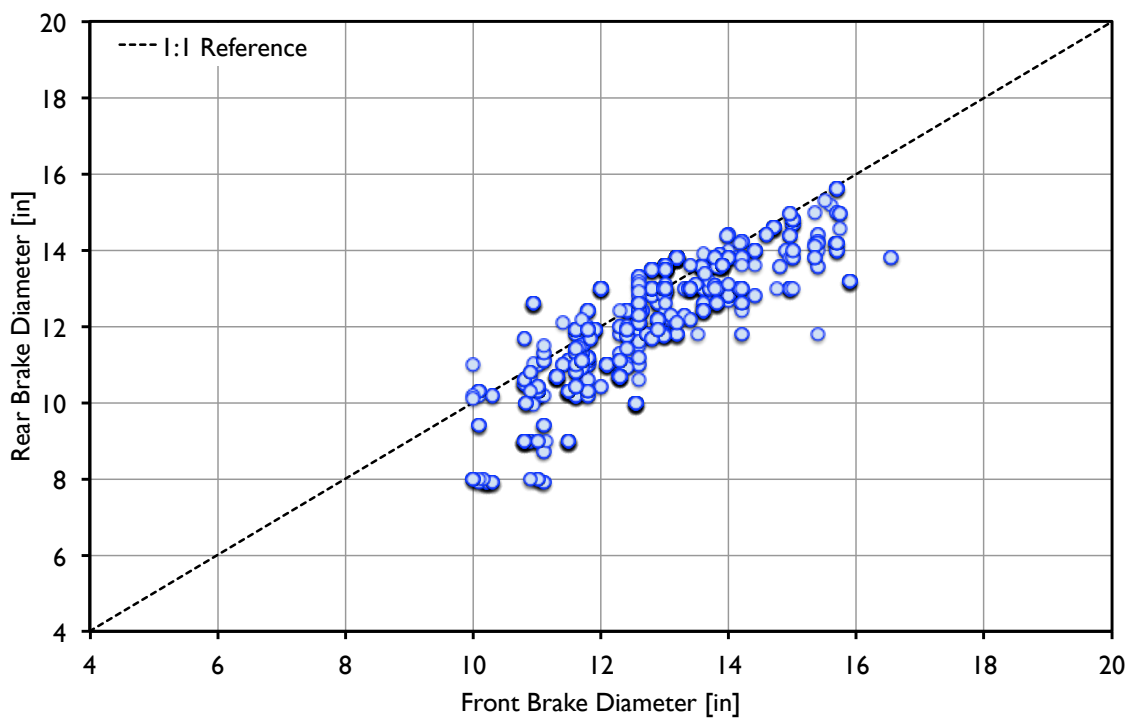

Figure 60: Rear Brake Diameter vs. Front Brake Diameter

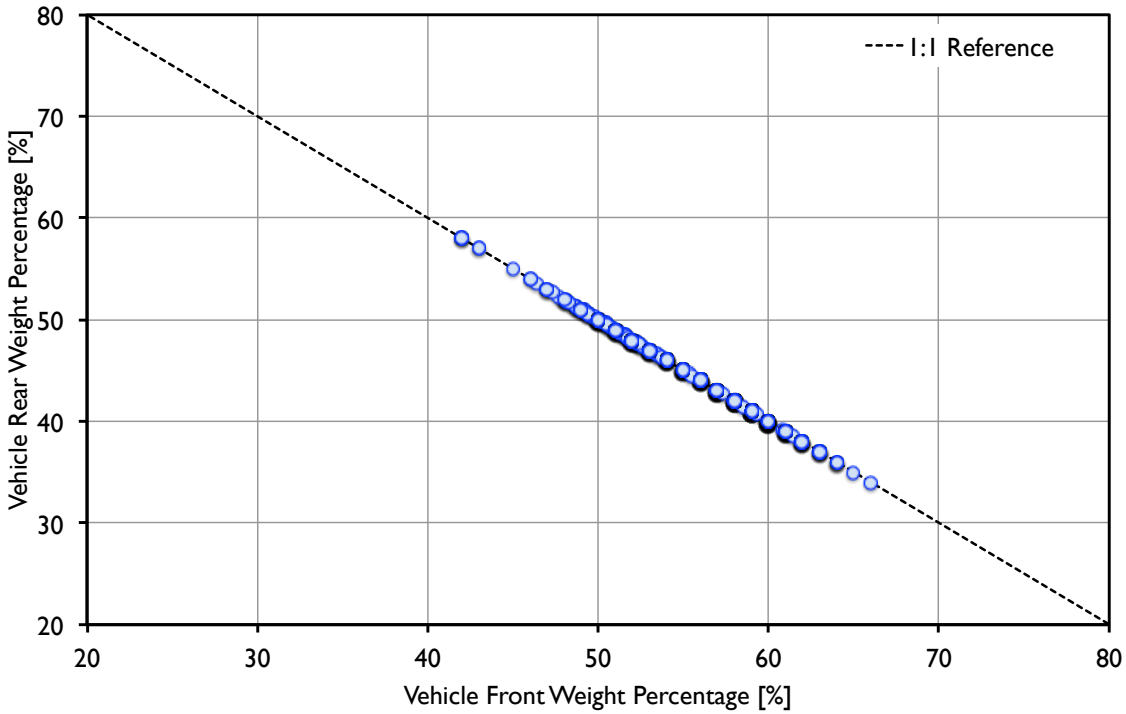

Figure 61: Rear Weight Distribution vs. Front Weight Distribution

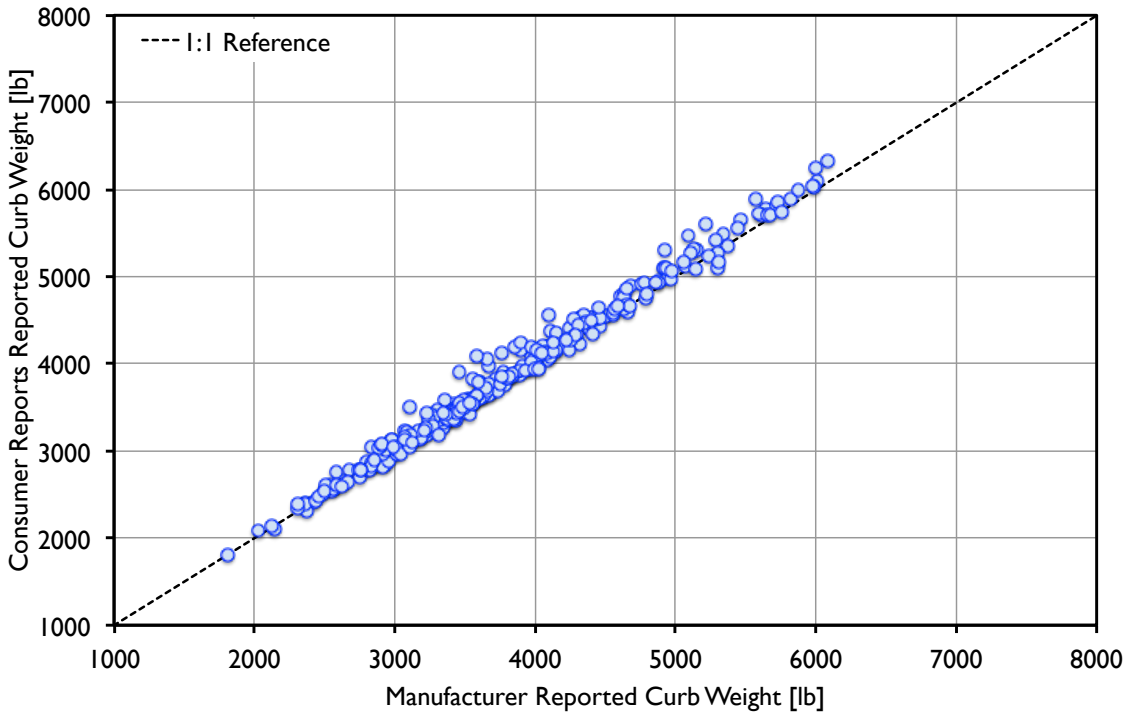

Figure 62: Consumer Reports vs. Manufacturer-Reported Curb Weight

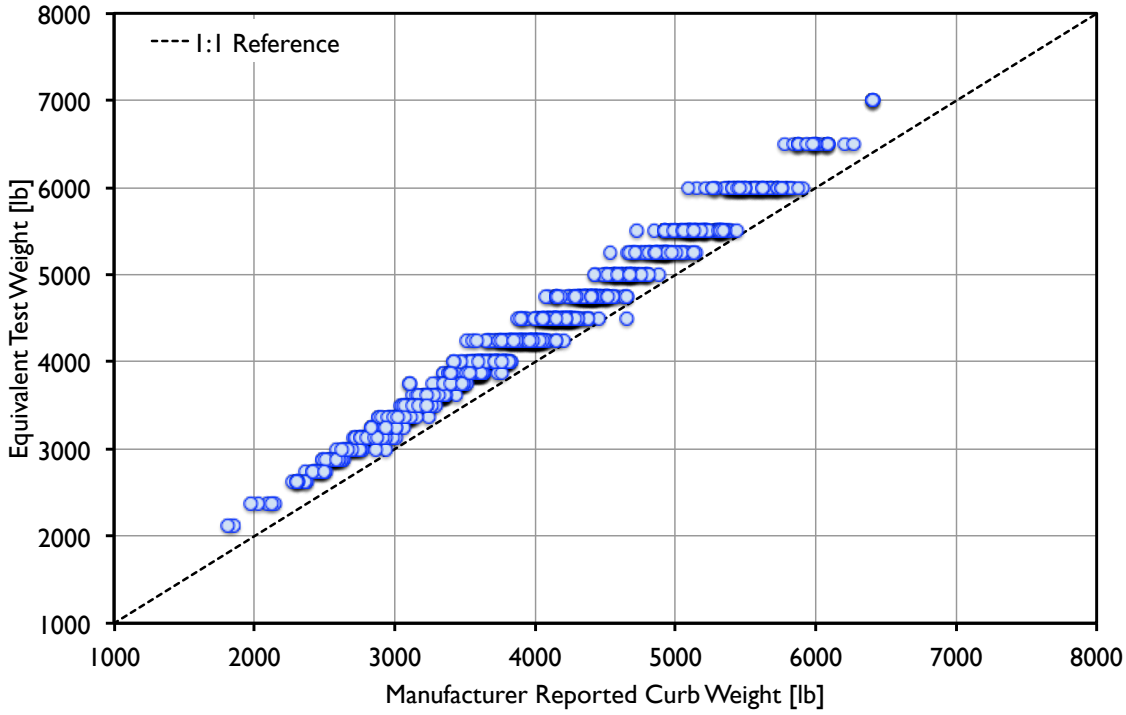

Figure 63: Equivalent Test Weight vs. Manufacturer-Reported Curb Weight

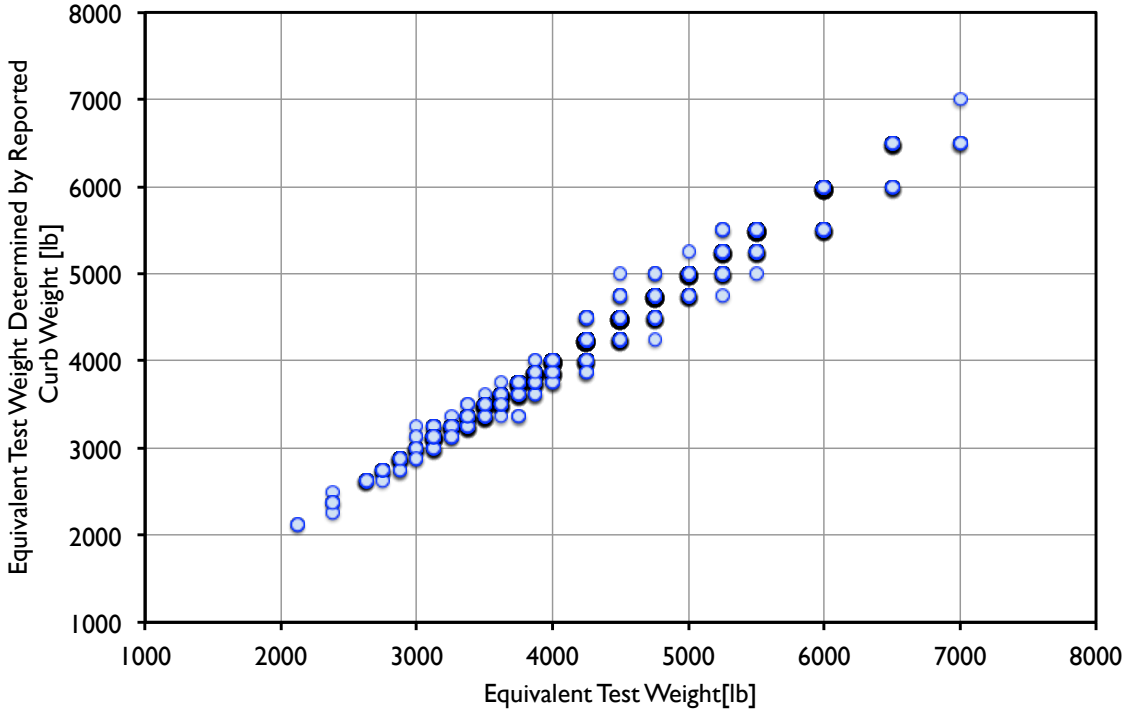

Figure 64: Equivalent Test Weight from Manufacturer-Reported Curb Weight vs. Equivalent Test Weight for Certification

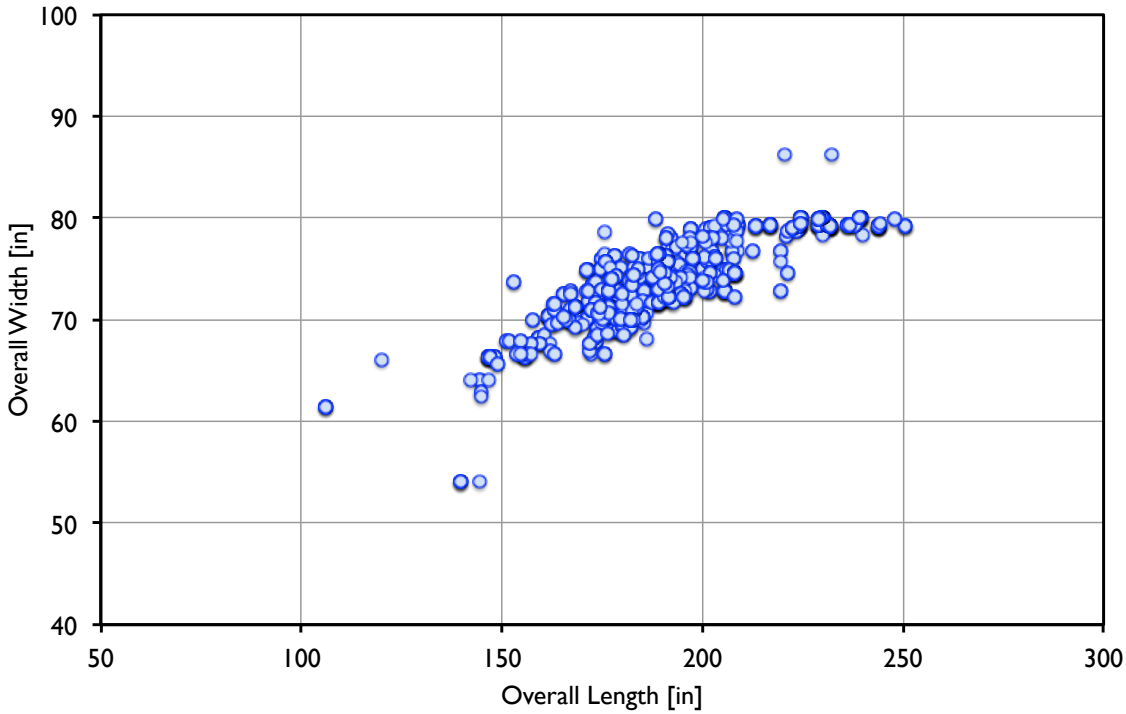

Figure 65: Overall Width vs. Overall Length

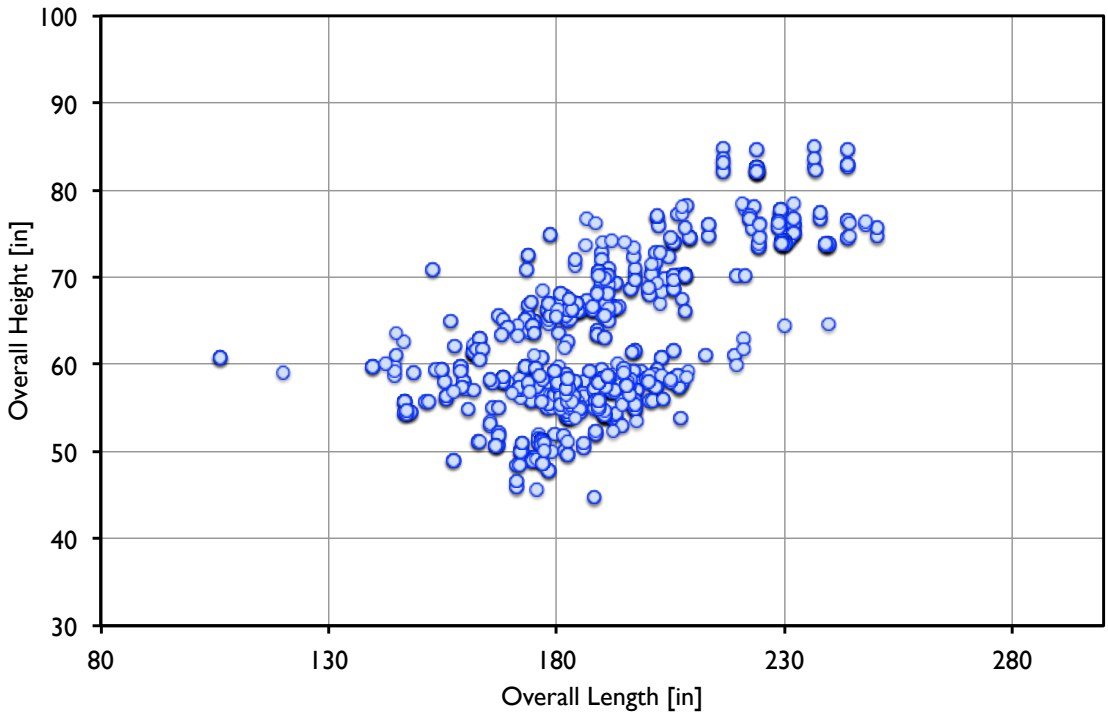

Figure 66: Overall Height vs. Overall Length

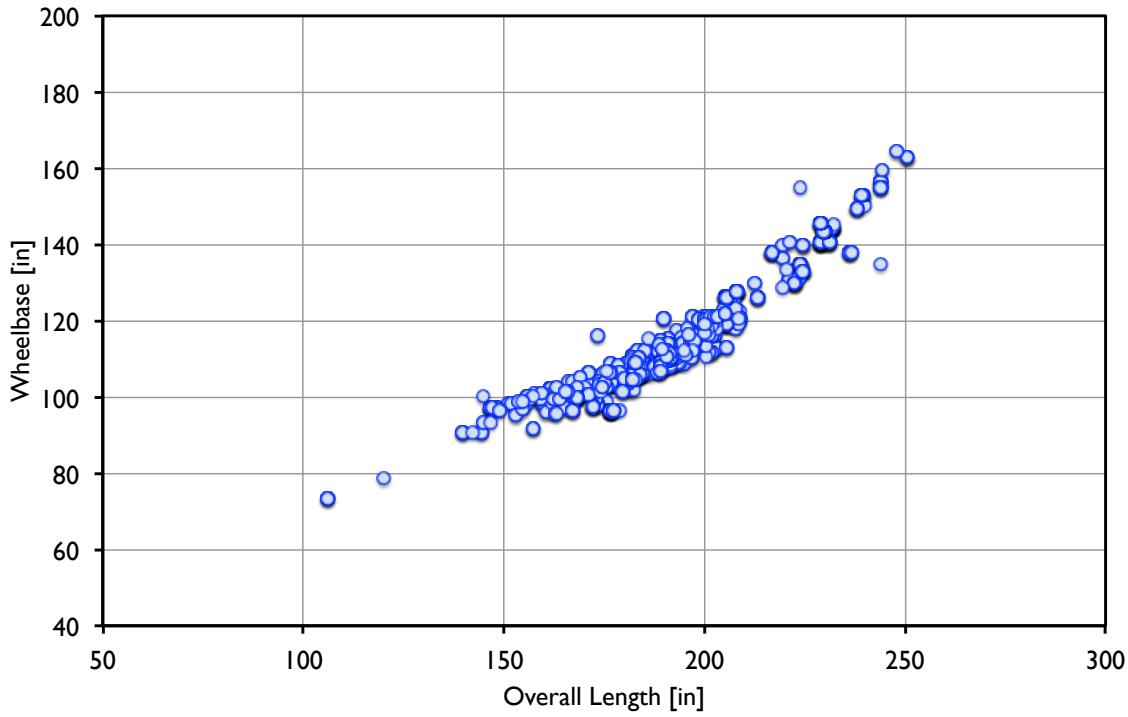

Figure 67: Wheelbase vs. Overall Length

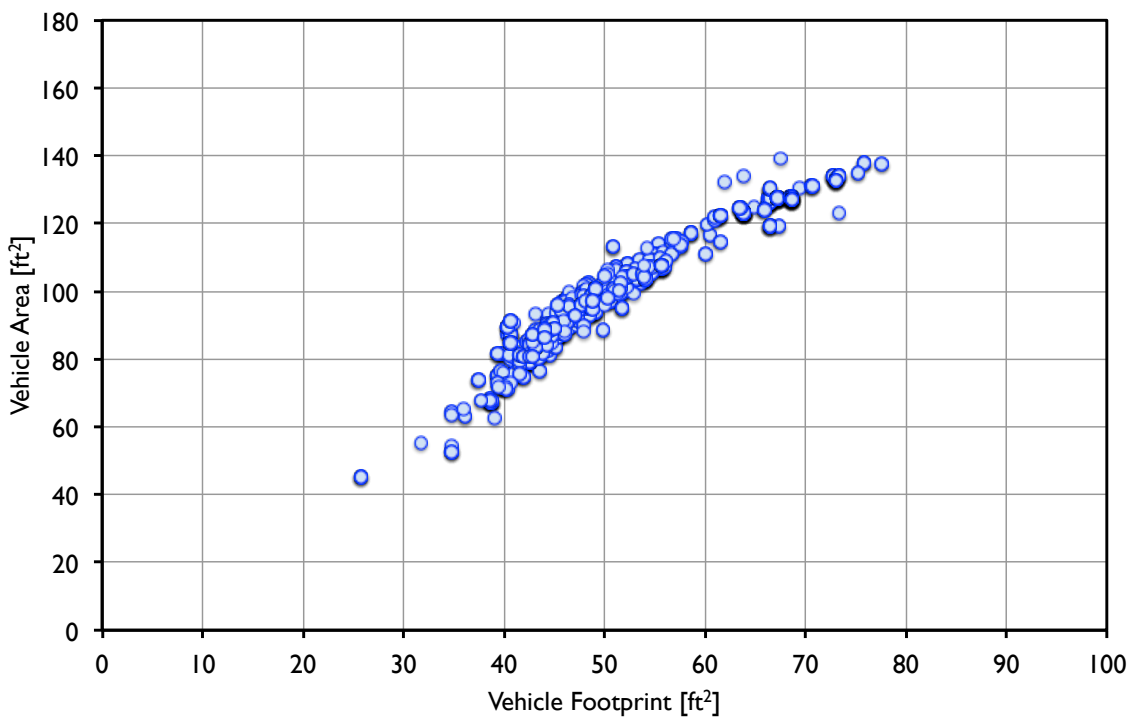

Figure 68: Vehicle Area vs. Vehicle Footprint

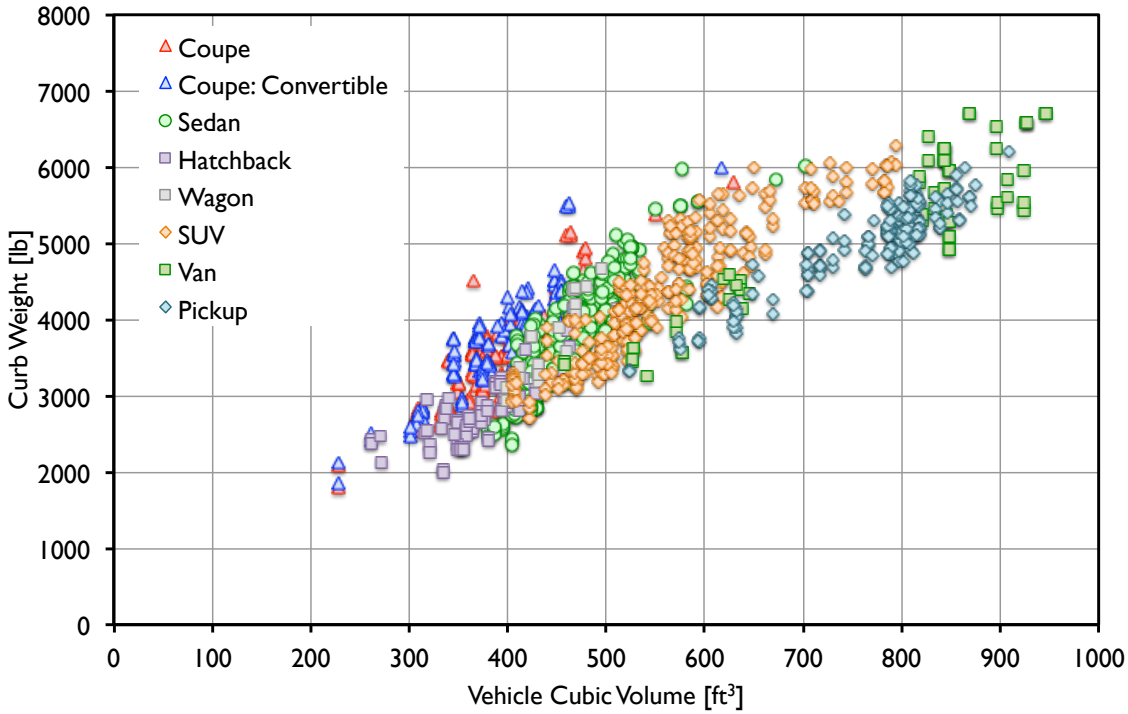

Figure 69: Manufacturer-Reported Curb Weight vs. Vehicle Cubic Volume

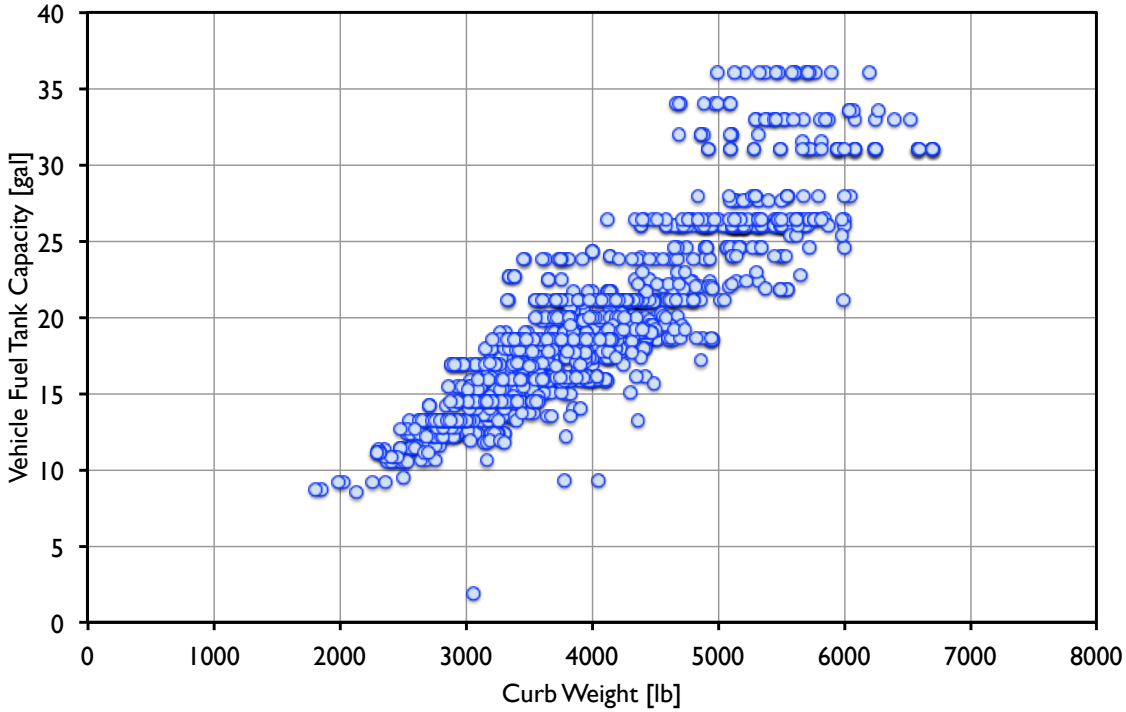

Figure 70: Fuel Tank Capacity vs. Curb Weight

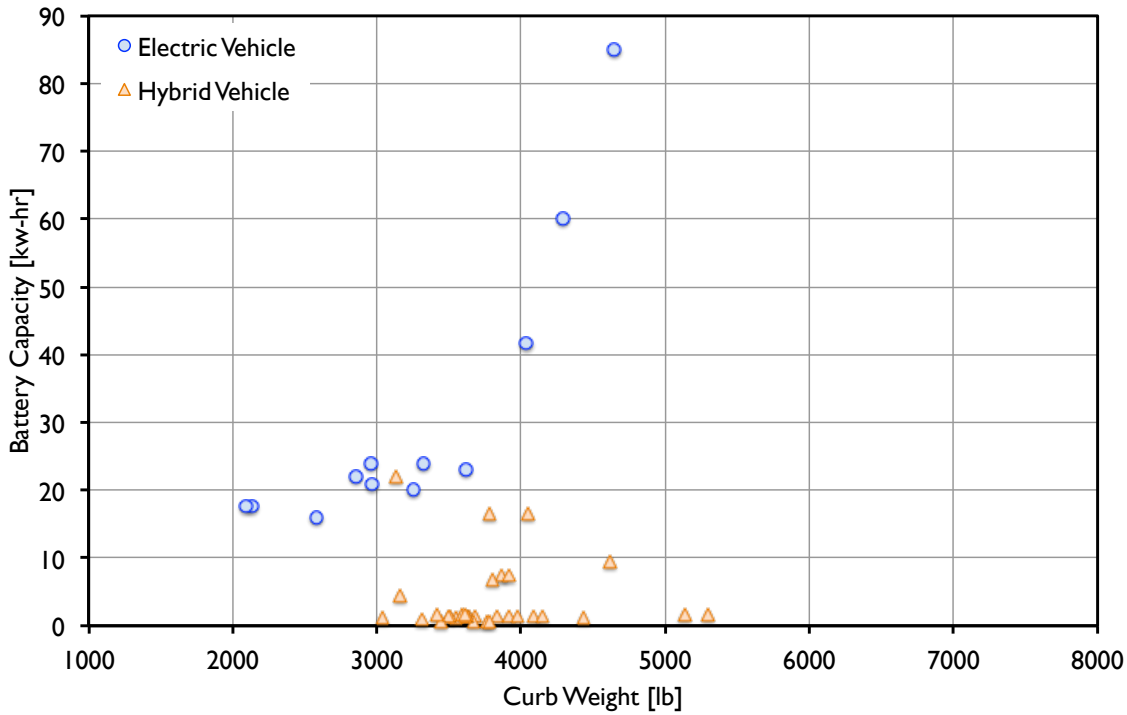

Figure 71: Battery Capacity vs. Manufacturer-Reported Curb Weight

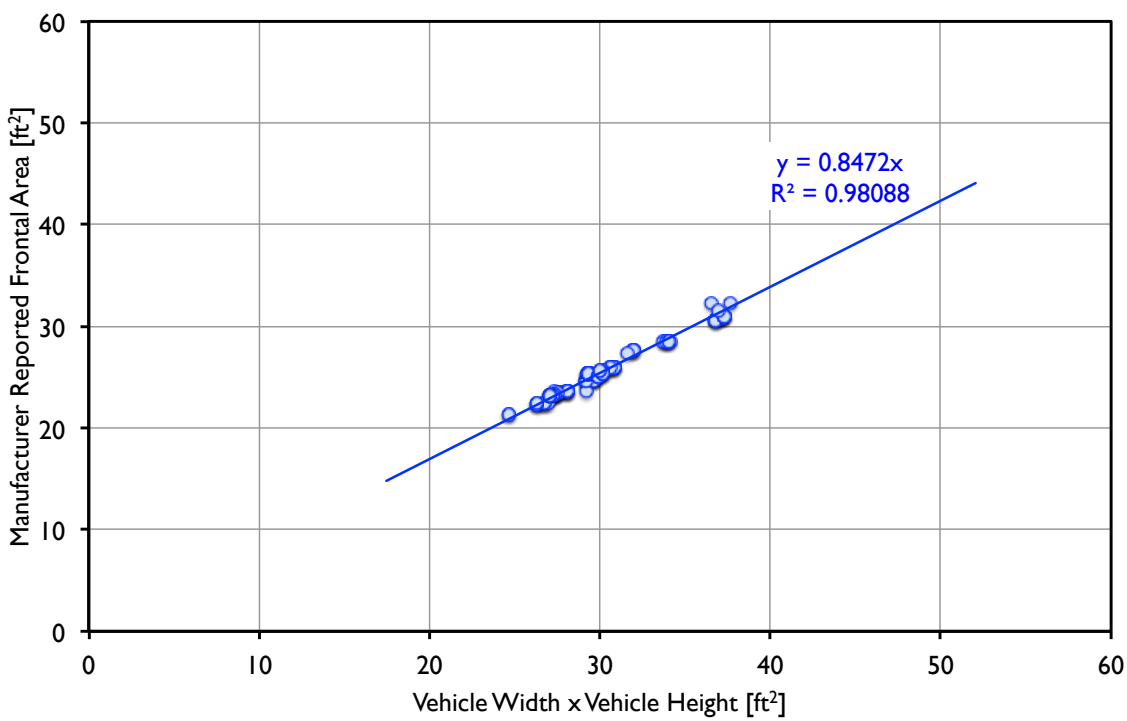

Figure 72: Manufacturer-Reported Frontal Area vs. Square Frontal Area

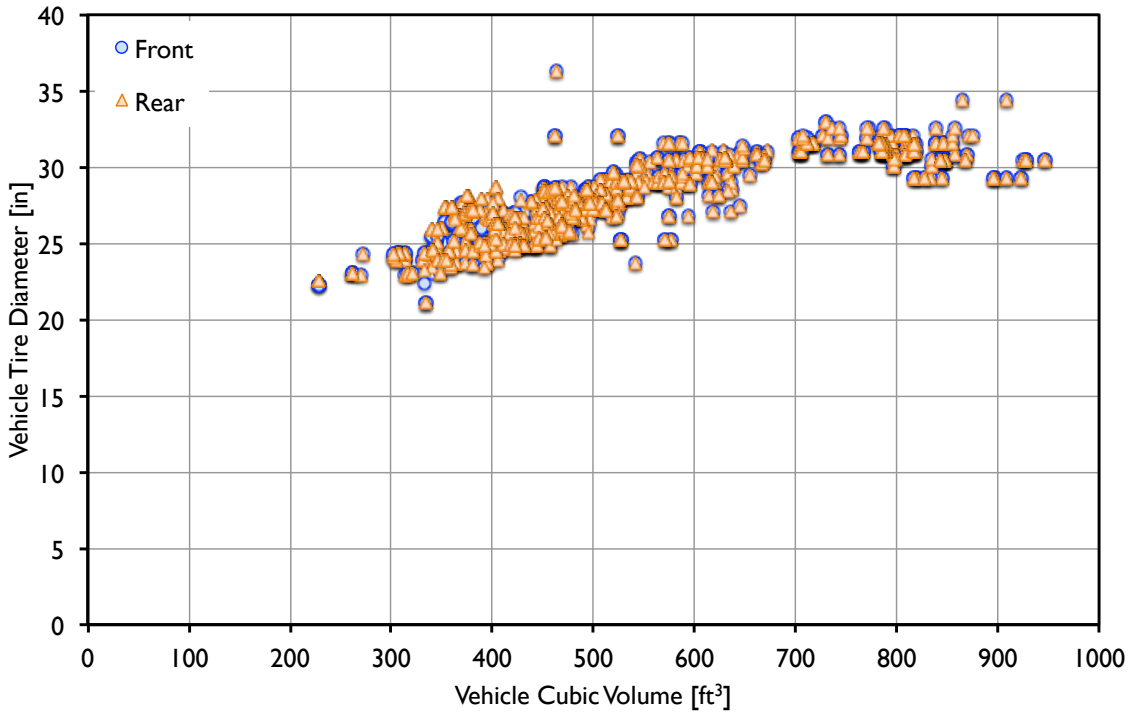

Figure 73: Tire Diameter vs. Vehicle Cubic Volume

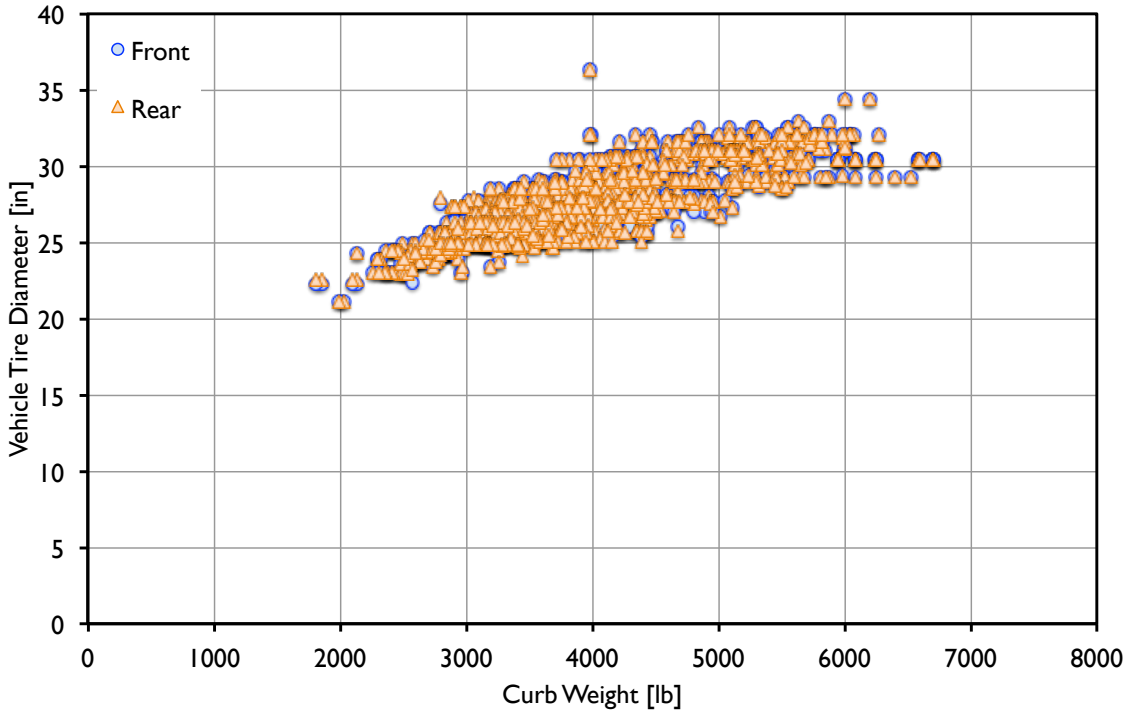

Figure 74: Tire Diameter vs. Manufacturer-Reported Curb Weight

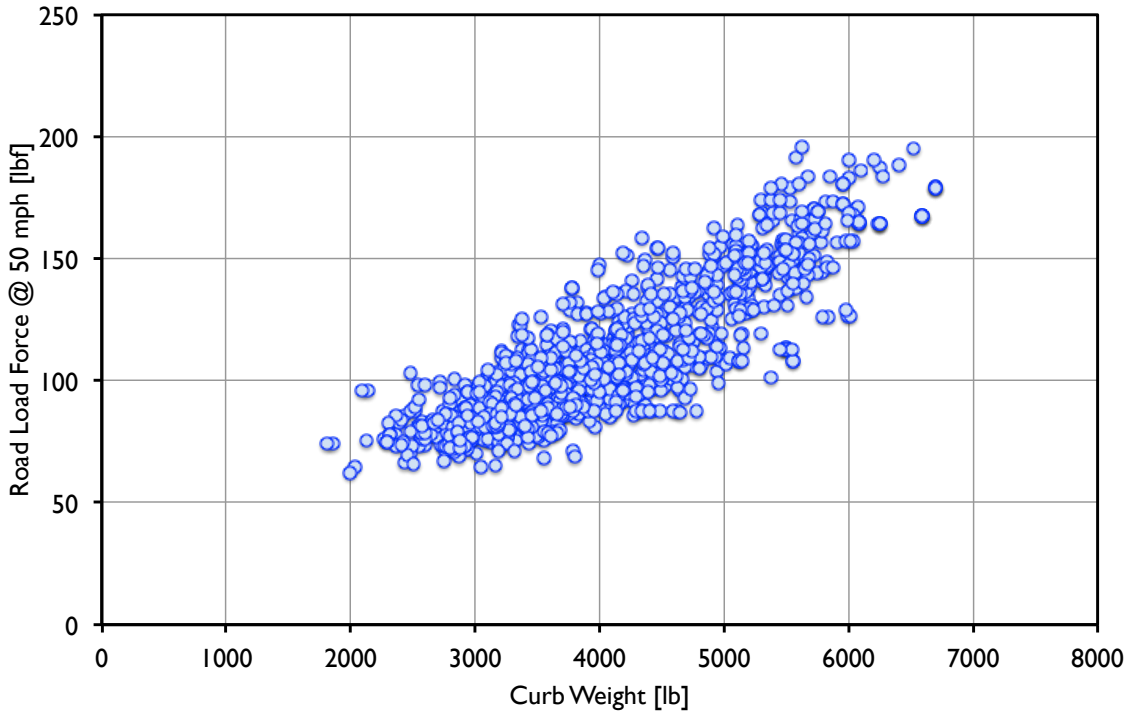

Figure 75: Road Force vs. Manufacturer-Reported Curb Weight

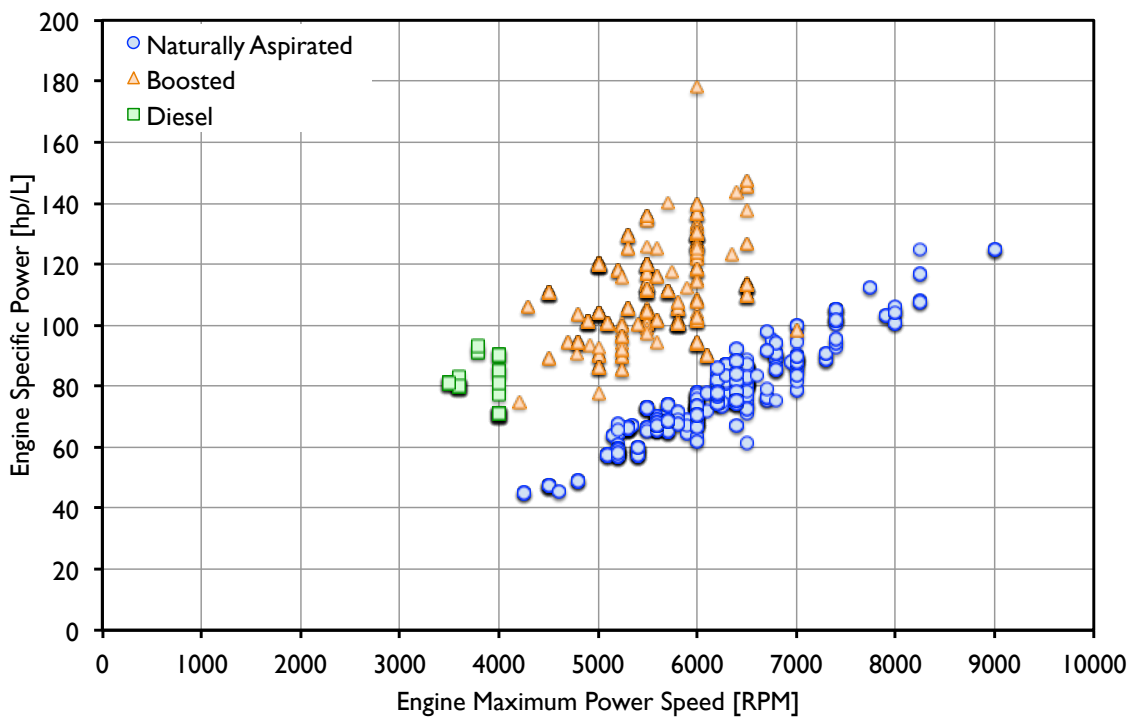

Figure 76: Engine Specific Power vs. Rated Power Speed

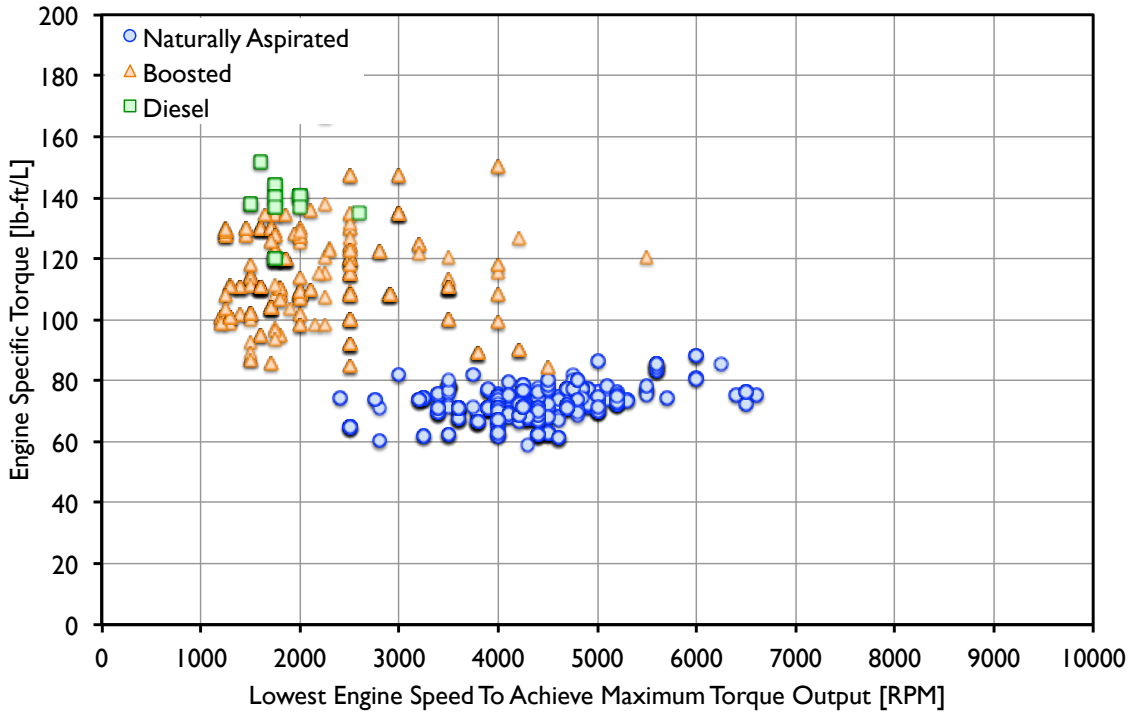

Figure 77: Engine Specific Torque vs. Rated Torque Speed

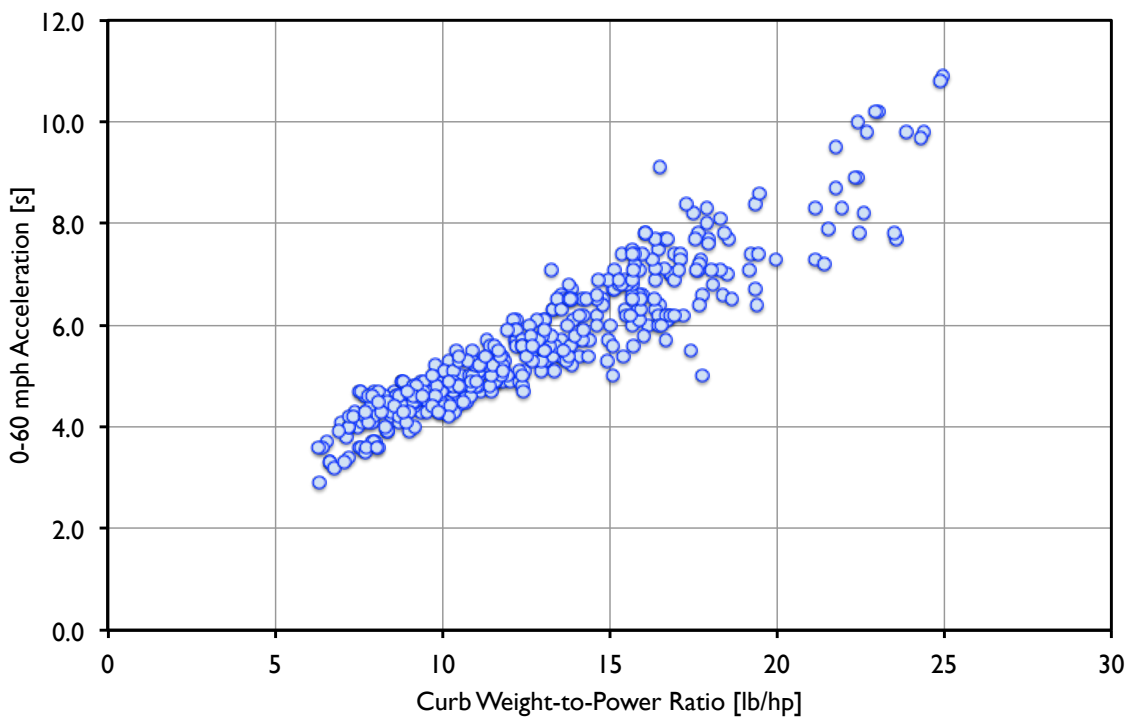

Figure 78: 0-60 mph Acceleration vs. Weight-to-Power Ratio

APPENDIX B: TABULAR RESULTS

Table XVI: Coefficient of Drag vs. Load Scenario

Coefficient of Drag (Cd)				
Load Scenario	Unweighted Average	Change from Baseline	Sales-Weighted Average	Change from Baseline
	[-]	[%]	[-]	[%]
Baseline	0.349	0.0	0.333	0.0
Reduced Cd	0.308	-11.6	0.298	-10.6
+ Reduced Tire RRC	0.308	-11.6	0.298	-10.6
+ Mass Reduction	0.308	-11.6	0.298	-10.6
+ Engine Downsize	0.308	-11.6	0.298	-10.6
+ Reduced On-Board Energy	0.308	-11.6	0.298	-10.6

Table XVII: Effective Frontal Area vs. Load Scenario

Effective Frontal Area (CdA)				
Load Scenario	Unweighted Average	Change from Baseline	Sales-Weighted Average	Change from Baseline
	[m2]	[%]	[m2]	[%]
Baseline	0.898	0.0	0.827	0.0
Reduced Cd	0.795	-11.6	0.739	-10.7
+ Reduced Tire RRC	0.795	-11.6	0.739	-10.7
+ Mass Reduction	0.795	-11.6	0.739	-10.7
+ Engine Downsize	0.795	-11.6	0.739	-10.7
+ Reduced On-Board Energy	0.795	-11.6	0.739	-10.7

Table XVIII: Tire RRC @ 80 kph vs. Load Scenario

Tire Rolling Resistance Coefficient @ 80 kph				
Load Scenario	Unweighted Average	Change from Baseline	Sales-Weighted Average	Change from Baseline
	[kg/1000 kg]	[%]	[kg/1000 kg]	[%]
Baseline	9.0	0.0	8.2	0.0
Reduced Cd	9.0	0.0	8.2	0.0
+ Reduced Tire RRC	7.6	-15.1	7.2	-11.4
+ Mass Reduction	7.6	-15.1	7.2	-11.4
+ Engine Downsize	7.6	-15.1	7.2	-11.4
+ Reduced On-Board Energy	7.6	-15.1	7.2	-11.4

Table XIX: Tire Rolling Force @ 80 kph vs. Load Scenario

Tire Rolling Force @ 80 kph				
Load Scenario	Unweighted Average	Change from Baseline	Sales-Weighted Average	Change from Baseline
	[N]	[%]	[N]	[%]
Baseline	174	0.0	142	0.0
Reduced Cd	174	0.0	142	0.0
+ Reduced Tire RRC	147	-15.1	126	-11.4
+ Mass Reduction	135	-22.2	117	-17.8
+ Engine Downsize	135	-22.2	117	-17.8
+ Reduced On-Board Energy	135	-22.3	116	-18.0

Table XX: Curb Weight vs. Load Scenario

Curb Weight				
Load Scenario	Unweighted Average	Change from Baseline	Sales-Weighted Average	Change from Baseline
	[kg]	[%]	[kg]	[%]
Baseline	1825	0.0	1633	0.0
Reduced Cd	1825	0.0	1633	0.0
+ Reduced Tire RRC	1825	0.0	1633	0.0
+ Mass Reduction	1667	-8.7	1505	-7.8
+ Engine Downsize	1667	-8.7	1505	-7.8
+ Reduced On-Board Energy	1662	-8.9	1502	-8.0

Table XXI: Equivalent Test Weight vs. Load Scenario

Equivalent Test Weight				
Load Scenario	Unweighted Average	Change from Baseline	Sales-Weighted Average	Change from Baseline
	[kg]	[%]	[kg]	[%]
Baseline	1964	0.0	1771	0.0
Reduced Cd	1964	0.0	1771	0.0
+ Reduced Tire RRC	1964	0.0	1771	0.0
+ Mass Reduction	1802	-8.3	1642	-7.3
+ Engine Downsize	1802	-8.3	1642	-7.3
+ Reduced On-Board Energy	1798	-8.5	1638	-7.5

Table XXII: Vehicle Energy Intensity vs. Load Scenario

Vehicle Energy Intensity				
Load Scenario	Unweighted Average	Change from Baseline	Sales-Weighted Average	Change from Baseline
	[MJ/km]	[%]	[MJ/km]	[%]
Baseline	0.554	0.0	0.488	0.0
Reduced Cd	0.535	-3.5	0.472	-3.3
+ Reduced Tire RRC	0.513	-7.4	0.458	-6.1
+ Mass Reduction	0.485	-12.4	0.436	-10.6
+ Engine Downsize	0.485	-12.4	0.436	-10.6
+ Reduced On-Board Energy	0.485	-12.5	0.436	-10.7

Table XXIII: Energy Conversion Efficiency vs. Load Scenario

Energy Conversion Efficiency				
Load Scenario	Unweighted Average	Change from Baseline	Sales-Weighted Average	Change from Baseline
	[%]	[%]	[%]	[%]
Baseline	21.3	0.0	22.0	0.0
Reduced Cd	21.0	-1.4	21.8	-1.3
+ Reduced Tire RRC	20.7	-3.1	21.5	-2.5
+ Mass Reduction	20.2	-5.3	21.1	-4.3
+ Engine Downsize	20.5	-3.6	21.5	-2.6
+ Reduced On-Board Energy	20.5	-3.6	21.5	-2.6

Table XXIV: Fuel/Electrical Intensity vs. Load Scenario

Fuel/Electrical Energy Intensity				
Load Scenario	Unweighted Average	Change from Baseline	Sales-Weighted Average	Change from Baseline
	[MJ/km]	[%]	[MJ/km]	[%]
Baseline	2.599	0.0	2.215	0.0
Reduced Cd	2.544	-2.1	2.170	-2.0
+ Reduced Tire RRC	2.483	-4.5	2.132	-3.8
+ Mass Reduction	2.403	-7.5	2.068	-6.6
+ Engine Downsize	2.361	-9.2	2.032	-8.3
+ Reduced On-Board Energy	2.360	-9.2	2.030	-8.3

Table XXV: Fuel Economy vs. Load Scenario

Fuel Economy				
Load Scenario	Unweighted Average	Change from Baseline	Sales-Weighted Average	Change from Baseline
	[mpg]	[%]	[mpg]	[%]
Reported Baseline	30.5	-0.8	33.7	1.3
Projected Baseline	30.7	0.0	33.3	0.0
Reduced Cd	31.4	2.2	34.0	2.1
+ Reduced Tire RRC	32.1	4.7	34.6	3.9
+ Mass Reduction	33.2	8.1	35.7	7.1
+ Engine Downsize	33.8	10.1	36.3	9.0
+ Reduced On-Board Energy	33.8	10.1	36.3	9.1
+ Baseline Efficiency	35.1	14.3	37.3	12.0

Table XXVI: Tailpipe CO_2 Emissions vs. Load Scenario

Tailpipe CO2 Emissions				
Load Scenario	Unweighted Average	Change from Baseline	Sales-Weighted Average	Change from Baseline
	[g/mile]	[%]	[g/mile]	[%]
Reported Baseline	326	3.0	263	0.1
Projected Baseline	316	0.0	263	0.0
Reduced Cd	310	-2.0	258	-2.0
+ Reduced Tire RRC	303	-4.3	253	-3.8
+ Mass Reduction	293	-7.4	246	-6.6
+ Engine Downsize	286	-9.4	241	-8.3
+ Reduced On-Board Energy	286	-9.5	241	-8.3
+ Baseline Efficiency	268	-15.3	236	-10.4